Sustainable process development for microalgae cultivation and product exploration: a biorefinery approach

A Thesis

submitted for the of degree of
Doctor of Philosophy

Submitted by

Ankan Sinha
Roll No: 166106019

Under the supervision of
Prof. Debasish Das

January 2022
Department of Biosciences and Bioengineering
Indian Institute of Technology Guwahati
Guwahati 781 039, Assam, India

TH-2951_166106019

INDIAN INSTITUTE OF TECHNOLOGY GUWAHATI

Department of Biosciences and Bioengineering

STATEMENT

I do hereby declare that the content embodied in this thesis is the result of investigations carried out by me in the Department of Biosciences and Bioengineering, Indian Institute of Technology Guwahati, Guwahati, Assam, India under the supervision of Prof. Debasish Das.

In keeping with the general practice of reporting scientific observations, due acknowledgements have been made wherever the work described is based on the findings of other investigators.

January 2022 **Ankan Sinha**

TH-2951_166106019

INDIAN INSTITUTE OF TECHNOLOGY GUWAHATI

Department of Biosciences and Bioengineering

CERTIFICATE

It is certified that the work described in this thesis entitled "**Sustainable process development for microalgae cultivation and product exploration: a biorefinery approach**" by Mr. Ankan Sinha for the award of degree of Doctor of Philosophy is an authentic record of the results obtained from the research work carried out under my supervision in the Department of Biosciences and Bioengineering, Indian Institute of Technology Guwahati, Guwahati, India. The work embodied in this thesis has not been submitted elsewhere for a degree.

Dr. Debasish Das

Professor

(Thesis Supervisor)

Department of Biosciences & Bioengineering

Indian Institute of Technology Guwahati

Guwahati 781 039, India

TH-2951_166106019

Acknowledgements

I would like to express my heartiest gratitude to my thesis supervisor, ***Prof. Debasish Das***, Department of Biosciences and Bioengineering, IIT Guwahati, for giving me the opportunity to pursue this research work. I must acknowledge the freedom of thinking, planning, execution and expression I was given in every step of my research work, while keeping faith and confidence on my capabilities.

I am indebted to my doctoral committee members, ***Dr. S. Senthilkumar, Prof. Vaibhav V. Goud*** and ***Dr. Soumen Kumar Maiti*** for their careful evaluation and constructive suggestions, which helped me to improve my work pertaining to Ph.D. thesis.

My sincere thanks to all the ***faculty members, technical officers and staffs*** of Department of Biosciences and Bioengineering for their kind support during my Ph.D. work.

I owe my thanks to the ***Department of Biosciences and Bioengineering,*** and ***Central Instrumentation Facility***, IIT Guwahati for providing me the necessary facilities to fulfil my Ph.D. thesis objectives.

I would also like to thank ***ONGC Ltd***. for providing financial assistance during my Ph.D. and ***MHRD*** for regular funding of the Ph.D. work, which made this study possible.

I would like to acknowledge the post-doctoral fellows of my lab ***Dr. Gargi Goswami, Dr. Basavaraj Palabhanvi, Dr. D Vijayan, Dr. Parveez Ahamed, Dr. Dineshbabu Ganasekaran and Dr. Chandan Mukherjee*** for their precious advice and guidance throughout my Ph.D. I would also like to thank my lab seniors ***Dr. Mehak, Dr. Saumya, Dr. Mayur,Dr. Payel*** for their suggestions, time, help in practical things. It was pleasure working with my lab mates ***Ratan, John, Noor, Krishna, Pavan, Boudhnath, Rashid, and Gobinda***. Their continuous support and kindness made the journey an unforgettable experience.

TH-2951_166106019

My heartiest thanks to my friends ***Subhojit, Saddam, Manish, Gaurav, Heeramoni, Anjali, Uttariya, Samrat, Jayabrata, Aniruddha*** for support and encouragement throughout the time. My deepest gratitude goes to my beloved parents, ***Mr. Amit Sinha*** and ***Mrs. Mitul Sinha*** as well as my ***family members*** for their blessings, love, patience, support and understanding throughout my studies and most of all to the ***Almighty God*** who made everything possible.

January 2022 **Ankan Sinha**

TH-2951_166106019

Abstract

The growing atmospheric emission of greenhouse gases (GHG), especially CO_2 from the combustion of hydro-carbon fuels currently hold significant impact on the increasing global carbon footprint. As a global concern, this situation has mandated the search for feasible carbon capture strategies (CCS). To that end, biological CCS offer sustainable methods free from energy intensive and complex chemical treatments. Microalgae, a natural and efficient cell factory for CO_2 capture, have gained impetus owing to its faster growth rate compared to other terrestrial plants, marginal cultivation requirements and diverse product portfolio. However, commercial feasibility of microalgae-based carbon capture and product generation process lies on several factors, which motivated the current research.

At the onset of the present study, the search of suitable microalgal strain with high CO_2 sequestration capability was materialized through screening of carbon rich industrial effluent using novel CO_2 selection pressure-based strategy. *Tetradesmus obliquus* CT02, an indigenous microalgal strain isolated through the novel screening process, found to exhibit a high CO_2 tolerance of 20% v/v. In order to understand the elementary requirements, the growth of the isolated microalgal strain was evaluated under different medium, initial pH and limiting nutrient (Nitrogen and phosphate) sources. Under selected nutritional and growth conditions, CT02 was found to have high protein and lipid content of 35.96% w/w and 41.21% w/w respectively, which clearly hypothesised the presence of vast product array. Keeping in mind the evident drawbacks of single product strategy, a biorefinery approach has been adopted for the isolated microalgal strain towards synthesis of different value-added products. Bioprospecting was performed in two sequential steps, resulting in alternate product cascades of bioactive molecules and biodiesel or biofertilizer. In the first step, crude microalgal extracts

TH-2951_166106019

in five different solvents were screened for their antioxidant and anticancer activities. While acetone extract showed the highest antioxidant activity with an IC_{50} value of 137 µg mL^{-1}, ethyl acetate extract exhibited maximum anticancer activity with an IC_{50} value of 306.67 µg mL^{-1}. This antioxidant and anticancer activity may be attributed to the coordinated action of multiple bioactive molecules as detected by HR-LCMS analysis. In the next step, post extracted residual biomass of CT02 was evaluated as feedstock for biodiesel production. The lipid content was found to be 35.7% - 39.1% w/w and further to that, FAME yield of 33.1% - 36.7% w/w was obtained via direct transesterification of both the acetone and ethyl acetate extracted biomass. Analysis of FAME composition revealed an abundance of palmitic acid (C16:0), stearic acid (C18:0), and elaidic acid (C18:1n9t) as the major constituents, making it suitable for use as biodiesel. The post extracted residual biomass was also evaluated for its application as biofertilizer through induced germination of *Solanum lycopersicum* seeds. The highest final germination percentage and germination index was estimated to be in the range of 75% - 80% and 117.5 - 118.5, respectively, comparable to that of commercial grade NPK (20:20:13).

Following the successful demonstration of biorefinery concept for CT02, a process engineering strategy was developed targeting improvement in its growth performance. The basic premise of the process relies on pH guided feeding of CO_2, enabling the growth of the isolate at optimal pH and without experiencing any possible limitation of carbon source. CT02 was first subjected to optimization of cultivation parameters under laboratory scale followed by evaluation of its growth and culture pH under diurnal variation of simulated sunlight intensity. The understanding of interdependent dynamics between growth, culture pH and incident light intensity led to the development of pH-based CO_2 feeding process for growth under quotidian variation of light intensity. The strategy was developed at laboratory scale bubble column photobioreactor under diurnal variation of simulated sunlight intensity and was further validated through growth of the strain in a 100 L airlift bioreactor under fluctuating outdoor

TH-2951_166106019

environmental conditions, which considered to be economical way of biomass generation. Under laboratory condition, an improvement of 53.3% in biomass titer and 85.16% in biomass productivity was achieved as compared to the batch with uncontrolled pH. The positive impact of the strategy was more prominent even under outdoor condition where, biomass titer and productivity of 1.14 g L^{-1} and 59.4 mg L^{-1} day^{-1}, was an improvement of 225.7% and 121.6% respectively, compared to the pH uncontrolled batch. In context of CO_2 fixation rate, 121 % improvement was achieved at outdoor cultivation process engineering strategy compared to batch with uncontrolled pH.

TH-2951_166106019

Contents

TH-2951_166106019

TH-2951_166106019

TH-2951_166106019

TH-2951_166106019

TH-2951_166106019

List of figures

TH-2951_166106019

TH-2951_166106019

TH-2951_166106019

	culture pH; (D) light intensity; (E) phosphate utilization and (F) nitrate utilization	

TH-2951_166106019

List of tables

TH-2951_166106019

Chapter 1

Introduction

1.1. Background and Motivation

The growing atmospheric emission of greenhouse gases (GHG), especially CO_2 from the combustion of hydro-carbon fuels has created a certain environmental crisis, driving us towards a severe climate change. The global average of atmospheric CO_2 concentration for the year 2019 stands at 409.8 ppm, with an annual growth rate of 2.3 ppm [Lindsey et. al., 2020] which holds significant impact on the increasing global carbon footprint. Another Recent survey revealed that almost 33.4 giga tonnes of CO_2 is being emitted every year due to various anthropogenic activities [Cheng. et., al 2019]. The urgency to neutralize this situation has mandated the scientific search for feasible carbon capture strategies (CCS). Though, conventional CCS like absorption, adsorption, membrane separation offer decent process efficiency, most of them are high energy intensive and certainly lack from the point of economic sustainability [Al-Mamoori et. al., 2017]. In contrast to this, biological CCS are based on natural CO_2 sequestration by microbial bio-factories, free from costly and complex chemical methods. As a choice of organism for bio-CCS, microalgae have gained huge impetus owing to their higher photosynthetic rate which accelerates the CO_2 fixation capacity 10 to 50 times than that of terrestrial crops [Patil et. al., 2017]. With a faster growth rate and ease of cultivation, this photosynthetically active unicellular organism proved to mitigate up to 1.8 kg of CO_2 per kg of biomass generated [Pavlik et. al., 2017]. Moreover, the multiproduct profile of microalgae makes them a viable third generation feedstock for producing vast range of high value bioactive molecules, healthcare supplements as well as low value products like biofuels

TH-2951_166106019

and biofertilizers. However, to realise the microalgal cell factories at commercial scale, selection of the robust strains with potential of sequestering CO_2 and subsequent conversion into multiple value-added products is of utter importance. Furthermore, the commercial processes involving microalgae as a feedstock are in dormancy owing to low net energy ratio (NER) and sub-optimal economic output. One of the potential solutions to these bottlenecks could be a biorefinery approach which enables sequential valorization of the microalgal biomass towards co-production of high-value metabolites (biotherapeutics, nutraceuticals and pigments), biofuels (biodiesel, bio-crude oil and bioethanol) and other low-value products (biofertilizer and bioplastics). In contrast to the process with single product strategy, biorefinery with multiple products may offer a sustainable and efficient process via maximizing the economic, environmental, and social benefits. For instance, a biorefinery strategy was demonstrated for generation of *Scenedesmus* sp. [Ferreira et. al., 2019] utilizing waste water and subsequent conversion of biomass into a wide range of high-value products such as phenols or flavonoids and low-value products such as biofuel or biofertilizer. Techno-economic analysis [Kothari et. al., 2017] has shown that, in-spite of having a vast global market, commercial availability of microalgal products is still in dormancy due to high capital cost and operational cost. To that end, the integrated approach of biofuel production coupled with bioprospecting of value-added products has been found to offer process sustainability and economic viability.

Another challenge towards commercialization of microalgae cultivation process is low biomass titer and productivity which, in turn incurs higher operational cost. To that end, understanding the limiting factors as well as selection of optimal process engineering strategies are vital. Efforts have been made by several research groups to realize the dynamics of microalgal growth under differential factors like CO_2 fixation, substrate utilization, light availability to cells, mass transfer and so on. For instance, growth-based feeding of limiting nutrients and

TH-2951_166106019

dynamic increase in illumination has been reported to substantially upsurge both biomass titer and productivity in case of *Chlorella* sp. FC2 IITG [Goswami et. al., 2019]. Another study involving various microalgal strains suggested that the optimal aeration to the culture have positive effect on growth and CO_2 utilization performance through betterment in mass transfer [Zhao et. al., 2015]. The culture pH, with direct control on solubility of CO_2 and nutrients, stands as one of the most critical factors for the dynamics of microalgal growth [Qiu et. al., 2017]. In addition to that, several reports revealed the effect of pH on cell metabolism which has impact on biomass composition i.e. protein and lipid content [Qiu et. al., 2017; Difusa et. al., 2017]. Owing to these facts, designing a sustainable method for controlling pH in microalgae cultivation is the need of the hour. While developing an effective process engineering strategy for improved biomass and product generation, laboratory scale studies are important talk. But it is even more important to assess the performance of the developed strategy at large scale cultivation under fluctuating outdoor environmental condition.

1.2. Objective of the study

Based on the current bottlenecks in microalgal research, the present study was carried out with the following objectives:

- **Screening & isolation of potential CO_2 tolerant microalgal strain from industrial hotspot in India.**
- **Characterization of growth and biochemical composition of the isolated microalgal strain *Tetradesmus obliquus* CT02.**
- **Establishment of biorefinery for bioactive molecules, biofuel, and biofertilizer using *Tetradesmus obliquus* CT02.**
- **Development of process engineering strategy for high cell density cultivation of *Tetradesmus obliquus* CT02 coupled with CO_2 sequestration.**

1.3. Approach

At the onset of the study, sampling was performed at steel plant effluent in search of potential CO_2 tolerant microalgae. Screening and isolation of the indigenous CO_2 tolerant strain was

TH-2951_166106019

performed by a novel CO_2 selection pressure-based screening strategy. The isolate was evaluated in terms of growth under different physicochemical parameters and biochemical composition, thereby obtaining insight about prospective product options. This motivated the development of biorefinery concept for the isolated microalgal strain with multiple product sequences. For assorting the primary product, solvent based crude microalgal extracts were screened for antioxidant and anticancer activity and the bioactive molecules prompting these activities were identified through mass spectroscopy. Further, the residual biomass post solvent extraction was evaluated for their potential as feedstock for biodiesel synthesis. Also, the induced germination of *Solanum lycopersicon* plants using the residual microalgal biomass recognized its quality as biofertilizer. This cumulatively portrayed a biorefining model for effective conversion of CO_2 into high value products, biofuel and biofertilizer using microalgae as a cell factory.

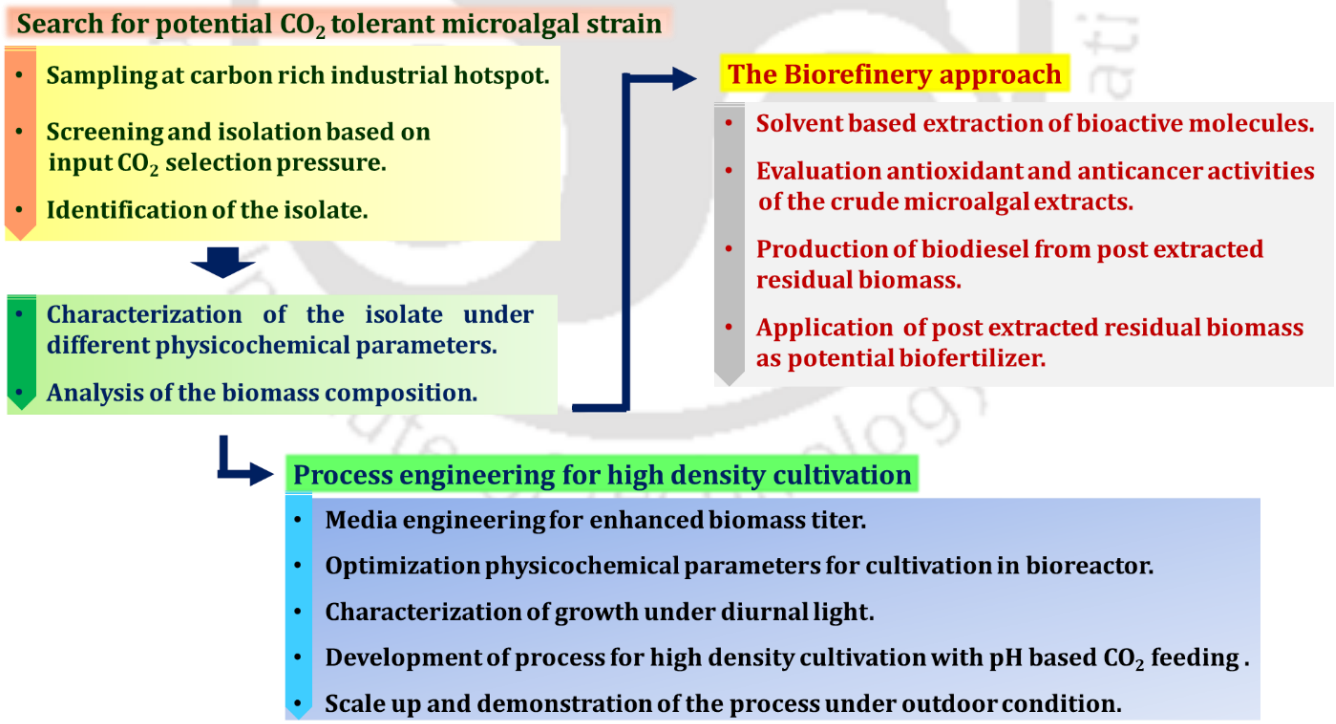

Fig. 1.1. Approach of the thesis towards development of sustainable microalgal biorefinery

TH-2951_166106019

In order to further explore and enhance the commercial viability of the strain, a process engineering strategy was developed aiming the improved biomass titer and CO_2 sequestration ability. Aiming to develop a sustainable process for cultivation of CT02, the nutrient requirements for growth were optimized through statistical tools followed by selection of suitable input aeration rate and culture pH. Characterization of the organism under diurnal variation of simulated sunlight intensity revealed the complex interdependency between growth, culture pH and incident light. The understanding led to the development of process engineering strategy coupling CO_2 injection for maintenance of optimal culture pH during quotidian variation of natural sunlight. The pH based $CO_{2\ feeding}$ strategy was first demonstrated at lab scale under simulated diurnal light intensity. Subsequently, the growth performance of the organism was evaluated under fluctuating outdoor environmental condition at 100 L airlift bioreactor where the aeration rate was reasonably scaled up keeping the volumetric power consumption rate constant.

1.4. Organisation of the thesis

The thesis consists of six Chapters encompassing introduction to conclusions. **Chapter 1** presents a general introduction of the current study establishing the background and motivation, the futuristic objectives, and the approach taken to resolve the problems in the current state of art technology. **Chapter 2** presents a detailed survey of literature depicting the current global need of sustainable carbon capture technology in view of rapidly increasing CO_2 concentration in the atmosphere. the chapter debates the existing chemical and biological CO_2 mitigation technologies and their major bottlenecks and microalgae as a potential cell factory for CO_2 bio fixation with multiproduct paradigm. It also depicts the sustainability of microalgal biorefineries over single product strategies. In order to understand the commercial dormancy of current microalgae cultivation technologies, the existing cultivation systems and process engineering strategies were also discussed. **Chapter 3** describes the stepwise study comprising

TH-2951_166106019

sampling, screening and isolation of potential CO_2 tolerant strain. Further, it deals with the characterization of the isolated strain under different physicochemical parameters. **Chapter 4** demonstrates the microalgal biorefinery approach for production of bioactive molecules, biofuel, and biofertilizer using *Tetradesmus obliquus* CT02. The concept of biorefinery with multiple products has been demonstrated in two sequential steps resulting in alternate product cascades: option-1 being bioactive molecules and biodiesel or option-2 being bioactive molecules and biofertilizer. **Chapter 5** reports the stepwise development of a process engineering strategy which offered improved biomass titer and CO_2 sequestration ability even under fluctuating environmental condition at large scale outdoor cultivation. The basic premise of the process engineering strategy was that the pH of the culture is maintained at its optimal value via cascade control with CO_2 feeding. **Chapter 6** comprises the overall conclusion and summarizes key research highlights obtained from the present study.

References

1. Al-Mamoori, A., Krishnamurthy, A., Rownaghi, A. A., & Rezaei, F. (2017). Carbon capture and utilization update. Energy Technology, 5(6), 834-849.
2. Cheng, J., Zhu, Y., Zhang, Z., & Yang, W. (2019). Modification and improvement of microalgae strains for strengthening CO2 fixation from coal-fired flue gas in power plants. Bioresource technology, 291, 121850.
3. Difusa, A., Talukdar, J., Kalita, M. C., Mohanty, K., & Goud, V. V. (2015). Effect of light intensity and pH condition on the growth, biomass and lipid content of microalgae *Scenedesmus* species. Biofuels, 6(1-2), 37-44.
4. Ferreira, A., Ribeiro, B., Ferreira, A. F., Tavares, M. L., Vladic, J., Vidović, S., ... & Gouveia, L. (2019). *Scenedesmus obliquus* microalga-based biorefinery–from brewery effluent to bioactive compounds, biofuels and biofertilizers–aiming at a circular bioeconomy. Biofuels, Bioproducts and Biorefining, 13(5), 1169-1186.

TH-2951_166106019

5. Goswami, G., Sinha, A., Kumar, R., Dutta, B. C., Singh, H., & Das, D. (2019). Process engineering strategy for cultivation of high density microalgal biomass with improved productivity as a feedstock for production of bio-crude oil via hydrothermal liquefaction. Energy, 189, 116136.
6. Kothari, R., Pandey, A., Ahmad, S., Kumar, A., Pathak, V. V., & Tyagi, V. V. (2017). Microalgal cultivation for value-added products: a critical enviro-economical assessment. 3 Biotech, 7(4), 1-15.
7. Lindsey, R. (2020). https://www.climate.gov/news-features/understanding-climate/climate-change-atmospheric-carbon-dioxide.
8. Patil, L., & Kaliwal, B. (2017). Effect of CO 2 concentration on growth and biochemical composition of newly isolated indigenous microalga *Scenedesmus bajacalifornicus* BBKLP-07. Applied biochemistry and biotechnology, 182(1), 335-348.
9. Pavlik, D., Zhong, Y., Daiek, C., Liao, W., Morgan, R., Clary, W., & Liu, Y. (2017). Microalgae cultivation for carbon dioxide sequestration and protein production using a high-efficiency photobioreactor system. Algal research, 25, 413-420.
10. Qiu, R., Gao, S., Lopez, P. A., & Ogden, K. L. (2017). Effects of pH on cell growth, lipid production and CO2 addition of microalgae *Chlorella sorokiniana*. Algal research, 28, 192-199.
11. Zhao, B., Su, Y., Zhang, Y., & Cui, G. (2015). Carbon dioxide fixation and biomass production from combustion flue gas using energy microalgae. Energy, 89, 347-357.

TH-2951_166106019

Chapter 2

Review of Literature

2.1 CO_2 emission: global crisis and solutions:

The concentration of carbon dioxide in the atmosphere has been increasing at a tormenting rate, mainly due to anthropogenic activities, leading us towards an alarming change in global climate. Recent reports by Intergovernmental Panel on Climate Change (IPCC) have already warned about atmospheric CO_2 concentration crossing 400 ppm which is quite beyond safety level (350 ppm) [Rahman et. al., 2017]. The key contributor to this situation is the increasing demand for technology due to population inflation. In 2019, 92% of the United States' overall anthropogenic emission of CO_2 was contributed by the combustion of fossil fuels (U.S. Energy Information Administration, 2019). Owing to this, the drastic increase in the earth's temperature has turned detrimental to the living ecosystem (Fig. 2.1) [Oh et. al., 2010]. The worldwide issue of global warming has a certain adverse impact on the health of living organisms [Lacetera et. al., 2019], availability of freshwater [Ferguson et. al., 2018], agriculture, and other socioeconomic factors.

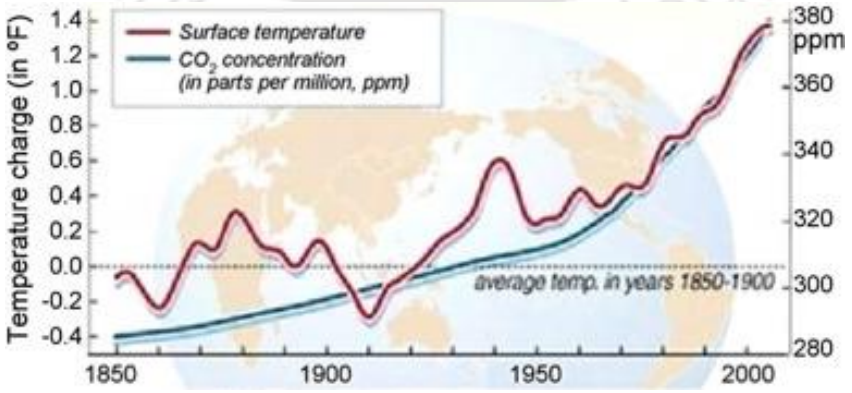

Fig. 2.1. The correlation between CO_2 concentrations in the atmosphere and the earth's surface Temperature [Oh., 2010].

TH-2951_166106019

According to the Global Carbon Project, the annual cumulative CO_2 emission has reached 34.8 gigatonnes in the year 2020, of which India has contributed 2.4 gigatonnes as the third most CO_2 emitter in the world (Fig 2.2).

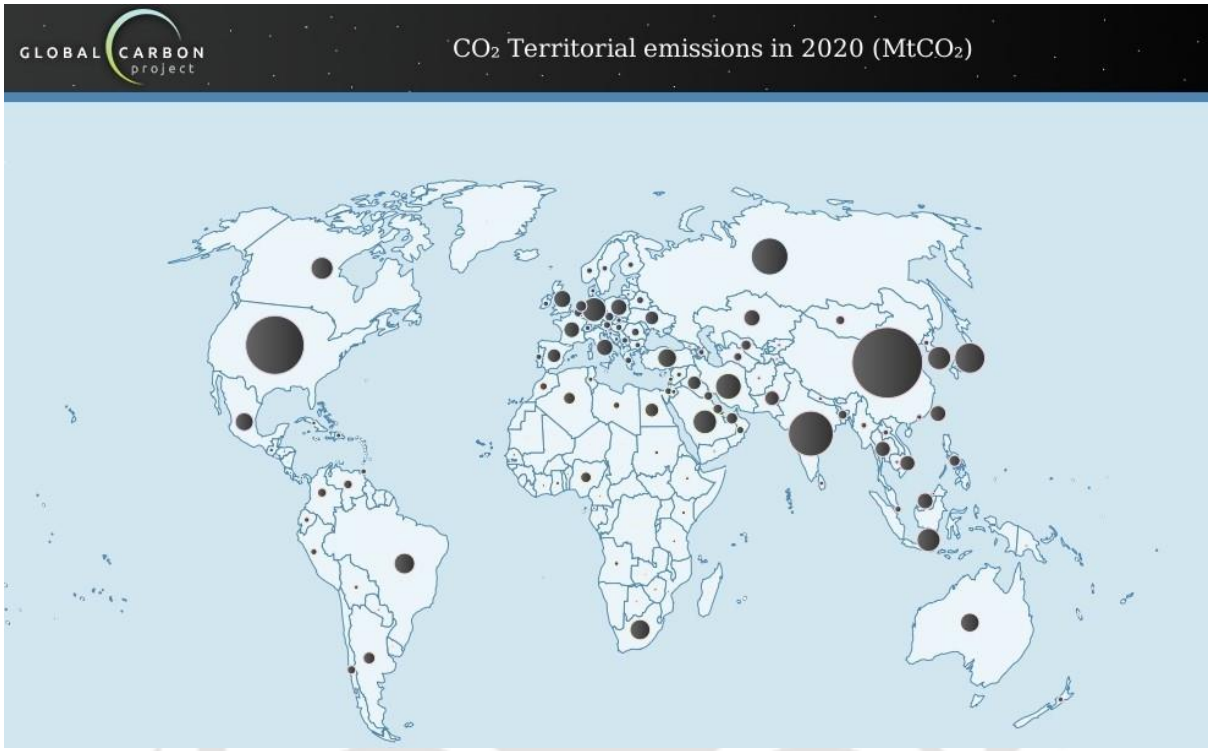

Fig. 2.2. Country-wise distribution of CO_2 emission [Global carbon atlas, 2020].

The situation has enforced the whole scientific community to search for economically and environmentally suitable CO_2 capture methods. Current science has been focusing on three broad strategies for reducing CO_2 emission: (i) Use of less carbon-intensive fuels, (ii) improved efficiency of energy products, and (iii) CO_2 sequestration from the direct environment [Shukla et. al., 2010]. Carbon capture technologies primarily involve the selective removal of CO_2 released from various industrial and energy sectors. Traditional concepts used for this purpose are precombustion: CO_2 removal of carbon before combustion; post-combustion: CO_2 removal from the off-gases post energy utilization; oxy-fuel combustion: Combustion in presence of oxygen which forms CO_2 and water, eliminates the requirement of CO_2 separation [Yaashikaa et. al., 2019]. Several CO_2 capture strategies(CCS) have been designed and regularly been utilized by the industries according to specific needs (Fig. 2.3). However, techno-economic

TH-2951_166106019

analysis of most of the current technologies revealed them as high energy-intensive processes, causing commercial infeasibility. For example, Absorption, despite being well-established process, have unavoidable and high energy requirements for solvent regeneration [Al-Mamoori et. al., 2017].

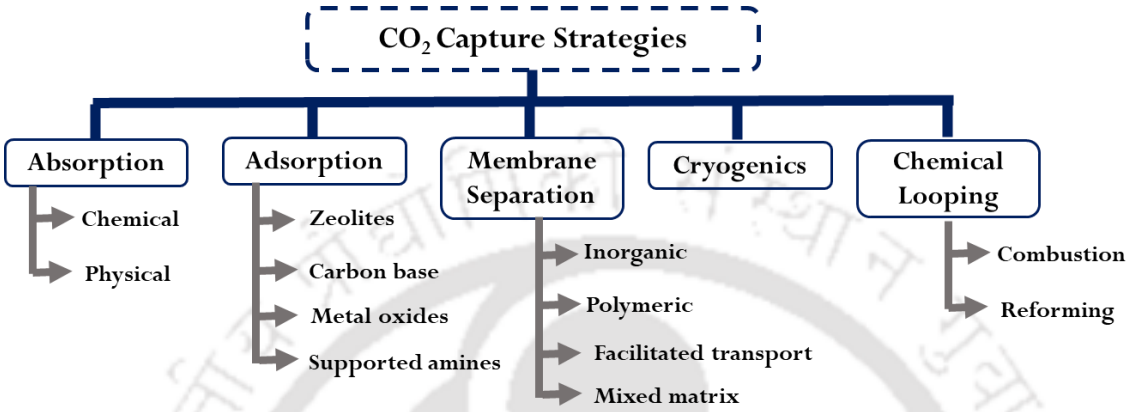

Fig. 2.3. Typical classification of current CCS technologies adopted by various Industries [Wilberforce et. al., 2019; Al-Mamoori et. al., 2017].

In contrast to the conventional methods, biological CCS through microbial cell factories offer efficient output without complex or energy-intensive chemical methods. The diverse range of microbes found to have CO_2 sequestration capability and explored for their expediency at a commercial scale. Microalgae are one of the most prominent amongst them, which utilizes photosynthetic machinery for the reduction of CO_2. These unicellular eukaryotes proved to exhibit ten times higher photosynthetic efficiency than terrestrial plants, resulting in enhanced growth rate and biomass productivity [Pires et. al., 2019]. However, to exploit the organism on commercial platforms, rigorous research, and careful process design are essential.

2.2. Microalgae: a sustainable cell factory

Microalgae are aquatic microorganisms with high photosynthetic efficiency and a faster growth rate. Their ease of cultivation and wide range of production capabilities have largely attracted the scientific community. These unicellular organisms have been found to naturally grow at various habitats like ponds, lakes, oceans, and even wastewater streams. As per the broad

TH-2951_166106019

classification, three types of microalgae i.e. Chlorophyta (green algae), Phaeophyta (brown algae), and Rhodophyta (red algae) are commonly found in nature [Khan et. al., 2018]. The simpler nutritional requirements than most microbial communities and the high tolerance to a wide range of pH, temperature, and salinities [Barsanti et. al., 2008]. Moreover, the vast pool of macromolecules present in microalgal cells can be realized through their multiproduct paradigm. Current science has already been able to utilize the organism for the production of high-value bioactive molecules (pharmaceuticals, health supplements, nutraceuticals), mid-value products (food supplements, cosmetic products), and low-value products (biofuels, biofertilizer, bioplastics) (Fig. 2. 4). The study revealed that the capacity of microalgae to make stable isotopes such as 13C, 15N, and 2H as part of algal biomass, drive their ability to generate an extensive range of products [Rizwan et. al., 2018]. Based on these facts, the commercialization of microalgae as a cell factory has been rigorously debated.

Fig. 2.4. An end-to-end technology for utilization of microalgae as a cell factory for CO_2 sequestration and Bioproduction

2.2.1. Microalgae based CO_2 sequestration:

The application of photosynthetic microorganisms for the biological sequestration of CO_2 is a promising approach attributed to the capability of these microorganisms to transform CO_2 into biomass, which in turn can be subsequently converted into various value-added products. Several cyanobacteria and microalgae such as *Synechococcus*, *Spirulina*, *Scenedesmus*,

TH-2951_166106019

Rhodobacter, *Monoraphidium*, *Emiliania*, *Chlorella*, *Chlamydomonas*, *Botryococcus*, *Anacystis*, and so on, have been studied for biological CO_2 sequestration [Tripathi et. al., 2015]. Most microalgal species are decorated to utilize bicarbonate, a form of dissolved inorganic carbon, which works as a supplier of CO_2 for the Calvin cycle during photosynthesis [Azov et. al. 1982]. During this event, the bicarbonate (HCO_3^-) ion dehydrates to produce CO_2 which further helps Ribulose-1,5-biphosphate carboxylase (RuBisCo) to reduce the counterproductive oxygenase activity.

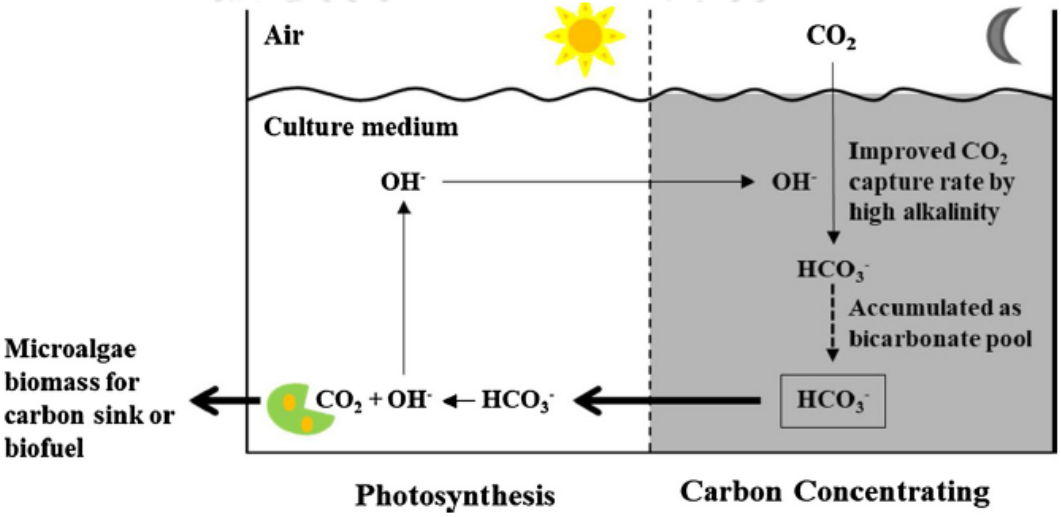

Fig. 2.5. Mechanism of the bicarbonate pool's role in the efficient capture of CO_2 from the air and rapid carbon supply for photosynthesis [Zhu et. al., 2020].

This carbon concentrating mechanism (Fig. 2.5) drives the CO_2 fixation efficiency of the organism through the continuous utilization of bicarbonate ions produced by the speciation of CO_2 in water. Also, this event leaves hydroxyl ions in the media, causing an increment in culture pH. In this state, the on-demand CO_2 input can rebuild the equilibrium between carbonaceous compounds in the culture and bring down the pH to an optimal level. To that end, the on-demand CO_2 injection based on culture pH can be a perfect response to balance the growth and biosequestration of CO_2 [Pawlowski et. al., 2014]. This strategy also ensures maximum utilization of input gas abating the re-emission of CO_2 back to the environment. Furthermore, the CO_2 fixation rate of the individual microalgal strains was observed to be

TH-2951_166106019

strongly affected by physicochemical parameters like input CO_2 concentration, airflow rate, mass transfer and mixing, incident light intensity, light/dark cycle length, culture pH, and temperature. [Cao et. al., 2019, Gendy et. al, 2013]. Yadav et. al., 2015 studied the effect of varying CO_2 concentrations in CO_2-air and flue gas-air mixtures on *Chlorella* sp. The species was reported to tolerate up to 5% v/v of CO_2 and could overcome the toxicity of flue gas under approaches like high initial biomass concentration, leading to an enhancement in the bio sequestration efficiency by 54% and an increment in biomass titer by 21-36%. Authors have reported that strains of microalgae isolated from locations having abundant content of limestone or carbonate are efficient candidates for CO_2 fixation [Tripathi et. al., 2015].

2.2.2. Microalgal based biorefinery:

Microalgae have drawn enough attention as a substrate for biofuel production to tackle the emergency of exhaustion of natural non-renewable energy reserves, global climate transformation, and energy crisis. However, the investments made towards operational and capital expenses for the production of microalgal biofuel overwhelmingly exceed the economic outcome of the process, questioning the economic viability of such processes [Subhash et. al., 2021]. To that end, processes are being designed to co-produce and recover value-added compounds from microalgal biomass, to achieve economic viability in commercialization. Microalgal biorefineries are being established to produce an array of value-added products carbohydrates, lipids, proteins, pigments, antioxidants as well as biofuels, biofertilizers, bioplastics, thus making the process techno-economically viable and sustainable. The fundamental principle of a biorefinery stands comparable to the conventional petroleum refinery in the way that microalgal biomass is transformed into high-value compounds and fuels. The conventional petroleum refinery is distinguished from the biorefinery based on the application of crude oil or microalgal biomass as raw feedstock, and the technology involved [Chew et. al., 2017]. Furthermore, microalgae-based biorefinery can be largely benefited as the

TH-2951_166106019

cultivation process can facilitate environmental remediation like CO_2 sequestration and wastewater treatment. Fig. 2.6 depicts a schematic for circular bioeconomy integrating the environmental remediation with multiproduct generation. The lesser cultivation requirements of microalgae like atmospheric CO_2 as carbon source, commercial-grade nitrogen, and phosphate sources, and sunlight as the sole energy source makes the process cost-effective than any other microbial community, hence more acceptable to the industrial standards. Also, microalgal species are well-characterized for their ability to propagate on degraded land, hence do not compete against food crops for the requirement of fertile land area. Moreover, the ability of microalgal biomass to sequester the environmental carbon dioxide originating from industrial flue-gases and off-gases aids in cutting down the atmospheric greenhouse gas concentration [Chew et. al., 2017]. In a nutshell, microalgal biomass is a futuristic potential reservoir for renewable energy owing to its photosynthetic characteristics that drive bio-energy production efficacies.

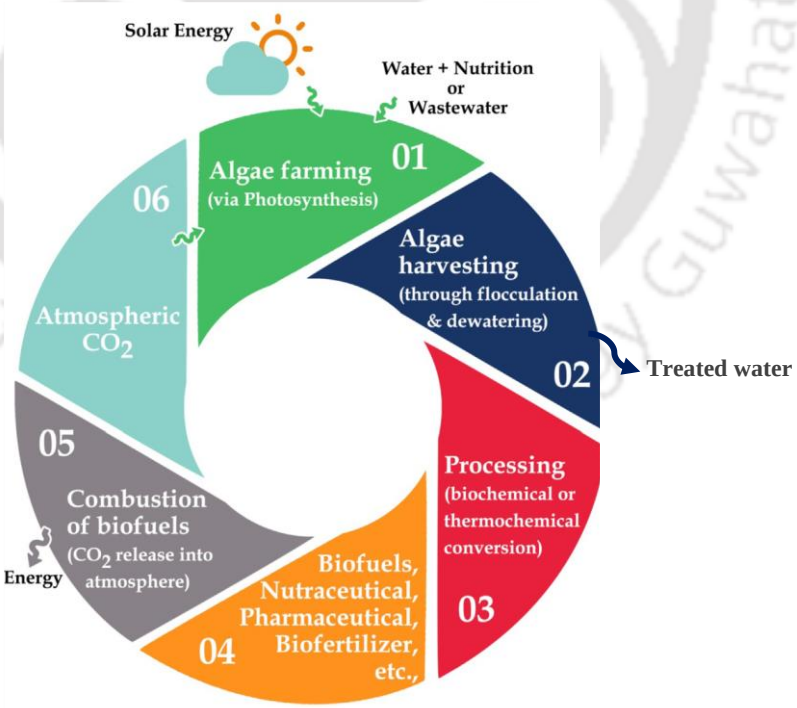

Fig. 2.6. A schematic of integrated microalgal biorefinery coupled with wastewater treatment and CO_2 sequestration [SundarRajan et. al., 2019].

TH-2951_166106019

A concept biorefinery demonstrated for *Scenedesmus* sp. have utilized wastewater for microalgal growth and subsequent production of bioactive products like phenols, flavonoids, different biofuels like biohydrogen and bio-oil, and biofertilizer [Ferreira et. al., 2019]. Another study exploited the microalgal biomass to produce to high value omega-3 fatty acids (especially eicosapentaenoic acid), and the residual biomass post-extraction have been sequentially used for biodiesel and biohydrogen production [Nobre et. al., 2013].

A typical microalgal biorefinery can be divided into major sections namely, upstream and downstream processing. The efficiency of upstream processing is affected by four crucial parameters, especially, the light source, choice of phosphorous and nitrogen substrates, carbon dioxide availability [Muthuraj et. al., 2015; Gonçalves et. al., 2016; Difusa et. al., 2015], and the microalgal strain. On the other hand, the choice of the downstream processing steps, employed towards the recovery and purification, play a crucial role in determining the quality and value of the finally extracted compounds from the microalgal biomass. The choice of the technologies for the implementation of the upstream and downstream processes is imperative to be implemented in such a way that the overall process cost is justifiable against the value of the final product, with minimum energy utilization, thus making the biorefinery sustainable.

2.3. Microalgal product paradigm

Global imbalance of supply and demand has driven the search for natural sources of several essential products. Immense efforts are made every day to understand and manipulate the biological systems for various production purposes. To that end, microalgae have repeatedly been evidenced as the perfect cell factory for multiproduct generation (Fig.2.7).

TH-2951_166106019

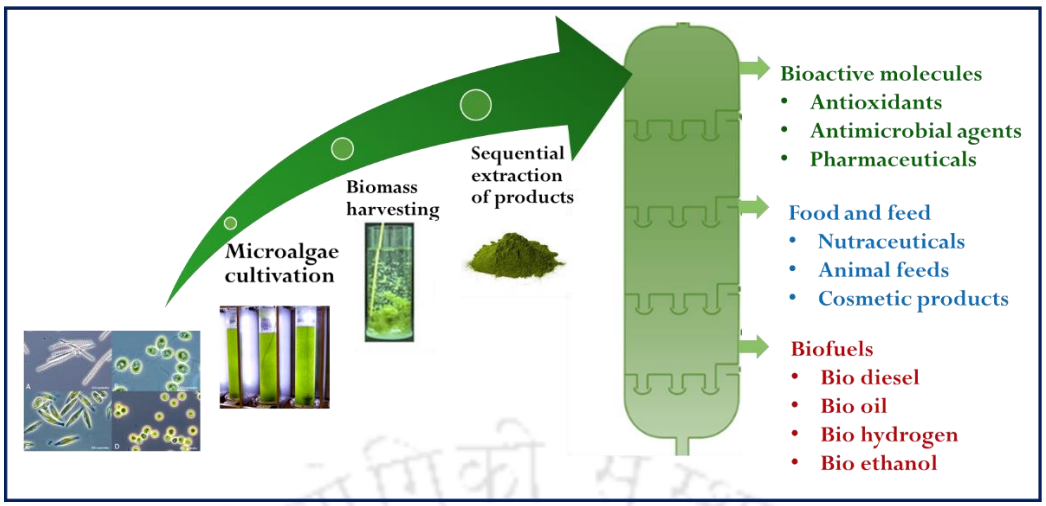

Fig. 2.7. A typical process flow in microalgal biorefinery with the common range of products.

2.3.1. Bioactive molecules:

Microalgal biomass is well-known for its potential to produce a wide range of products that find application in a variety of industries including pharmaceuticals. Although proteins, carbohydrates, and lipids are the predominant components of the microalgal biomass, pigments hold comparatively higher significance owing to their pharmaceutical, nutritional, anti-inflammatory, antibiotic, and neuroprotective properties. Pigments from microalgae, such as phycobilins, carotenoids, chlorophylls, play a crucial role in the channelization of energy to maintain the integrity and function of the microalgal cells, harnessing light and facilitating photosynthesis. The pigments such as fucoxanthin, lutein, violaxanthin, astaxanthin, β-carotene, and chlorophylls, find application as ingredients in cosmetics, nutritional supplements, and color-additives, owing to their anti-oxidant properties.

β-carotene is well-known for being a potential anti-oxidant and a precursor for vitamin A. Pourkarimi et. al., 2020 reported that the biomass titer of *Dunaliella salina* and the production of β-carotene thereof, are predominantly influenced by factors like illumination intensity, temperature, and salinity. Luo et. al., 2021 reported the application of exogenous addition of molybdenum disulfide nanoparticles in the cultures of *Dunaliella salina*, which resulted in 1.33- and 1.48-fold increments in biomass titer and β-carotene production, respectively.

TH-2951_166106019

Fucoxanthin, a pigment of the carotenoid family, is well recognized for its anti-cancer properties. The pigment has been reported to stimulate autophagy, apoptosis, arrest of cell proliferation, and DNA repair mechanisms. Treatment of cancer animal models or cell lines with fucoxanthin has been known to induce angiogenesis, and inhibit invasion and migration resulting from metastasis Méresse et. al., 2020. Using optimized cultivation conditions in an acrylic pipe-based photobioreactor, *Pavlova* sp. OPMS 30543 could produce up to 4.88 mg fucoxanthin L^{-1} day^{-1} in outdoor growth conditions [Kanamoto et. al., 2021].

2.3.2. Fatty acids

Arachidonic acid, ɣ-linolenic acid, DHA, EPA belong to the range of PUFA synthesized by microalgae, which are potential substitutes for fish oil. The synthesis of PUFA through microalgal cultivation is predominantly influenced by the choice of the microalgal strain, and exogenous abiotic parameters like carbon source, temperature, and illumination, since these factors directly play a role in modulating the formation of long-chain fatty acids inside the microalgal cell. The intake of PUFA provides several benefits to health from the perspective of protection against mental anomalies like depression, cognitive disorders, cardiovascular ailments, etc. [Koutra et. al., 2020].

Nannochloropsis oceanica CY2 has been reported to produce 2.38% per DCW of EPA (Eicosapentaenoic acid) in BG11 medium under optimum conditions, where further optimization of the nitrogen source was found to double the content of EPA, and the illumination of the cultures with red LED could further shoot up the EPA production to 5.5% [Chen et. al., 2013]. Authors have reported the production of docosahexaenoic acid (DHA) through the fermentation of crude glycerol originating from the biodiesel industry using a microalgal strain of *Schizochytrium limacinum.* Under optimum conditions of temperature and optimum concentrations of ammonium chloride, ammonium acetate, and trace metals, a maximum titer of 4.91 g L^{-1} d^{-1} of DHA was achieved, along with 22.1 g $L^{-1}$of dry cell biomass

TH-2951_166106019

[Chi et. al., 2007]. Su et. al., 2016 reported the production of 115.47 mg L^{-1} arachidonic acids from a red microalgal species *Porphyridium purpureum*, under optimum aeration rate and the illumination of 3 L min^{-1} and 110 µmol m^{-2} s^{-1}, respectively. For the production of α-linolenic acid from *Chlorella sorokiniana*, the supplementation of acetylcholine could improve the production of α-linolenic acid, total fatty acids, and biomass by 60, 80, and 126%, respectively [Parsaeimehr et. al., 2015].

2.3.3. Biofuels

The extensive usage of fossil fuels has proven to be detrimental to the environment owing to excessive emissions of greenhouse gases and the resulting global warming. The current scenario calls for the need to look for alternative sources of clean energy. At present, there are various clean energy alternatives that are being explored and executed, for example, biofuels derived from living species, offer huge ecological advantages, attributed to the minimized release of noxious greenhouse gases, like carbon dioxide and other hydrocarbon compounds, oxides of sulfur and nitrogen, and consequent reduction of global warming effects. However, the sources or substrates which are currently being utilized for the production of biofuels, are also potential resources for the production of food and other traditional agricultural commodities, giving rise to the popular "food versus fuel" controversy. A probable way to eradicate this issue is to derive biofuels through the cultivation of microalgal biomass, and shifting into the 3rd-generation class of biofuels. Microalgal species can effectively transform carbon dioxide, water, and sunlight into a wide array of products with potential applications as a source of renewable energy. Microalgal species possess huge potential as a host for biofuel production, due to their high-yield and low-input prospective [Shuba et. al., 2018].

Biodiesel is a popular biofuel derived from microalgal biomass well-known for improved fuel characteristics like an engine compatibility, low emission of pollutants resulting from combustion, and high energy density. Biodiesel forms as a result of transesterification of

TH-2951_166106019

triacylglycerols, a form of neutral lipids from microalgal biomass, which in the presence of catalysts or alcoholic cofactors results in the production of fatty acid alkyl esters. Chandra et. al., 2021 reported the production of 1152.37 ± 0.065 mg L^{-1} of lipids using a microalgal consortium for four strains cultivated on dairy wastewater. Fatty acid methyl ester (FAME) characterization of the produced lipid indicated the presence of linolenic acid, linoleic acid, stearic acid, palmitoleic acid, palmitic acid, and myristic acid, confirming its potential to be utilized as biodiesel. A study reported the effect of nutrient starvation on lipid production in *Scenedesmus obliquus* and *Micractinium reisseri*, wherein starvation of iron or phosphorous resulted in a 1.2-fold increment in lipid production from both species, while starvation of nitrogen elevated the lipid accumulation by 1.6-folds and 1.54-folds in *Scenedesmus obliquus* and *Micractinium reisseri*, respectively. Starvation of nitrogen resulted in the accumulation of lipids with greater content saturated fatty acids, making it suitable for biodiesel applications greater oxidative stability, and improved fuel characteristics Srinuanpan et. al., 2018. Microalgal biomass also finds application as a feedstock for the production of biogas through anaerobic digestion. Anaerobic digestion is a potential technology for the production of biofuels as well as the management of organic wastes. A study outlined the production of biogas with a methane content of 91% v/v from microalgae grown in airlift photobioreactors using swine manure as digestate. The produced biogas was reported to have a characteristic lower heating value of 33,294 kJ m^{-3} [Miyawaki et. al., 2021].

Microalgae have also been widely explored for the production of biohydrogen. Hydrogen has been regarded as a potential biofuel owing to its high yield of energy, which is three-times relative to that resulting from common hydrocarbon fuels; augmented with higher cleanliness attributed to the release of water vapor as the sole by-product of its combustion and no emission of greenhouse gases [Koutra et. al., 2020]. Authors have reported biohydrogen yield of 60.6 mL g^{-1} dry biomass through *Enterobacter aerogenes* -mediated dark fermentation of residual

TH-2951_166106019

Nannochloropsis sp. biomass as feedstock, which was left over after the extraction of pigments (70%) and lipids (45 g lipids/100 g dry biomass) [Nobre et. al., 2013]. Moreover, microalgae present a promising platform for the production of bioethanol as compared to the substrates used for first and third-generation biofuel production, since, microalgae-facilitated biofuel production bypasses the requirement for lignocellulosic biomass or edible crops as substrate material. Acid hydrolysis of *Scenedesmus* sp. is has been reported to yield up to 93% sugars, which could subsequently yield up to 86% ethanol through *Saccharomyces cerevisiae*-mediated fermentation [Sivaramakrishnan et. al., 2018]. A study reported the production of 18.57 g L^{-1} bioethanol through the *Saccharomyces cerevisiae*-mediated fermentation of microalgal biomass under optimum conditions of fermentation time (43.6 h), the yeast volume (% v/v) (15.09%), and algal biomass amount (98.7 g L^{-1}) [El-Mekkawi et. al., 2019].

2.3.4. Biofertilizers

Microalgal biomass finds application as fertilizers, owing to their potential to release potassium, phosphorous, and nitrogen. The pattern in which microalgae release these nutrients falls in synchronization with the pattern in which plants demand them. This in turn minimizes the loss of nutrients relative to chemical fertilizers. Microalgae are also known to possess compounds that stimulate plant growth, in addition to anti-fungal substances which protect the plant species from specific fungal infections. Although the potassium, phosphorous, and nitrogen content of microalgal biomass is relatively less as compared to that of chemical fertilizers, still they are potentially more effective owing to their greater content of micronutrients [Koutra et. al., 2020]. Coppens et. al., 2016 reported comparable results in terms of tomato plant growth with the application of commercial and microalgal fertilizers. However, microalgal fertilizers were observed to enhance the qualitative richness of the fruit in terms of elevated carotenoid and sugar contents. Another study reported the application of *Spirulina*

TH-2951_166106019

platensis and *Chlorella vulgaris* as biofertilizers augmented with cow dung manure. The resulting impact of the formulation was assessed on maize plants in greenhouse conditions for 75 days, which led to an improvement in growth characteristics at a primary phase of growth, along with enhanced yield and germination of seeds [Dineshkumar et. al., 2019]. Authors have reported the effect of treating onion plants with a combination of cow dung and *Spirulina platensis* or *Chlorella vulgaris*. These treatments resulted in improved yield and growth characteristics in terms of bulb weight, bulb diameters, bulb length, neck thickness, leaf area, the composition of pigments, total indoles, amino acids, total phenols, total carbohydrates, mineral content, and other non-nutritional factors [Dineshkumar et. al., 2020].

2.3.5. Miscellaneous products

Microalgae are also known to produce extracellular polymeric substances (EPS) to facilitate the adhesion of cells and sustain the cell's viability. EPS are generally composed of lipids, proteins, polysaccharides, and several inorganic and organic constituents, of pharmaceutical significance. Authors have reported an increment in EPS production by 3.4-fold in *Porphyridium sordidum* and 1.2-fold in *Porphyridium purpureum* under the optimized intensity of white light, and concentrations of calcium chloride, sodium chloride, and potassium dihydrogen phosphate [Medina-Cabrera et. al., 2020]. Another important product synthesized by microalgae is vitamin E (tocopherols), which are fat-soluble bioactive compounds possessing antioxidant properties. They are known to play a crucial in the electron transport chain and maintain the stability of the cell membrane from the perspective of fluidity and permeability. *Nannochloropsis oculata* have been reported to produce up to 2325.8 ± 39 μg g^{-1} DCW of tocopherol with sodium nitrate as a nitrogen source in the medium [Durmaz, et. al, 2007]. Microalgae also produce sterols, which are well-recognized for their role in improvising cardiovascular health owing to their ability to reduce LDL blood cholesterol. Sterols are also known to possess anti-atherogenic, anti-oxidative, anti-cancer, and anti-inflammatory

TH-2951_166106019

properties. *Pavlova lutheri* could synthesize high concentrations of sterols (chondrillasterol, dihydrochondrillasterol, fungisterol, methylergostenol, epicampesterol, and poriferasterol) when exposed to 100 mJ m^{-2} of UV-C radiation [Ahmed et. al., 2017].

2.4. Microalgae cultivation: process and challenges:

The faster growth rate and ease of cultivation at minimal nutritional requirements have already established microalgae as a choice of organism for environmental remediation and different production purposes. However, the commercial scale production technologies get hindered owing to low biomass titer and productivity incurring higher operational cost [Chen et. al., 2021]. Technoeconomic analysis of various pilot scale projects have repeatedly reported low feasibility of commercialization. Hence, redesigning the microalgal cultivation process is the need of the hour.

2.4.1 Microalgae cultivation systems

Large scale cultivation of microalgae necessitates the selection of an optimally designed photobioreactor satisfying the specific growth requirements of the microalgal strain. These include the maintenance of certain physicochemical parameters such as temperature, pH, and agitation (in order to achieve a homogenous suspension eliminating concentration and temperature or pH gradients), and so on. The selection of an optimum photobioreactor design configuration relies on the process requirement.

Most microalgae cultivation systems practise two fundamental classes of photobioreactors available are closed and open type photobioreactors. The open-type culture systems possess direct interaction with the external environment. Examples include inclined-surface systems (thin-layer), paddle wheel driven raceway systems, tanks and synthetic ponds [Kumar et. al., 2015]. In contrast to these, the closed type photobioreactors like flat panels, tubular loops, and bubble columns are characterised by possessing no interaction with the external environment [Zuccaro et. al., 2020]. Open photobioreactors offer several advantages over the closed ones,

TH-2951_166106019

with respect to the ease of cleaning, continuous release of the oxygen produced directly into the environment preventing excessive build-up, evaporation-driven self-cooling, direct sunlight availability, and low-cost fabrication and set-up. However, open systems have several associated shortcomings as well. For instance, their operation relies to a greater extent on the climate or weather conditions, require larger amount of space or area than the closed reactors, and greater vulnerability to possible contamination by other microbes. In general, open systems offer very restricted control over contamination and other culture parameters, owing to which their application gets limited to few specific species of microalgae, including *Nannochloropsis*, *Scenedesmus*, *Chlorella*, *Dunaliella*, *Arthrospira*, etc., which are characteristically robust in nature [Acién et. al., 2017]. On the other hand, closed systems offer a culture environment with contamination-free and better controlled conditions, thus extending their usage to a broader range of microalgal species, including *Porphyridium* sp., *Isochrysis* sp., *Haematococcus* sp., etc. [Acién et. al., 2017].

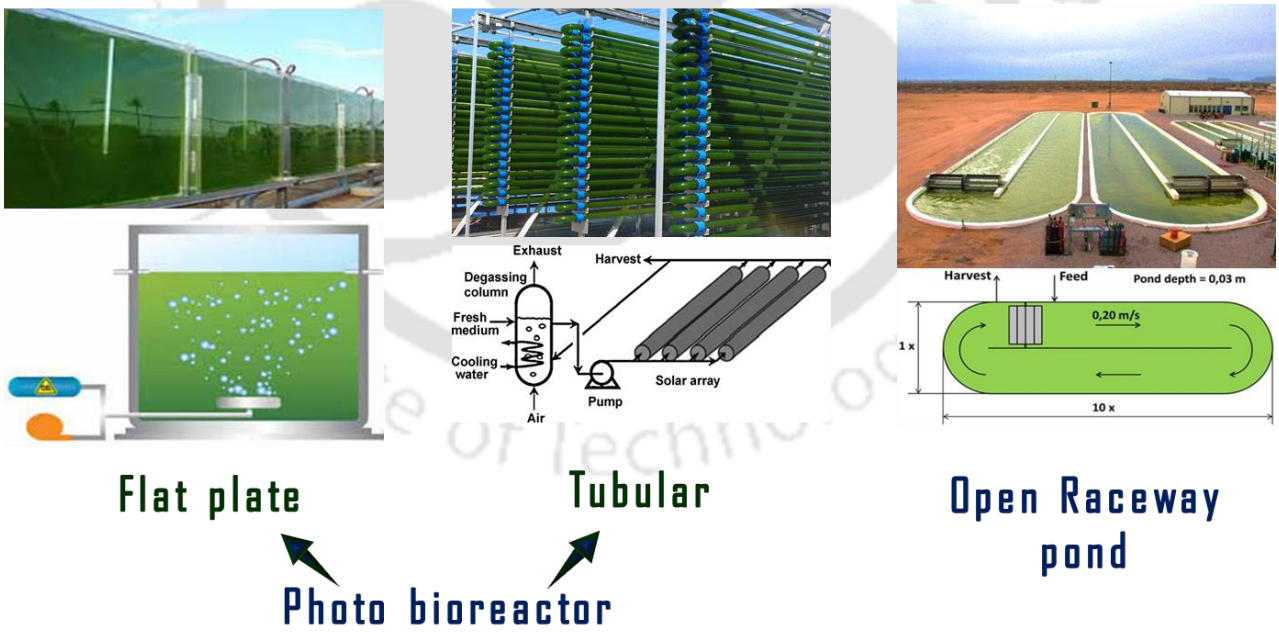

Fig. 2.8. Typical cultivation systems used for commercial scale production of microalgal biomass.

TH-2951_166106019

In case of open systems, **raceway ponds** have gained popularity owing to their economic viability for the large-scale production of microalgal biomass. Raceway cultivation systems are mainly characterised by their overall area which generally varies between 100 and 5000 sq. meter, while systems larger than this are demonstrated by increasing the total number of raceway ponds. The cumulative area of the raceway systems is segregated into 2 to 4 different channels for facilitating the recirculation of the culture. The channel length is varied proportionally in accordance with the channel width, whereby, the length-to-width ratios are varied between range of 10 to 20. Lower ratios of channel length to width, and lesser bend numbers, are known to decrease head losses. The depth of the channels for raceway systems are maintained within a limit of 0.2 to 0.4 meters. This limitation on the channel depth is attributed to the fact that the titre of the biomass in the culture and the availability of light to the cells inside the bulk medium, depend inversely on the depth of the channel [Acién et. al., 2017]. As the open raceway systems are exposed to the external environment, the biomass productivity is liable to get affected by the variations in external parameters such as temperature. Ryu et. al., 2019 reported the application of waste streams from industries as a source of heat (using a heat exchanger) to maintain the consistency in temperature throughout the year. This led to 44% increase in biomass productivity, coupled with 95% improvement in economic viability. Authors have drawn a comparison between different types of culture systems for microalgae, such as, closed photobioreactors, open raceway systems and a hybrid two-phase system, where, the production of biomass is carried out in closed airlift bioreactors, and the induction of lipid synthesis is carried out in open raceway systems [Narala et. al., 2016]. Such hybrid systems have not only proved to eradicate the problem of culture contamination during growth phase, but also have aided in achieving higher lipid productivity as compared to either of these systems operated alone. Authors have reported the application of alternatively permutated conic baffles inside open raceway systems in order to induce vortex flow to

TH-2951_166106019

enhance mass transfer and mixing. The installation of these baffles led to 48.1% reduction in mixing time, 34% increment in mass transfer, which in turn caused 39.6% enhancement in the productivity of *Spirulina* biomass [Cheng et. al., 2018].

One of the prevalent kinds closed systems for large-scale production of microalgal biomass are the **tubular photobioreactors**, generally fabricated out of plastic or glass tubing within which the circulation of the culture is facilitated either by gaseous streams in airlift mode or via pumps. The surface area-to-volume ratio in case of tubular systems is about 80 m^{-1}, facilitating the maintenance of high-density cultures [Acién et. al., 2017]. These systems are fabricated from transparent tubes having approximate diameter of 7 to 10 cm. The dimensions of the tube in terms of diameter and length are a critical parameter which can aid in alleviating the build-up of oxygen and decreasing the head loss in the reactor [Camacho-Rubio et. al., 1999]. The angle at which the tube faces the sunlight in chosen in such a way that light is captured efficiently while simultaneously curtailing radiation on adjacent tubes.

TH-2951_166106019

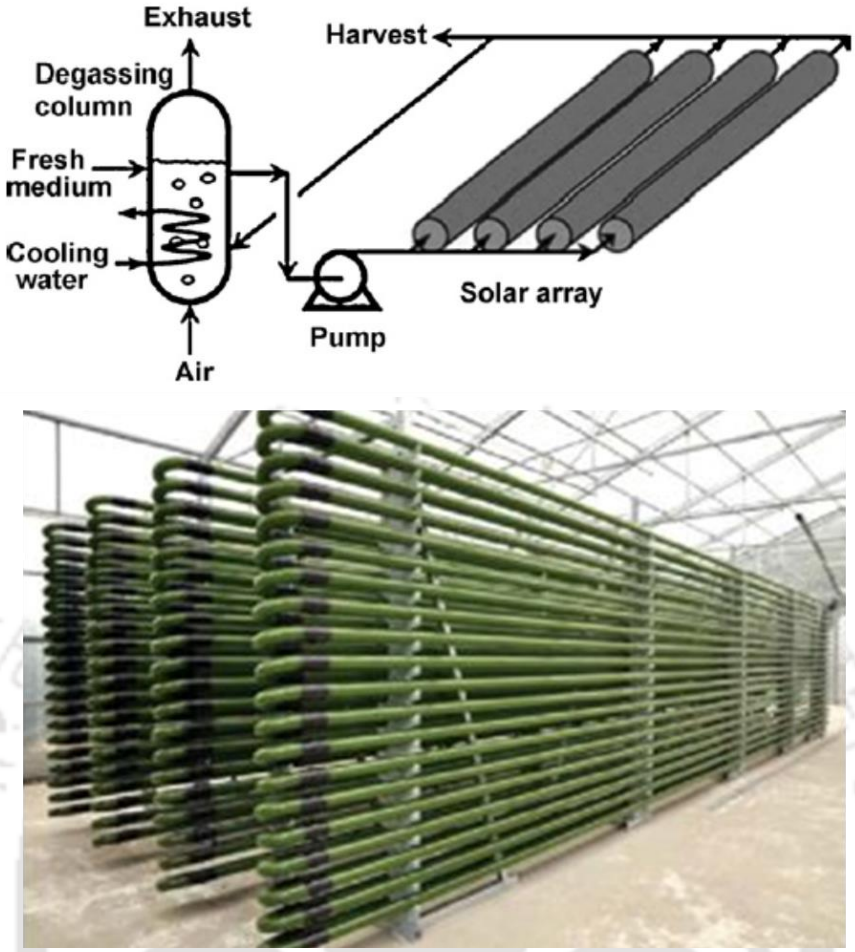

Fig. 2.9. Tubular photobioreactor and its process flow diagram used for pilot scale cultivation of microalgae [Singh et. al., 2012].

Despite of these measures, excessive heat might be captured by the biomass in the absence of an appropriate temperature control system. To overcome this, tubular systems are sometime cooled down by spraying water on the surface of the tube, or by arranging the tubes in an overlapping manner to create shade, or by submerging the tube in thermally controlled water bath. The typically designed tubular system comprise of a photostage loop and a mixing tank (Fig 2.9). The photostage loop is the portion of the reactor which houses photosynthesis and the production of algal biomass, while the mixing tank is the region which facilitates the elimination of oxygen and regulates the influential culture conditions [Acien Ferna´ndez et. al., 2001].

TH-2951_166106019

Out of different closed tubular systems, one primitive type is the **serpentine photobioreactors**. Their structure comprises of flat loops made up of straight tubes joined through U-shaped curved tubes. These tubes may be aligned either horizontally or vertically. Addition of nutrients and exchange of gases are carried out in a different container. Generally, a gaseous stream-induced airlift or a pump is used to maintain the circulation of the culture at a rate of 0.2-0.3 ms^{-1} [Fernandez-Sevilla et. al., 2010].

Manifold photobioreactors and **helical photobioreactors** are examples of some other closed tubular systems. Manifold reactors comprise of sequentially arranged tubes in parallel manner, and joined at their either terminal by two separate manifolds. One of the manifold aids in the distribution, while the other manifold facilitates withdrawal of the cultivated biomass. Manifold reactors are advantageous over serpentine systems attributed to decreased head loss, and lesser oxygen build-up, thereby encouraging industrial scale application [Tredici et. al., 2010]. Helical bioreactors comprise of low-diameter elastic tubular structures arranged in a helical manner about an erect auxiliary support [Richmond et. al., 2013].

Flat-panel airlift photobioreactors the most efficient and high-capacity closed reactor system, reported to be yielding comparatively higher biomass productivity. These are commonly fabricated out of narrow transparent panels for appropriate exposure to sunlight. Generally, a narrow layer of biomass suspension flows in between two transparent panels arranged parallelly [Carvalho et. al., 2006]. Key advantage to this kind of design is the high surface to vaolume ratio which certainly facilititates a better mixing capacity [Gupta et. al., 2015]. The transparent plates are fabricated out of polyethylene, glass, polymethyl methacrylate, polycarbonate [Acién et. al., 2017]. The two panels are separated by such a distance that the incident light intensity can be continuously available to the maximum number of cells, resulting in high photosynthetic efficiency [Hu et. al., 1998]. Flat panel photobioreactors are advantageous over other systems owing to the fact that they have a large

TH-2951_166106019

surface area to facilitate absorption of solar radiation relative to the culture volume used for the biomass synthesis. Mixing is carried out using pump aided turbulence wherein enhanced mass transfer and reduced oxygen accumulation is obtained by circulating the biomass suspension from an open headspace. Reduced oxygen accumulation can also be achieved by positioning many flat-plates parallelly in a horizontal manner [Acién et. al., 2017].

Barbosa et. al., 2005 reported the production of 2.36 mg g^{-1} β-carotene, 5.65 mg g^{-1} lutein, 0.33 mg g^{-1} vitamin E and 3.48 mg g^{-1} vitamin C, from cultures of *Dunaliella tertiolecta* cultivated in a flat panel photobioreactor. In another study, cultures of *Phaeodactylum tricornutum* were studied for the production of eicosapentaenoic acid (EPA) in a flat panel airlift photobioreactor. At a light illumination of 250 µmol photon m^{-2} s^{-1}, the efficiency of photosynthesis reached 10.6%, while it reduced to 4.8% on increasing the illumination intensity to 1000 µmol photon m^{-2} s^{-1}. However, the volumetric productivity improved by 35% for flat panel photobioreactor operating at higher light intensities, in contrast to bubble column reactors. Biomass productivity of up to 1.04 g L^{-1} d^{-1} were achieved at 1.25% v/v of carbon dioxide, and EPA titres of 5% DCW, and productivity 52 mg L^{-1} d^{-1} were obtained in continuous mode of operation with 16 hours of light phase [Meiser et. al., 2004]. In order to overcome the limitations associated with necessity for energy and cooling in closed photobioreactors, authors have reported a novel kind of flat panel photobioreactor comprising of spectrally-selective insulated glazed photovoltaic (IGP) system [Nwoba et. al., 2020]. IGP has been reported to operate without the provision for cooling water, with significantly higher productivity of biomass as compared to open raceway systems. IGP provided a stress-free environment with respect to temperature, and was capable of generating 2.5-times greater electrical energy relative to the energy expended for mixing, thus demonstrating it to be a stand-alone system for the co-production of electricity and biomass, without any cooling and electricity requirements.

TH-2951_166106019

Table 2.1 Performance of different microalgal species in terms of growth kinetic parameters and CO_2 fixation, during their outdoor cultivation.

Sl. No.	Microalgal species	Cultivation conditions	Biomass productivity (mg L^{-1} day^{-1})	CO2 fixation rate (mg L^{-1} day^{-1})	References
1	*Scenedesmus obliquus* CNW-N	Tubular photobioreactor (60L)	245.8 ± 27.9	430.2 ± 48.8	Ho et. al., 2017
2	*Anabaena* sp. ATCC 33047	Vertical Flat Panel Reactor (350 L)	170 ± 20	250 ± 60	Clares et. al., 2014
3	*Chlorella* sp. NJ-18	Airlift photobioreactor (70 L)	91.8	172.6	Zhou et. al., 2013
4	*Scenedesmus obtusus* XJ-15	airlift bag photobioreactor (140-L)	86.5	170	Xia et. al., 2013
5	*Chlorella vulgaris*	Open raceway pond (60 L)	---	33.79 ± 4.02	Yadav et. al., 2020
6	*Chlorella zofingiensis*	Flat plate photobioreactor (60L)	58.4	109.8	Feng et. al., 2011
7	*Anabaena* sp. ATCC 33047	Open raceway pond (100 L)	50 ± 10	100 ± 20	Clares et. al., 2014

Flat panel photobioreactors have been extensively used for evaluating the influence of optical illumination on microalgal biomass. The thickness of the plates is generally kept within a range of 1 to 3 cm to facilitate homogenous distribution of light inside the bulk culture broth. To guarantee this homogeneity, the applications are restricted to cultures having low biomass density. To this end, authors have reported flat panel reactors with plate thickness as low as a millimetre [Jiang et. al., 2021]. Using numerical design and experimental validation, they could deduce the minimum thickness of the panel which could facilitate the biomass growth without imposing much shear stress. Table 2.1 compares some recent microalgal cultivation studies performed in different open or closed setups under outdoor condition.

TH-2951_166106019

Additionally, there is a class of photobioreactors called the **thin-layer systems**, characterised by usage of thin-layer biomass suspensions to enhance biomass titre and to improve light capture efficacy. Irrespective of the regime of the operation and design of the system, it is imperative to establish the appropriate layer thickness or optical path, density of the culture, pattern of movement of the cells, duration of dark and light phases, regime of mixing and mass transfer. A key design aspect of these reactors is the surface area directly being exposed to the sunlight. Greater the surface area exposed to light, and lower the culture volume, the higher will be the availability of the solar radiation, leading to higher efficacy of photosynthesis and thus biomass productivity [Masojıdek et. al., 2015]. In this context, thin layer systems are superior to raceways or open ponds owing to their larger surface area exposed to sunlight relative to the volume. A vital benefit of thin layer systems is their efficacy of mixing, leading to rapid dark-light cycle of the microalgal culture owing to the smaller path of light within the reactor. The pattern of the dark-light phases conveys significant idea about the photosynthetic efficiency of the cells when the path of light measures less than 1 cm [Zarmi et. al., 2013]. Some recent pilot scale setups have been exploited for high density biomass generation using different microalgal sytrains like *Chlorella fusca* [Malapascua et. al., 2014], *Scenedesmus* sp. [Morales-Amaral et. al., 2015] *Nanochloropsis* sp. [Torzillo et. al., 2010]. Schädler et. al. (2019) demonstrated an open thin-layer cascade photobioreactor system for lipid bio-synthesis using microalgae *Microchloropsis salina*. The process was carried out in two phases in two separate thin-layer photobioreactors operating in cascade, where the microalgal biomass was produced in the first phase and lipid was produced thereof in the second phase. 6.6 g/l of total lipid titre was obtained the photobioreactor cascade was operated in batch mode, whereas, continuous operation resulted in 3 g L^{-1} of total lipids. Moreover, this set-up could aid in achieving 84-87% of CO_2 conversion. Schädler et. al., 2020 reported the operational feasibility of open thin-layer photobioreactors coupled with the recycling of water, with enhanced growth

TH-2951_166106019

performance, and reduced nutrient utilization, and minimal production of wastewater. This study demonstrated repeated water recycling irrespective of high culture of density of *Microchloropsis salina* even at biomass titres greater than 30 g L^{-1} dry cell weight. Another study reported the effect of surface area to volume ratio of a thin layer photobioreactor on the growth characteristics of *Scenedesmus obliquus* [Venancio et al., 2020]. Higher biomass titre (20.14 g L^{-1}) and higher biomass productivity (2.42 g L^{-1} d^{-1}) were obtained at higher surface area to volume ratio of 80 m^{-1}, as compared to the biomass titre (14.60 g L^{-1}) and biomass productivity (1.85 g L^{-1} d^{-1}) obtained at a lower surface area to volume ratio of 60 m^{-1}. However, the same study reported a pattern of increase in CO_2 sequestration with the decrease in surface area to volume ratio.

2.4.2 Process engineering strategies

The key to a successful microalgal production technology lies on the simplicity and economic viability of the process. As discussed earlier, one of the greatest hindrance towards commercialization is low biomass titer and productivity under fluctuating outdoor conditions, which considered to be economical way of microalgal cultivation. To that end, understanding the limiting factors as well as selection of optimal process engineering strategies targeting better biomass growth is mandatory. Efforts are continuously being made in this purpose through upgradation of CO_2 fixation rate, substrate utilization, light availability to cells, mass transfer etc. For instance, growth-based feeding of limiting nutrients and dynamic increase in illumination has been reported to substantially upsurge both biomass titer and productivity in case of *Chlorella* sp. FC2 IITG [Goswami et. al., 2019]. Another study involving various microalgal strains suggested that the optimal aeration to the culture have positive effect on growth and CO_2 utilization performance through betterment in mass transfer [Zhao et. al., 2015]. Salvucci et. al., 2004 have studied the dependency of CO_2 fixation rate on temperature, which has clear impact on growth performance of the microorganism. Study revealed that the

TH-2951_166106019

temperature can cause alteration in activation conditions of RuBisCo, key enzyme involved in photosynthesis. Owing to this fact, the higher photosynthetic efficiency and in turn biomass titer and productivity can be achieved by cultivation under suitable temperature regime. The culture pH, with direct control on solubility of CO_2 and nutrients, stands as one of the most critical factors for the dynamics of microalgal growth [Qiu et. al., 2017]. In addition to that, several reports revealed the effect of pH on cell metabolism which has impact on biomass composition i.e. protein and lipid content [Qiu et. al., 2017; Difusa et. al., 2015]. Researchers have reported the use of submerged membrane contactor to facilitate the delivery of CO_2 sequestered to the microalgal broth using a chemical solvent through a semi-permeable membrane [Xu et. al., 2019]. In this study, reduction in the thickness of the layer supporting the membrane or by-passing the use of the support led to improvement in the mass transfer of CO_2. The application of flat-sheet-type pond liners under optimum conditions led to 90% CO_2 capture efficiency, which is 1.9-times higher than that achieved using hollow-fibre-type arrangement [Xu et. al., 2019]. In a nutshell, development of the process engineering strategies has repeatedly been proved to upregulate the performance of microalgal cultivation, thus a requirement towards improved biomass and product generation.

References

1. Acién, F. G., Molina, E., Reis, A., Torzillo, G., Zittelli, G. C., Sepúlveda, C., & Masojídek, J. (2017). Photobioreactors for the production of microalgae. Microalgae-based biofuels and bioproducts, 1-44.
2. Ahmed, F., & Schenk, P. M. (2017). UV–C radiation increases sterol production in the microalga Pavlova lutheri. Phytochemistry, 139, 25-32.
3. Al-Mamoori, A., Krishnamurthy, A., Rownaghi, A. A., & Rezaei, F. (2017). Carbon capture and utilization update. *Energy Technology*, *5*(6), 834-849.

TH-2951_166106019

4. Azov, Y. (1982). Effect of pH on inorganic carbon uptake in algal cultures. *Applied and environmental microbiology*, *43*(6), 1300-1306.
5. Barbosa, M. J., Zijffers, J. W., Nisworo, A., Vaes, W., Van Schoonhoven, J., & Wijffels, R. H. (2005). Optimization of biomass, vitamins, and carotenoid yield on light energy in a flat-panel reactor using the A-stat technique. Biotechnology and bioengineering, 89(2), 233-242.
6. Barsanti, L., Coltelli, P., Evangelista, V., Frassanito, A. M., Passarelli, V., Vesentini, N., & Gualtieri, P. (2008). Oddities and curiosities in the algal world. In *Algal toxins: nature, occurrence, effect and detection* (pp. 353-391). Springer, Dordrecht.
7. Cao, X., Xi, Y., Liu, J., Chu, Y., Wu, P., Yang, M., ... & Xue, S. (2019). New insights into the CO2-steady and pH-steady cultivations of two microalgae based on continuous online parameter monitoring. *Algal Research*, *38*, 101370.
8. Carvalho, A. P., Meireles, L. A., & Malcata, F. X. (2006). Microalgal reactors: a review of enclosed system designs and performances. Biotechnology progress, 22(6), 1490-1506.
9. Chandra, R., Pradhan, S., Patel, A., & Ghosh, U. K. (2021). An approach for dairy wastewater remediation using mixture of microalgae and biodiesel production for sustainable transportation. Journal of Environmental Management, 297, 113210.
10. Chen, C. Y., Chen, Y. C., Huang, H. C., Huang, C. C., Lee, W. L., & Chang, J. S. (2013). Engineering strategies for enhancing the production of eicosapentaenoic acid (EPA) from an isolated microalga Nannochloropsis oceanica CY2. Bioresource technology, 147, 160-167.
11. Chen, M., Chen, Y., & Zhang, Q. (2021). A Review of Energy Consumption in the Acquisition of Bio-Feedstock for Microalgae Biofuel Production. *Sustainability*, *13*(16), 8873.

TH-2951_166106019

12. Cheng, J., Guo, W., Cai, C., Ye, Q., & Zhou, J. (2018). Alternatively permutated conic baffles generate vortex flow field to improve microalgal productivity in a raceway pond. Bioresource technology, 249, 212-218.
13. Chi, Z., Pyle, D., Wen, Z., Frear, C., & Chen, S. (2007). A laboratory study of producing docosahexaenoic acid from biodiesel-waste glycerol by microalgal fermentation. Process Biochemistry, 42(11), 1537-1545.
14. Coppens, J., Grunert, O., Van Den Hende, S., Vanhoutte, I., Boon, N., Haesaert, G., & De Gelder, L. (2016). The use of microalgae as a high-value organic slow-release fertilizer results in tomatoes with increased carotenoid and sugar levels. *Journal of applied phycology*, *28*(4), 2367-2377
15. Difusa, A., Talukdar, J., Kalita, M. C., Mohanty, K., & Goud, V. V. (2015). Effect of light intensity and pH condition on the growth, biomass and lipid content of microalgae *Scenedesmus* species. Biofuels, 6(1-2), 37-44.
16. Difusa, A., Talukdar, J., Kalita, M. C., Mohanty, K., & Goud, V. V. (2015). Effect of light intensity and pH condition on the growth, biomass and lipid content of microalgae Scenedesmus species. Biofuels, 6(1-2), 37-44.
17. Dineshkumar, R., Subramanian, J., Gopalsamy, J., Jayasingam, P., Arumugam, A., Kannadasan, S., & Sampathkumar, P. (2019). The impact of using microalgae as biofertilizer in maize (Zea mays L.). Waste and Biomass Valorization, 10(5), 1101-1110.
18. Dineshkumar, R., Subramanian, J., Arumugam, A., Rasheeq, A. A., & Sampathkumar, P. (2020). Exploring the microalgae biofertilizer effect on onion cultivation by field experiment. *Waste and Biomass Valorization*, *11*(1), 77-87.

TH-2951_166106019

19. Durmaz, Y. (2007). Vitamin E (α-tocopherol) production by the marine microalgae Nannochloropsis oculata (Eustigmatophyceae) in nitrogen limitation. Aquaculture, 272(1-4), 717-722.

20. El-Mekkawi, S. A., Abdo, S. M., Samhan, F. A., & Ali, G. H. (2019). Optimization of some fermentation conditions for bioethanol production from microalgae using response surface method. Bulletin of the National Research Centre, 43(1), 1-8.

21. Ferguson, C. R., Pan, M., & Oki, T. (2018). The effect of global warming on future water availability: CMIP5 synthesis. *Water Resources Research*, *54*(10), 7791-7819.

22. Fernández, F. A., Sevilla, J. F., Pérez, J. S., Grima, E. M., & Chisti, Y. (2001). Airlift-driven external-loop tubular photobioreactors for outdoor production of microalgae: assessment of design and performance. *Chemical Engineering Science*, *56*(8), 2721-2732.

23. Fernández-Sevilla, J. M., Fernández, F. A., & Grima, E. M. (2010). Biotechnological production of lutein and its applications. *Applied microbiology and biotechnology*, *86*(1), 27-40.

24. Ferreira, A., Ribeiro, B., Ferreira, A. F., Tavares, M. L., Vladic, J., Vidović, S., & Gouveia, L. (2019). *Scenedesmus obliquus* microalga-based biorefinery–from brewery effluent to bioactive compounds, biofuels and biofertilizers–aiming at a circular bioeconomy. Biofuels, Bioproducts and Biorefining, 13(5), 1169-1186.

25. Gendy, T. S., & El-Temtamy, S. A. (2013). Commercialization potential aspects of microalgae for biofuel production: an overview. *Egyptian Journal of Petroleum*, *22*(1), 43-51.

26. Gonçalves, A. L., Rodrigues, C. M., Pires, J. C., & Simões, M. (2016). The effect of increasing CO_2 concentrations on its capture, biomass production and wastewater bioremediation by microalgae and cyanobacteria. Algal research, 14, 127-136.

TH-2951_166106019

27. Goswami, G., Sinha, A., Kumar, R., Dutta, B. C., Singh, H., & Das, D. (2019). Process engineering strategy for cultivation of high density microalgal biomass with improved productivity as a feedstock for production of bio-crude oil via hydrothermal liquefaction. *Energy*, *189*, 116136.
28. Gupta, P. L., Lee, S. M., & Choi, H. J. (2015). A mini review: photobioreactors for large scale algal cultivation. *World Journal of Microbiology and Biotechnology*, *31*(9), 1409-1417.
29. Hu, Q., Kurano, N., Kawachi, M., Iwasaki, I., & Miyachi, S. (1998). Ultrahigh-cell-density culture of a marine green alga Chlorococcum littorale in a flat-plate photobioreactor. *Applied Microbiology and Biotechnology*, *49*(6), 655-662.
30. Jiang, W., Levasseur, W., Casalinho, J., Martin, T., Puel, F., Perre, P., & Pozzobon, V. (2021). Shear stress computation in a millimeter thin flat panel photobioreactor: Numerical design validated by experiments. Biotechnology and applied biochemistry, 68(1), 60-70.
31. Kanamoto, A., Kato, Y., Yoshida, E., Hasunuma, T., & Kondo, A. (2021). Development of a Method for Fucoxanthin Production Using the Haptophyte Marine Microalga Pavlova sp. OPMS 30543. Marine Biotechnology, 23(2), 331-341.
32. Khan, M. I., Shin, J. H., & Kim, J. D. (2018). The promising future of microalgae: current status, challenges, and optimization of a sustainable and renewable industry for biofuels, feed, and other products. *Microbial cell factories*, *17*(1), 1-21.
33. Koutra, E., Tsafrakidou, P., Sakarika, M., & Kornaros, M. (2020). Microalgal biorefinery. In Microalgae Cultivation for Biofuels Production (pp. 163-185). Academic Press.

TH-2951_166106019

34. Koutra, E., Tsafrakidou, P., Sakarika, M., & Kornaros, M. (2020). Microalgal biorefinery. In *Microalgae Cultivation for Biofuels Production* (pp. 163-185). Academic Press.

35. Kumar, K., Mishra, S. K., Shrivastav, A., Park, M. S., & Yang, J. W. (2015). Recent trends in the mass cultivation of algae in raceway ponds. *Renewable and Sustainable Energy Reviews*, *51*, 875-885.

36. Lacetera, N. (2019). Impact of climate change on animal health and welfare. *Animal Frontiers*, *9*(1), 26-31.

37. Luo, S.W., Alimujiang, A., Cui, J., Chen, T.T., Balamurugan, S., Zheng, J.W., Wang, X., Yang, W.D. and Li, H.Y., 2021. Molybdenum disulfide nanoparticles concurrently stimulated biomass and β-carotene accumulation in Dunaliella salina. Bioresource Technology, 320, p.124391.

38. Malapascua, J. R., Jerez, C. G., Sergejevová, M., Figueroa, F. L., & Masojídek, J. (2014). Photosynthesis monitoring to optimize growth of microalgal mass cultures: application of chlorophyll fluorescence techniques. *Aquatic biology*, *22*, 123-140.

39. Masojídek, J., Sergejevová, M., Malapascua, J. R., & Kopecký, J. (2015). Thin-layer systems for mass cultivation of microalgae: flat panels and sloping cascades. In *Algal biorefineries* (pp. 237-261). Springer, Cham.

40. Medina-Cabrera, E. V., Rühmann, B., Schmid, J., & Sieber, V. (2020). Optimization of growth and EPS production in two Porphyridum strains. Bioresource Technology Reports, 11, 100486.

41. Meiser, A., Schmid-Staiger, U., & Trösch, W. (2004). Optimization of eicosapentaenoic acid production by Phaeodactylum tricornutum in the flat panel airlift (FPA) reactor. Journal of applied phycology, 16(3), 215-225.

TH-2951_166106019

42. Méresse, S., Fodil, M., Fleury, F., & Chénais, B. (2020). Fucoxanthin, a marine-derived carotenoid from brown seaweeds and microalgae: A promising bioactive compound for cancer therapy. International Journal of Molecular Sciences, 21(23), 9273.

43. Miyawaki, B., Mariano, A. B., Vargas, J. V. C., Balmant, W., Defrancheschi, A. C., Corrêa, D. O., ... & Kava, V. M. (2021). Microalgae derived biomass and bioenergy production enhancement through biogas purification and wastewater treatment. *Renewable Energy*, *163*, 1153-1165..

44. Morales-Amaral, M.M., Go´mez-Serrano, C., Aci?en, F.G., Fernandez-Sevilla, J.M., Molina-Grima, E., (2015). Outdoor production of Scenedesmus sp. in thin-layer and raceway reactor using generated from anaerobic digestion as the sole nutrient source. *Algal Research*. 12, 99–108.

45. Muthuraj, M., Chandra, N., Palabhanvi, B., Kumar, V., & Das, D. (2015). Process engineering for high-cell-density cultivation of lipid rich microalgal biomass of *Chlorella* sp. FC2 IITG. Bioenergy Research, 8(2), 726-739.

46. Narala, R. R., Garg, S., Sharma, K. K., Thomas-Hall, S. R., Deme, M., Li, Y., & Schenk, P. M. (2016). Comparison of microalgae cultivation in photobioreactor, open raceway pond, and a two-stage hybrid system. Frontiers in Energy Research, 4, 29

47. Nobre BP, Villalobos F, Barragán BE, Oliveira AC, Batista AP, Marques PASS *et al*., A biorefinery from Nannochloropsis sp. microalga – extraction of oils and pigments. Production of biohydrogen from the leftover biomass. *Bioresour Technol* **135**:128–136 (2013).

48. Nwoba, E. G., Parlevliet, D. A., Laird, D. W., Alameh, K., & Moheimani, N. R. (2020). Pilot-scale self-cooling microalgal closed photobioreactor for biomass production and electricity generation. Algal Research, 45, 101731.

49. Oh, T. H. (2010). Carbon capture and storage potential in coal-fired plant in Malaysia—A review. *Renewable and Sustainable Energy Reviews*, *14*(9), 2697-2709.

TH-2951_166106019

50. Parsaeimehr, A., Sun, Z., Dou, X., & Chen, Y. F. (2015). Simultaneous improvement in production of microalgal biodiesel and high-value alpha-linolenic acid by a single regulator acetylcholine. Biotechnology for biofuels, 8(1), 1-10.
51. Pawlowski, A., Mendoza, J. L., Guzmán, J. L., Berenguel, M., Acién, F. G., & Dormido, S. (2014). Effective utilization of flue gases in raceway reactor with event-based pH control for microalgae culture. *Bioresource technology*, *170*, 1-9.
52. Pires, J. C. M., & da Cunha Gonçalves, A. L. (Eds.). (2019). *Bioenergy with carbon capture and storage: using natural resources for sustainable development*. Academic Press.
53. Pourkarimi, S., Hallajisani, A., Alizadehdakhel, A., Nouralishahi, A., & Golzary, A. (2020). Factors affecting production of beta-carotene from Dunaliella salina microalgae. Biocatalysis and Agricultural Biotechnology, 29, 101771.
54. Qiu, R., Gao, S., Lopez, P. A., & Ogden, K. L. (2017). Effects of pH on cell growth, lipid production and CO_2 addition of microalgae Chlorella sorokiniana. Algal research, 28, 192-199.
55. Rahman, F. A., Aziz, M. M. A., Saidur, R., Bakar, W. A. W. A., Hainin, M. R., Putrajaya, R., & Hassan, N. A. (2017). Pollution to solution: Capture and sequestration of carbon dioxide (CO2) and its utilization as a renewable energy source for a sustainable future. *Renewable and Sustainable Energy Reviews*, *71*, 112-126.
56. Richmond, A., & Hu, Q. (2013). *Handbook of microalgal culture: applied phycology and biotechnology*. John Wiley & Sons.
57. Rizwan, M., Mujtaba, G., Memon, S. A., Lee, K., & Rashid, N. (2018). Exploring the potential of microalgae for new biotechnology applications and beyond: a review. *Renewable and Sustainable Energy Reviews*, *92*, 394-404.
58. Rubio, F. C., Fernández, F. A., Pérez, J. S., Camacho, F. G., & Grima, E. M. (1999). Prediction of dissolved oxygen and carbon dioxide concentration profiles in tubular

TH-2951_166106019

photobioreactors for microalgal culture. *Biotechnology and bioengineering*, *62*(1), 71-86.

59. Ryu, K. H., Lee, J. Y., Heo, S., & Lee, J. H. (2019). Improved microalgae production by using a heat supplied open raceway pond. Industrial & Engineering Chemistry Research, 58(21), 9099-9108.
60. Salvucci, M. E., & Crafts-Brandner, S. J. (2004). Relationship between the heat tolerance of photosynthesis and the thermal stability of Rubisco activase in plants from contrasting thermal environments. *Plant physiology*, *134*(4), 1460-1470.
61. Schädler, T., Cerbon, D. C., de Oliveira, L., Garbe, D., Brück, T., & Weuster-Botz, D. (2019). Production of lipids with Microchloropsis salina in open thin-layer cascade photobioreactors. Bioresource technology, 289, 121682.
62. Schädler, T., Neumann-Cip, A. C., Wieland, K., Glöckler, D., Haisch, C., Brück, T., & Weuster-Botz, D. (2020). High-Density Microalgae Cultivation in Open Thin-Layer Cascade Photobioreactors with Water Recycling. Applied Sciences, 10(11), 3883.
63. Shuba, E. S., & Kifle, D. (2018). Microalgae to biofuels:'Promising'alternative and renewable energy, review. Renewable and Sustainable Energy Reviews, 81, 743-755.
64. Shukla, R., Ranjith, P., Haque, A., & Choi, X. (2010). A review of studies on CO2 sequestration and caprock integrity. *Fuel*, *89*(10), 2651-2664.
65. Singh, R. N., & Sharma, S. (2012). Development of suitable photobioreactor for algae production–A review. *Renewable and Sustainable Energy Reviews*, *16*(4), 2347-2353.
66. Sivaramakrishnan, R., & Incharoensakdi, A. (2018). Utilization of microalgae feedstock for concomitant production of bioethanol and biodiesel. Fuel, 217, 458-466.
67. Srinuanpan, S., Cheirsilp, B., Prasertsan, P., Kato, Y., & Asano, Y. (2018). Strategies to increase the potential use of oleaginous microalgae as biodiesel feedstocks: nutrient starvations and cost-effective harvesting process. Renewable Energy, 122, 507-516.

TH-2951_166106019

68. Su, G., Jiao, K., Chang, J., Li, Z., Guo, X., Sun, Y., Zeng, X., Lu, Y. and Lin, L., 2016. Enhancing total fatty acids and arachidonic acid production by the red microalgae Porphyridium purpureum. Bioresources and Bioprocessing, 3(1), pp.1-9.

69. Subhash, G. V., Rajvanshi, M., Kumar, G. R. K., Sagaram, U. S., Prasad, V., Govindachary, S., & Dasgupta, S. (2021). Challenges in microalgal biofuel production: A perspective on techno economic feasibility under biorefinery stratagem. *Bioresource Technology*, *343*, 126155.

70. SundarRajan, P., Gopinath, K. P., Greetham, D., & Antonysamy, A. J. (2019). A review on cleaner production of biofuel feedstock from integrated CO2 sequestration and wastewater treatment system. *Journal of cleaner production*, *210*, 445-458.

71. Torzillo, G., Giannelli, L., Roldan, A. M., Verdone, N., De Filippis, P., Scarsella, M., & Bravi, M. (2010). Microalgae culturing in thin-layer photobioreactors. *Chemical Engineering Transactions*, *20*, 265-270.

72. Tredici, M.R., Zittelli, G.C., Rodolfi, L., (2010). Photobioreactors. In: Flickinger, M.C. (Ed.), Encyclopedia of Industrial Biotechnology: *Bioprocess, Bioseparation, and Cell Technology*. Wiley, Hoboken, NJ, pp. 3821–3838.

73. Tripathi, R., Singh, J., & Thakur, I. S. (2015). Characterization of microalga Scenedesmus sp. ISTGA1 for potential CO2 sequestration and biodiesel production. *Renewable Energy*, *74*, 774-781

74. Venancio, H. C., Cella, H., Lopes, R. G., & Derner, R. B. (2020). Surface-to-volume ratio influence on the growth of Scenedesmus obliquus in a thin-layer cascade system. Journal of Applied Phycology, 1-9.

75. Wilberforce, T., Baroutaji, A., Soudan, B., Al-Alami, A. H., & Olabi, A. G. (2019). Outlook of carbon capture technology and challenges. *Science of the total environment*, *657*, 56-72.

TH-2951_166106019

76. Xu, X., Martin, G. J., & Kentish, S. E. (2019). Enhanced CO2 bio-utilization with a liquid–liquid membrane contactor in a bench-scale microalgae raceway pond. Journal of CO2 Utilization, 34, 207-214.

77. Yaashikaa, P. R., Kumar, P. S., Varjani, S. J., & Saravanan, A. (2019). A review on photochemical, biochemical and electrochemical transformation of CO2 into value-added products. *Journal of CO2 Utilization*, *33*, 131-147.

78. Yadav, G., Karemore, A., Dash, S. K., & Sen, R. (2015). Performance evaluation of a green process for microalgal CO2 sequestration in closed photobioreactor using flue gas generated in-situ. *Bioresource Technology*, *191*, 399-406.

79. Zarmi, Y., Bel, G., & Aflalo, C. (2013). Theoretical analysis of culture growth in flat-plate bioreactors: the essential role of timescales. *Handbook of Microalgal Culture/Eds. A. Richmond, Q. Hu. Wiley-Blackwell*, 205-224.

80. Zhao, B., Su, Y., Zhang, Y., & Cui, G. (2015). Carbon dioxide fixation and biomass production from combustion flue gas using energy microalgae. Energy, 89, 347-357.

81. Zhu, C., Zhai, X., Xi, Y., Wang, J., Kong, F., Zhao, Y., & Chi, Z. (2020). Efficient CO2 capture from the air for high microalgal biomass production by a bicarbonate Pool. *Journal of CO2 Utilization*, *37*, 320-327.

82. Zuccaro, G., Yousuf, A., Pollio, A., & Steyer, J. P. (2020). Microalgae cultivation systems. *Microalgae cultivation for biofuels production*, 11-29.

TH-2951_166106019

Chapter 3

Screening, isolation & characterization of potential CO_2 tolerant microalgal strain from industrial hotspot in India.

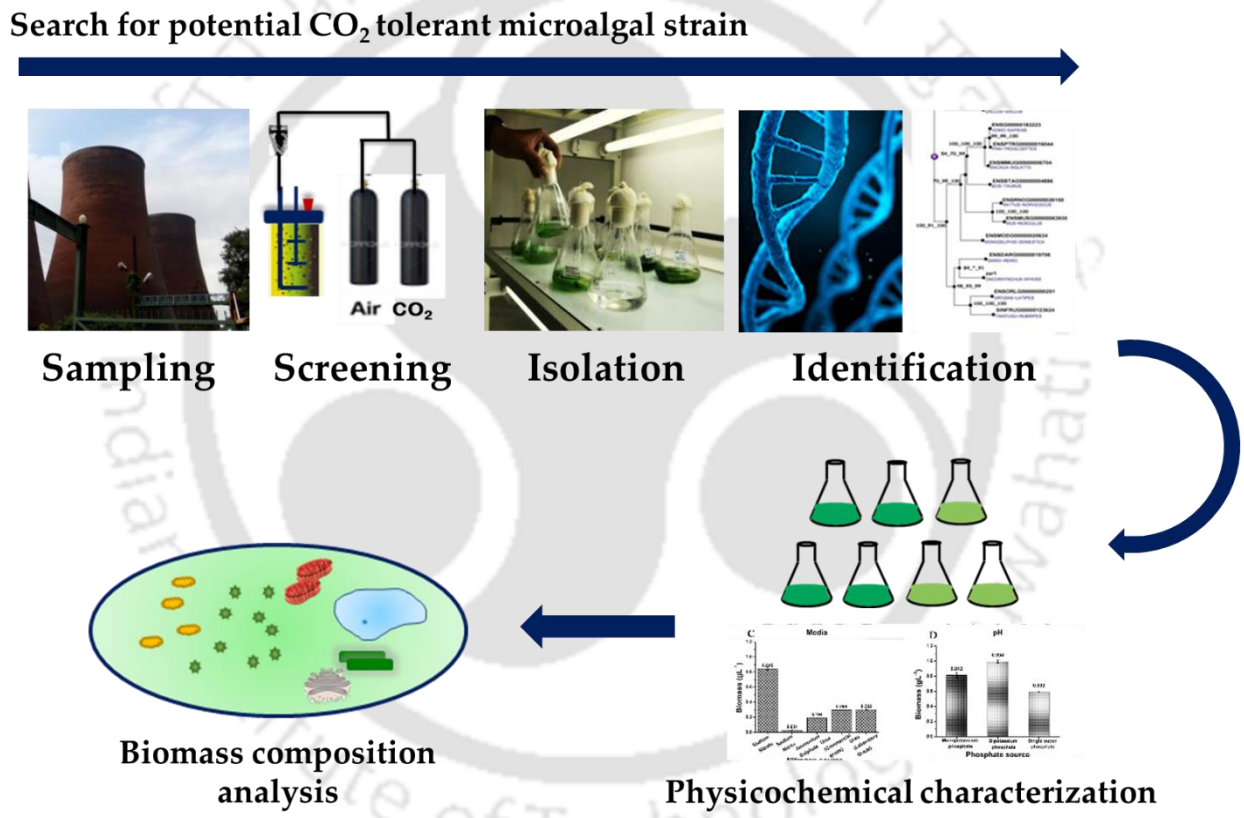

Fig. 3.1. Graphical abstract.

3.1. Background and Motivation

The alarming deterioration in air quality due to CO_2 emission from various anthropogenic activities has mandated the search for natural resources facilitating carbon capture. To that end, microalgae, photoautotrophic eukaryotes with the ability to produce high-value compounds and bulk chemicals, have shown promising outcome in terms of CO_2 sequestration. These

TH-2951_166106019

photosynthetic microorganisms are capable of exhibiting faster growth rate with fewer environmental requirements for cultivation [Benedetti et. al., 2018]. Compared to the terrestrial plants, microalgae have almost 10 times higher photosynthetic efficiency resulting in higher growth rate and biomass productivity [Pires et. al., 2019]. However, as microalgae are quite diverse in nature, there is a critical need to search for appropriate strains with high CO_2 sequestration capability and concomitant multiproduct portfolio. It has been reported that, with the progress of geological time, the CO_2 sequestration capabilities of chlorophytes have gradually decreased while the other microalgal communities have emerged as better CO_2 capturing capacity [Wang et. al., 2018]. Also, the CO_2 tolerance levels of an individual microalgal strain depends on factors like photosynthetic efficiency, CO_2 availability, mixing rates, [Ho et. al., 2011] culture pH. This makes the selection process complex and cumbersome, resulting in low economic efficiency. To that end, the development of high throughput process for screening and selection of indigenous microalgal strains with potential of sequestering CO_2 and subsequent conversion into value-added products, is the key to sustainable biorefinery. Furthermore, the character of most microalgae have been observed to be greatly influenced by basic environmental factors like pH, temperature, incident light intensity, availability of limiting nutrients, etc. [Qiu et. al., 2017; Difusa et. al., 2015]. This motivated the careful selection of right nutritional and physicochemical parameters for the growth of the organism.

3.2. Materials and Methods

3.2.1 Sampling, screening, and isolation of potential CO_2 tolerant microalgal strain

As a CO_2 rich industrial hotspot, sample was collected from effluent of Bokaro Steel plant, Jharkhand, India (23.6693° N, 86.1511° E) was inoculated in BG11 medium (Table 3.1) in a bubble column reactor (Spectrochem Instruments Pvt. Ltd., India) of 500 mL with working volume of 300 mL (Fig. 3.2) and enriched to obtain sufficiently large cell population. Screening

TH-2951_166106019

of CO_2 tolerant strains was performed by a novel CO_2 selection pressure-based screening strategy where, the enriched mixed culture was exposed to sequentially elevated concentrations of CO_2 starting from 5% to 20% v/v, with step-wise increase by 2.5% v/v.

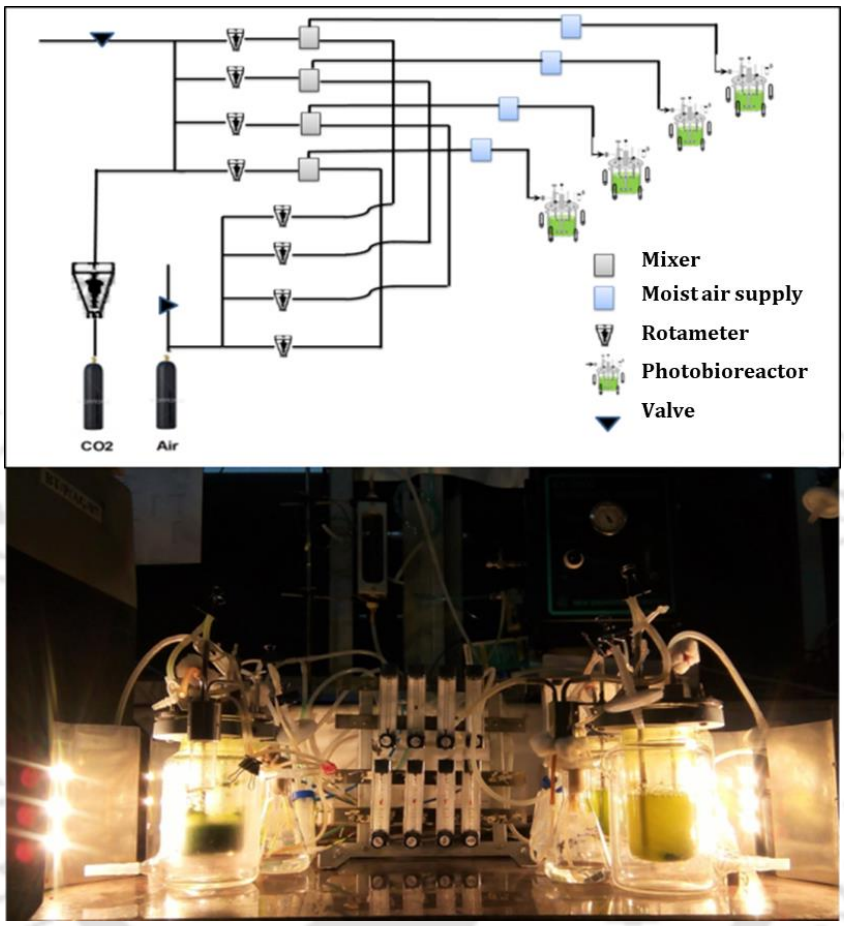

Fig. 3.2. Bubble column photobioreactor with customized aeration

The CO_2 concentration of the input gas stream was varied by ratiometric mixing of compressed air and CO_2 through rotameters (Fig. 3.2). The culture was maintained at room temperature with a light-dark cycle of 16:8 h and light intensity of approximately 250 µE m^{-2} s^{-1}. In order to eliminate any possible nutritional stress, the concentrations of nitrate and phosphate were maintained higher than 50% of their initial value via intermittent feeding. Dynamic profiles of phosphate and nitrate utilization & pH were obtained by sampling every 24 h at the end of the light cycle. The screened CO_2 tolerant culture, at the end of the batch of 53 days, was subjected to serial dilution and streak plating to isolate axenic unialgal culture.

TH-2951_166106019

3.2.2 Identification of the isolated strain

The morphology of the strain was studied using bright field microscopy (Nikon, Japan) and field emission scanning electron microscopy (FESEM) (Sigma, Carl Zeiss Microscopy, Germany). For molecular identification of the strain, genomic DNA was isolated using HiPurA^{TM} plant genomic DNA purification kit and partial 28s rDNA sequence was amplified using D2 region Specific Primers (Forward being ACCCGCTGAACTTAAGC and reverse being GGTCCGTGTTTCAAGACGG) in a thermal cycler (Veriti$^{®}$, Thermo Fisher Scientific, USA). PCR amplification conditions involved an initial denaturation step at 94 °C for 5 min, followed by 35 cycles of 94 °C for 1 min, 52 °C for 1 min and 72 °C for 2 min and final extension of 10 min at 72 °C. Further, sequencing of the PCR amplicon was performed using BDT v3.1 Cycle sequencing kit on ABI 3730xl Genetic Analyzer. The sequence obtained was compared with the existing database through NCBI BLAST and the phylogenetic tree was constructed in MEGA X using Neighbor-Joining method with 1000 bootstrap replications.

3.2.3 Characterization of the strain under different physiochemical parameters in shake flask

Characterization experiments were performed to study the effect of different medium composition, initial pH of the medium, nitrogen and phosphate sources on growth of the organism. In order to understand the suitable medium supporting maximum biomass titer, growth characterization was carried out in five different medium compositions such as Watanabe (AF6), Beijerinck (BJA), BG 11, Bold Basal medium (BBM), and Algae Culture Broth (ACB). Details about the composition of these media are given in supporting information (Table 3.1). Further, the growth of the strain was evaluated under various initial pH (4, 6, 8, 10, and 12), different nitrogen sources (sodium nitrate, sodium nitrite, ammonium sulphate, analytical grade urea, and commercial grade urea) with equimolar nitrogen (0.011 M) and

TH-2951_166106019

different phosphate sources (monopotassium phosphate, dipotassium phosphate, and single super phosphate) containing equimolar phosphate (0.0015 M). All characterization experiments were performed in 250 mL Erlenmeyer flasks with working volume of 100 mL, incubated at 28 °C temperature and 150 rpm agitation in a shaker incubator (Orbitek, Scigenics Biotech, India). 10%, v/v of seed culture with absorbance (A_{690}) of 1.0 was used as inoculum and the light intensity was maintained at 20 µE $m^{-2}s^{-1}$ with a light:dark cycle of 16:8. Samples were withdrawn at the end of every light cycle to monitor the growth.

After completion of growth characterization, the biochemical composition of the biomass and CO_2 fixation rate was evaluated under selected physiochemical parameters supporting improved growth. Biomass productivity (P, mg L^{-1} day^{-1}) and CO_2 fixation rate (R_{CO_2}, mg L^{-1} day^{-1}) was calculated as follows:

$$P = \frac{x_f - x_0}{t_f - t_0} \quad (3.1)$$

where x_0 and x_f are the dry cell weights (g L^{-1}) obtained at initial and final time points t_0 and t_f respectively.

$$R_{CO_2} = C_C P \frac{M_{CO_2}}{M_C} \quad (3.2)$$

where, C_C is elemental carbon content of biomass. M_{CO_2} and M_C are the molar mass of CO_2 and C (g mol^{-1}), respectively. C_C was estimated at the end of the batch using elemental analyser (EuroEA3000, Italy).

TH-2951_166106019

Table 3.1. Detailed composition of different microalgal growth media

Medium	Suitable for Algal Family	Compositions (g L^{-1})*
Watanabe (AF6)	Euglenophyceae, Volvocalean algae, Xanthophytes, many Cryptophytes, Dinoflagellate and green ciliates; specific for algae requiring slightly acidic medium	$NaNO_3$ 0.14, NH_4NO_3 0.022, $MgSO_4$ 0.03, KH_2PO_4 0.01, K_2HPO_4 0.005, $CaCl_2$. 4H2O 0.01, ammonium ferric citrate 0.002, citric acid 0.002, biotin 0.002, thiamine 10 µg, vitamin B6 1 µg, vitamin B12 1 µg, Na_2-EDTA 0.005, $FeCl_3$ 0.098, $MnCl_2 \cdot 4H_2O$ 0.18, $ZnCl_2 \cdot 4H_2O$ 57 µg, $Na_2MoO_4 \cdot 2H_2O$ 12.5 µg
Beijerincki (BJA)	Chlorophyceae	NH_4NO_3 0.15, K_2HPO_4 0.02, $MgSO_4 \cdot 7H_2O$ 0.02, $CaCl_2 \cdot 2H_2O$ 0.01, KH_2PO_4 0.363, K_2HPO_4 0.69, H_3BO_3 0.01, $MnCl_2 \cdot 4H_2O$ 0.005, EDTA 0.05, $CuSO_4 \cdot 5H_2O$ 0.0015, $ZnSO_4 \cdot H_2O$ 0.022, $CoCl_2 \cdot 6H_2O$ 0.0015, $FeSO_4 \cdot 7H_2O$ 0.005, $(NH_4)_6Mo_7O_{24} \cdot 4H_2O$ 0.001
BG 11	Cyanophyceae	$NaNO_3$ 1.5, $K_2HPO_4 \cdot 3H_2O$ 0.004, $MgSO_4 \cdot 7H_2O$ 0.075, $CaCl_2 \cdot 2H_2O$ 0.036, Na_2CO_3 0.02, citric acid 0.006, ferric ammonium citrate 0.006, EDTA 0.001, and A5 + Co solution (1 mL L^{-1}) that consists of H_3BO_3 2.86, $MnCl_2 \cdot H_2O$ 1.81, $ZnSO_4 \cdot 7H_2O$ 0.222, $CuSO_4 \cdot 5H_2O$ 0.079, $Na_2MoO_4 \cdot 2H_2O$ 0.39, and $Co(NO_3)_2 \cdot 6H_2O$ 0.049
Bold Basal (BBM)	Broad spectrum medium for Chlorophyceae, Xantophyceae, Chrysophyceae and Cyanophyceae; unsuitable for algae with vitamin requirements	KH_2PO_4 0.175, $CaCl_2 \cdot 2H_2O$ 0.025, $MgSO_4 \cdot 7H_2O$ 0.075, $NaNO_3$ 0.25, K_2HPO_4 0.075, NaCl 0.025, H_3BO_3 0.011, $ZnSO_4 \cdot 7H_2O$ 0.00882, $MnCl_2 \cdot 4H_2O$ 0.00144, MoO_3 0.00071, $CuSO_4 \cdot 5H_2O$ 0.00157, $Co(NO_3)_2 \cdot 6H_2O$ 0.00049, Na_2EDTA 0.05, KOH 0.0031, $FeSO_4$ 0.005, H_2SO_4 1 µL
Algae Culture Broth (ACB)	Commercial medium obtained from Himedia Pvt. Ltd., India	$NaNO_3$ 1, $MgSO_4.7H_2O$ 0.513, K_2HPO_4 0.25, NH_4Cl 0.050, $CaCl_2.2H_2O$ 0.058, $FeCl_3$ 0.003

TH-2951_166106019

3.2.4 Analysis of growth and substrate utilization

For monitoring the growth of the organism, absorbance of the culture was measured at 690 nm (A_{690}) using UV-Vis spectrophotometer (Cary 100, Agilent Technologies, USA). The absorbance values were converted into dry cell weight (DCW) using the correlation, one cell density = 0.1853 g dry cells L^{-1} (R^2 = 0.99). Cell free supernatant obtained from centrifugation of the sample at 10000 rpm for 10 min was analysed for substrate utilization.

3.2.4.1. Analysis of phosphate utilization

Phosphate estimation was carried out using ascorbic acid method with potassium hydrogen phosphate (dibasic) as standard [Parsons et. al., 1984]. Combined reagent (0.16 mL) comprising (5 N) sulfuric acid, (0.018 M) antimony potassium tartrate, (0.102 M) ammonium molybdate and (0.1 M) ascorbic acid was used for estimating the phosphate content in the supernatant of 1mL. The absorbance was read at 880 nm after incubation for 10 minutes at room temperature.

3.2.4.2. Analysis of nitrate utilization

Estimation of nitrate present in the supernatant was done using salicylic acid method and keeping sodium nitrate as the standard [Cataldo et. al., 1975]. In this method, 0.1 mL of the supernatant was mixed with 0.4 mL of 5 % (w/v) salicylic acid in sulfuric acid followed by incubation for 20 minutes at room temperature which yields a yellow-coloured solution after neutralization with 9.5 mL of 2N NaOH. The absorbance was observed at 410 nm after cooling the tubes to room temperature.

3.2.5. Analysis of intracellular biochemical composition

For biochemical composition analysis, stationary phase culture was collected and centrifuged at 7000 rpm at 4 ℃ for 10 min. Cell pellet was washed twice with distilled water and lyophilized overnight.

TH-2951_166106019

3.2.5.1. Estimation of total protein

To extract the intracellular protein, biomass resuspended in phosphate buffer (pH 6.8) was subjected to ultrasonication at 35% amplitude (a maximal power of 350 W) in a pulse mode (5 s ON / 10 s OFF) under cold condition. Repeating 3 rounds of sonication for 5 min each, the supernatant was collected after every round. Total protein estimation of the whole supernatant done by Bradford method [Bradford 1976] using bovine serum albumin as standard. 0.25 mL of protein sample extracted was mixed with 2.5 mL of Bradford reagent and absorbance was recorded wavelength of 595 nm.

3.2.5.2. Estimation of total Lipid

Intracellular lipid extraction was performed following the protocol described by [Bligh & Dyer, 1959]. 2 ml of Chloroform: Methanol (2:1) was added to 50 mg of biomass followed by ultrasonication for 30 minutes at 35% amplitude (a maximal power of 350 W) in a pulse mode (10 s ON / 5 s OFF) under cold condition. Further, the mixture was incubated at room temperature for 6 hours with continuous shaking of 150 rpm. A combination of 1 ml chloroform and 2 ml of 0.9% NaCl in water was added post incubation and lipid was extracted as dissolved in chloroform layer. The extracted lipid was weighed and compared to the initial biomass for valuation of total intracellular lipid.

3.2.5.3. Estimation of total carbohydrate

Prior to determination of carbohydrate content, the dried microalgal biomass was subjected to acid hydrolysis according to the protocol described by [Van Wychen and Laurens, 2013]. 50 mg of biomass was hydrolyzed with 500 µl of 72% (w/v) H_2SO_4 for 1 h. Concentration of H_2SO_4 was reduced to 4% by the adding distilled water and autoclaved at 121 for 1 h. After cooling down to room temperature, the mixture volume was made up to 50 ml. The solution was then centrifuged at 10,000 rpm for 10 min and the supernatant was analysed for total

TH-2951_166106019

carbohydrate content was estimated via phenol sulfuric acid method [Dubois et al., 1956] considering glucose as standard.

3.2.5.4. Estimation of total chlorophyll content

For extraction of intracellular chlorophyll, 50 mg of dry biomass was resuspended in 10 mL of 99.9% methanol and incubated in dark at 45 ℃ for 30 min. The sample was then centrifuged and supernatant was analysed for absorbance at wavelength of 652 nm and 665 nm. Total chlorophyll content (sum of chlorophyll a and chlorophyll b) was estimated based on the following Eq. **3.3 and Eq. 3.4** [Pruvost et al., 2011].

$$Chlorophyll\ a\ (\mu g\ mL^{-1}) = 16.5169 \times A_{665} - 8.0962\ \times\ A_{652} \quad (3.3)$$

$$Chlorophyll\ b\ (\mu g\ mL^{-1}) = 27.4405 \times A_{652} - 12.1688\ \times\ A_{665} \quad (3.4)$$

3.2.5.5. Estimation of ash content

Ash content was calculated by subjecting 1 gm of dry biomass to 575℃ in a muffle furnace for 4 hours. Weight of the residual ash was converted to the percent fraction of initial weight of microalgal biomass.

3.3. Results and Discussion

3.3.1 Screening and isolation of CO_2 tolerant microalgal strain from industrial hotspot

Under photoautotrophic condition, microalgae grow by fixing CO_2 from different sources such as the atmosphere and exhausts from industries including flue and flare gas. The growth rate of microalgae is directly proportional to the photosynthetic efficiency which, in turn depends on the available CO_2 concentration. It has been reported that, atmospheric concentration of CO_2 (0.036%) is sub-optimal for photosynthesis [Bhola et. al., 2011] and the photosynthesis apparatus appears to be adapted to much higher concentrations of CO_2 [Solovchenko et. al., 2013]. Further, microalgal bioprocess is typically based on flue gas from various industries,

TH-2951_166106019

CO_2 concentration in which varies from 3% – 30% [Bhola et. al., 2011]. Therefore, screening and isolation of an indigenous CO_2 tolerant strain remains the first key step towards development of a sustainable bioprocess. In the present study, a CO_2 selection pressure-based strategy was adopted for rapid screening and isolation of CO_2 tolerant microalgal strain. The water sample collected from carbon rich industrial hotspot was subjected to culturing under sequentially elevated CO_2 concentration of 5% - 20% v/v, with a step wise increase by 2.5%. In the beginning of the screening process, starting with 5% CO_2 v/v, presence of four morphologically distinct microalgal strains was accounted in the mixed culture and their growth was monitored in terms of differential cell count (Fig. 3.4). A consistent lag in the growth of the strains was observed at the beginning of each elevation of CO_2 selection pressure (Fig. 3.4). With the increase in CO_2 concentration, reduction in growth of the strains was observed and finally, three out of four strains could survive under the final CO_2 concentration of 20% v/v. Amongst the three survivors, only one strain was found to not only withstand but also grow significantly even at 20% CO_2 concentration v/v and was further isolated. The growth of the strain could be correlated with the decrease in concentration of nitrate and phosphate during the batch run under individual concentration of CO_2 (Fig 3.3). pH of the culture was found to be automatically maintained within the range of 7 - 8 even at higher CO_2 concentrations (Fig 3.3). This self-regulatory phenotypic response might be due to continuous utilization of CO_2 linked with growth of the organism, even at higher CO_2 selection pressure [Uggetti et. al., 2018]. In a similar study, microalgal community present in the waste water sample collected from sewage treatment plant, was enriched at high CO_2 concentration of 10% v/v and *Scenedesmus* sp. was found to grow dominantly amongst all microalgal strains present in the mixed culture [Wang et. al., 2018].

TH-2951_166106019

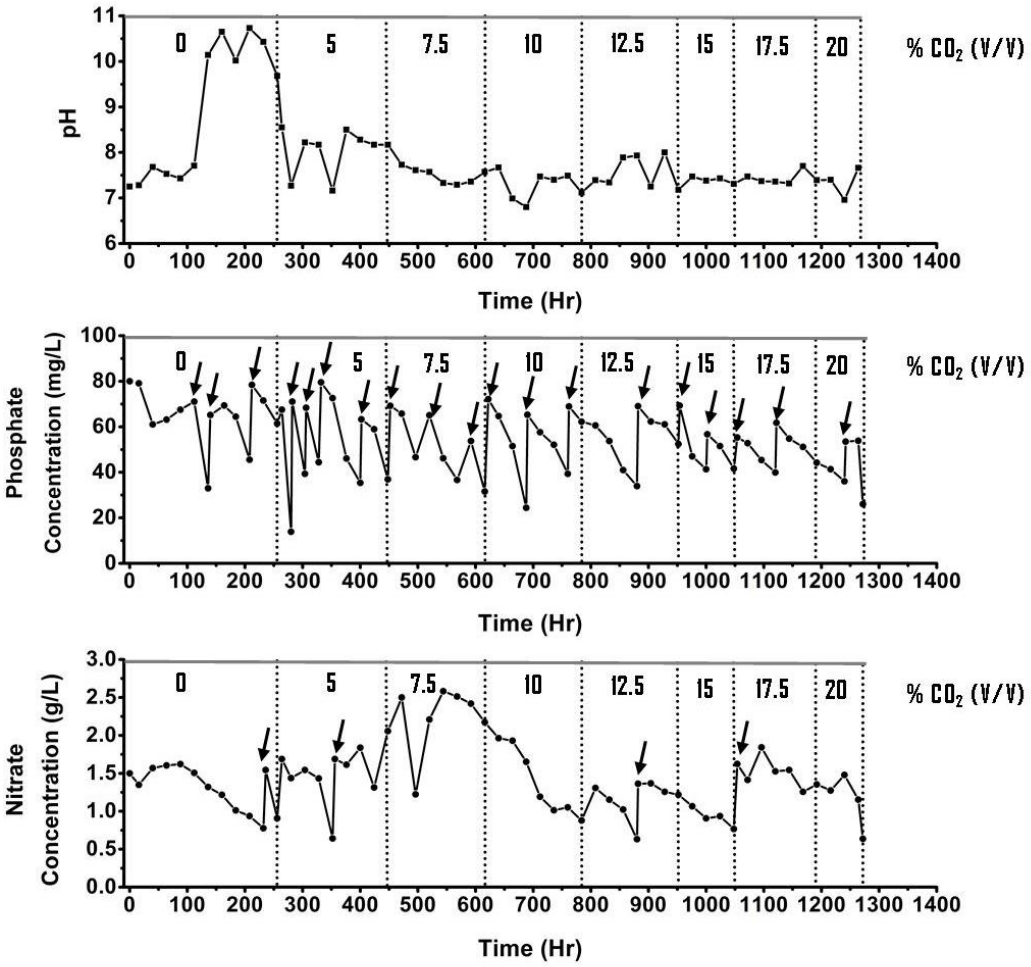

Fig. 3.3. Dynamic profiles of pH, phosphate concentration, nitrate concentration for screening of CO_2 tolerant strain from mixed algal culture under different CO_2 concentration in photoautotrophic growth condition. Arrows indicate intermittent feeding of nutrient in the reactor.

TH-2951_166106019

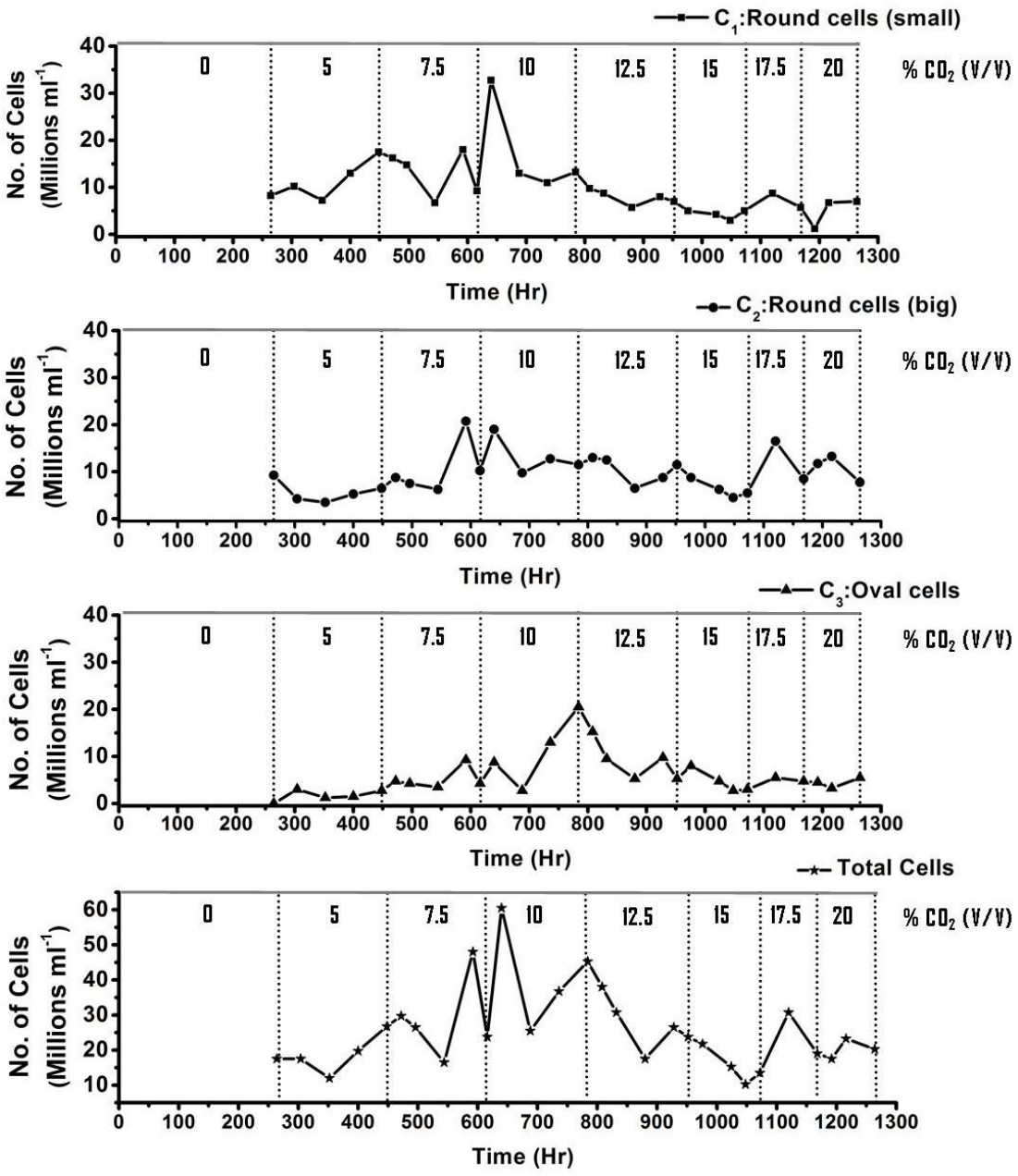

Fig. 3.4. Dynamic profiles of total and differential algal cell count for screening under different CO_2 concentration in photoautotrophic growth condition.

TH-2951_166106019

3.3.2 Identification of the isolated microalgal strain

Bright field microscopy and FESEM images (**Fig. 3.5A** and **Fig. 3.5B**) confirmed the oval shaped unicellular nature of the isolated microalgal strain and absence of any spike or flagella on the cell surface. The cells were visibly green in colour and about 6 to 9 µm in length. Molecular identification of the isolate was further carried out by 28s rDNA sequencing analysis as morphological resemblance is only presumptive and do not confirm the evolutionary position of an isolate. The isolate was found to be in closest homology with *Tetradesmus obliquus* KMC24 with maximum sequence similarity of 97.8%. To further depict the evolutionary position of the isolate, a phylogenetic tree was constructed based on the sequence of the isolate and 15 closest organisms (**Fig. 3.5 C**). In accordance with this finding, the isolated microalgal strain was identified as *Tetradesmus obliquus* CT02 (GenBank Accession # MZ267545). Hereafter, the organism is designated as CT02.

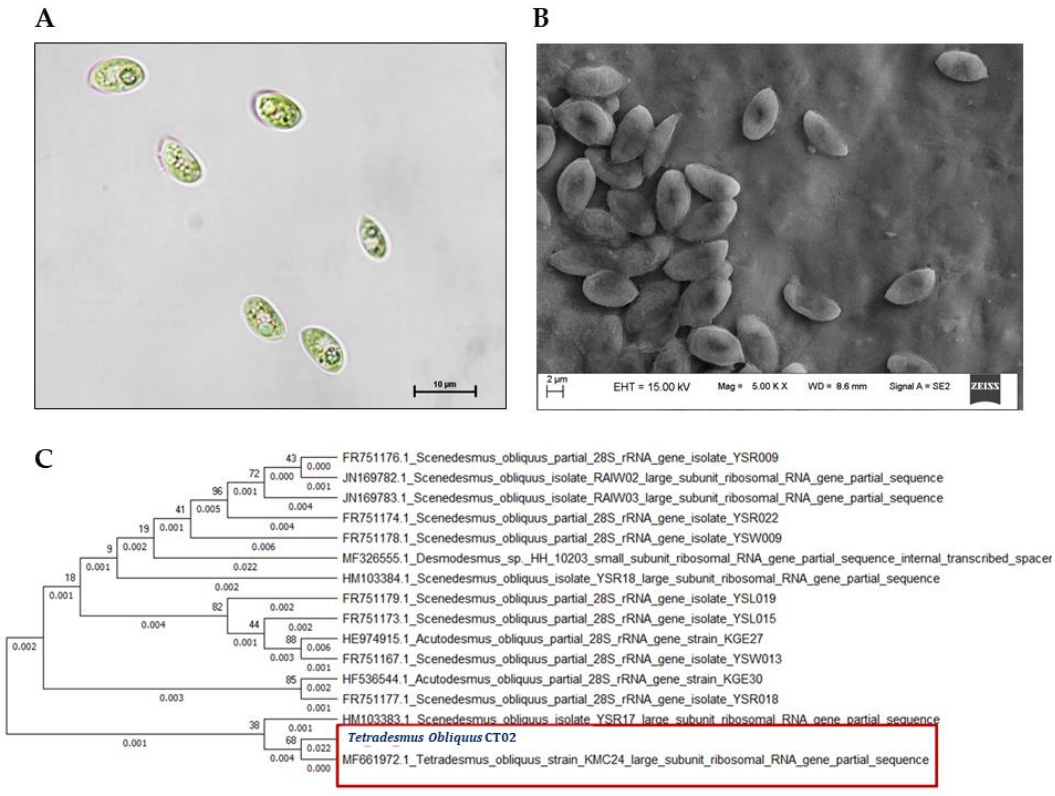

Fig. 3.5. Morphological identification of isolated microalgal strain under (A) bright field microscopy and (B) field emission scanning electron microscopy (FESEM). The molecular level identification was carried out based on phylogenetic tree generated using MEGA X (C).

TH-2951_166106019

Neighbour-joining showing phylogenetic position of isolate and related taxa is based on partial 28s rRNA gene sequence comparisons. Bootstrap values are indicated at nodes. Representative sequences in the dendogram were obtained from GenBank.

3.3.3. Characterization of the isolated microalgal strain

The growth of microalgae can substantially vary with the fulfilment of their nutritional requirements. In search of suitable nutritional and growth conditions for CT02, characterization of the strain was carried out under different media compositions, various initial pH, nitrogen sources, and phosphate sources of the medium supporting maximum growth of CT02. Dynamic profile of growth of CT02 was monitored under different nutritional and physicochemical conditions.

Although the strain was found to grow in a wide variety of culture media (**Fig. 3.6**), the highest biomass titer of 1.087 g L^{-1} was obtained using algae culture broth (ACB) medium. This emphasizes the importance of phosphate as a limiting macronutrient for growth CT02 as ACB contained highest phosphate concentration than other media.

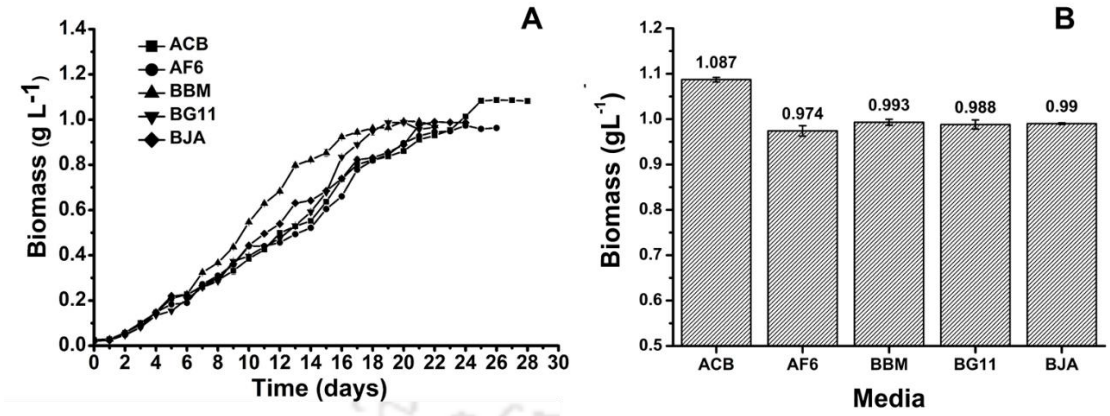

Fig. 3.6. Dynamic profile for growth (A) and maximum growth (B) obtained for CT02 in different growth media.

Further, the strain was able to favorably grow at lower initial pH of the medium. A maximum biomass titer of 0.826 g L^{-1} was obtained at a pH value of 6, while sub-optimal growth was observed at alkaline pH (**Fig. 3.7**). Studies depict the initial pH of the medium in the range of

TH-2951_166106019

6 to 9 as optimal for the growth of various microalgae [Muthuraj et. al., 2014; Ren et. al., 2013; Xin et. al., 2010]. In case of *Scenedesmus* sp., while higher growth was achieved at initial pH close to neutral, synthesis of different growth and non-growth associated products was induced at an acidic pH of 5 [Wu et. al., 2016]. This depicts a mutually exclusive nature of the initial pH conditions promoting growth and product formation. To that end, the present strain may be beneficial as the growth is favorable at lower initial pH of the medium (4 - 6) which might also promote synthesis of various value-added compounds.

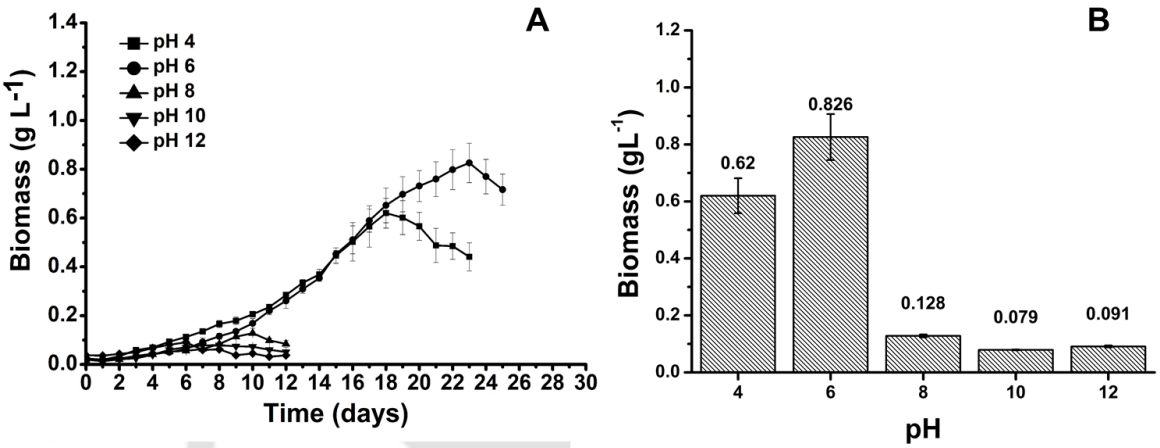

Fig. 3.7. Dynamic profile for (A) growth and (B) Maximum growth obtained by CT02 at different initial pH.

Amongst five different nitrogen sources, the strain exhibited a substantially higher biomass titer (0.845 g L^{-1}) with sodium nitrate as compared to others (**Fig. 3.8**). Sodium nitrate has been recognized as a favorable nitrogen source for growth of various microalgal strains [Arumugam et. al., 2013; Shen et. al., 2010]. The lower growth in case of ammonia-based nitrogen sources such as ammonium sulphate and urea may be due to the formation of H^+ ions during ammonia uptake from media [Muthuraj et. al., 2014].

TH-2951_166106019

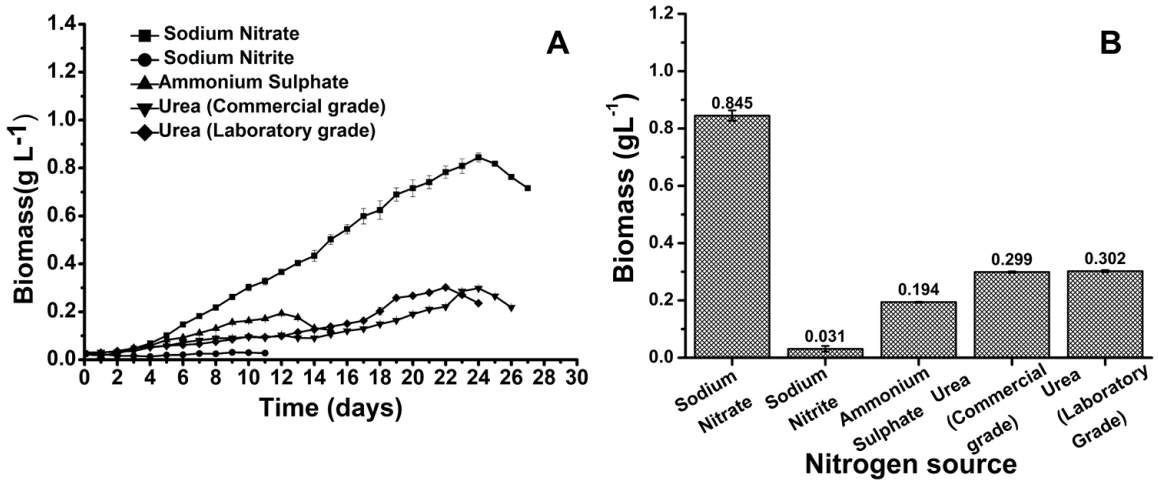

Fig 3.8: Dynamic profile for growth (A) and maximum growth (B) obtained for CT02 in different nitrogen sources.

Phosphate sources have been regularly reported as another vital limiting nutrient [Kang et. al., 2006; Goswami et. al., 2019] Amongst 2 most frequently used phosphate source and commercial phosphate, dipotassium phosphate was found to be the most suitable phosphate source for CT02, resulting highest biomass titer of 0.994 g L^{-1} (**Fig. 3.9**).

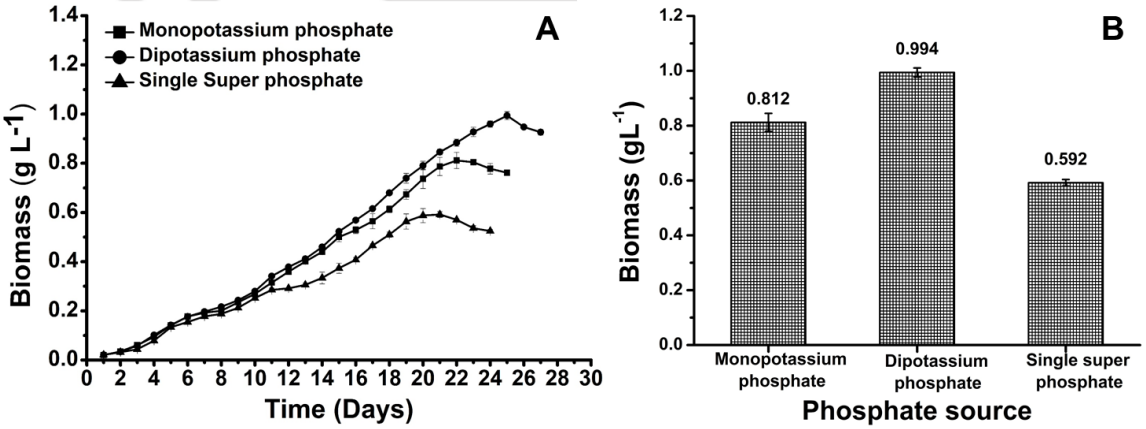

Fig 3.9: Dynamic profile for growth (A) and maximum growth (B) obtained for CT02 in different phosphate sources.

Under the nutritional conditions of sodium nitrate as nitrogen source, dipotassium phosphate as phosphate source, and initial pH of 6, the maximum biomass productivity and CO_2 fixation rate was found to be 39.7 mg $L^{-1}day^{-1}$ and 66.5 mg $L^{-1}day^{-1}$, respectively (**Table 3.2**). A lower biomass titer of less than 1 g L^{-1} might be a limiting factor for any biorefinery considering the use of CT02. In order to improve the biomass titer and productivity of CT02, different process

TH-2951_166106019

engineering strategies such as, growth kinetic driven feeding of limiting nutrients [Goswami et. al., 2019)], dynamic increase in incident light intensity [Goswami et. al., 2019; Muthuraj et. al., 2015] and substrate driven pH control [Palabhanvi et. al., 2016] can be implemented.

Table 3.2. Characterization of growth of CT02 under selected nutritional conditions.

Selected nutritional conditions for growth of CT02	
Growth Media	Algae culture broth (ACB)
Initial pH	6
Nitrogen source	Sodium nitrate
Phosphate source	Dipotassium phosphate
Growth kinetic parameters of CT02 under selected nutritional conditions	
Maximum biomass titer (g L^{-1})	0.99 ± 0.02
Biomass productivity (mg L^{-1} day^{-1})	39.7 ± 0.69
CO_2 fixation rate (mg L^{-1} day^{-1})	66.5 ± 1.15

3.3.4. Analysis of biomass composition of CT02 under suitable nutritional condition

To evaluate the application potential of the biomass with the ability to produce value-added compounds and biofuels, analysis of biochemical composition such as total protein, carbohydrate, lipid, and ash content was carried out (**Fig 3.10**).

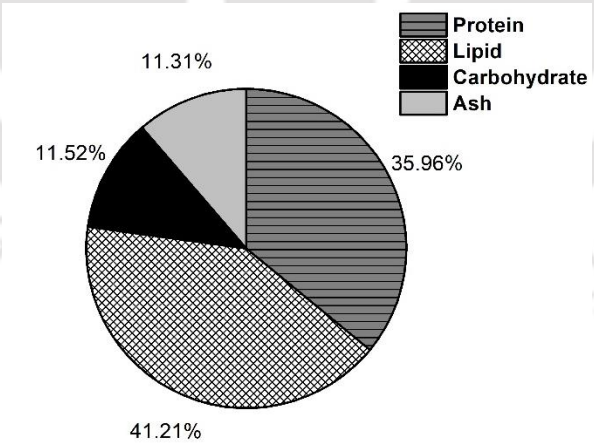

Fig. 3.10. Composition of CT02 biomass grown under suitable nutritional and physicochemical conditions.

A high protein content of 35.96 % w/w was estimated, which can be considered as potential source of bioactive metabolites [Surkatti et. al., 2018]. Total chlorophyll content was estimated to be 1.8 µg per mg of biomass. Further, substantially high lipid content of 41.21% w/w depicts

TH-2951_166106019

that the protein extracted biomass can be suitably used for synthesis of biodiesel. However, carbohydrate content was estimated to be lowest at 11.5% w/w, which, may be due to regular consumption of carbohydrate for cellular metabolism as explained by Mirón et. al., 2002. [Sánchez et. al., 2002]. Furthermore, the low carbohydrate and high lipid content of biomass at the end of the batch might be the effect of nutritional stress to the cells caused by exhaustion of limiting nutrients nitrate and phosphate, which redirect the carbon flux from carbohydrate or protein fractions of the biomass to the accumulation of neutral lipid [Muthuraj et. al., 2014]. The residual ash content was calculated to be 11.31% w/w.

3.4. Conclusions

As the foremost step towards microalgae-based carbon capture, a novel CO_2 selection pressure based strategy was developed for screening and selection of potential CO_2 tolerant strains from indigenous hotspots. *Tetradesmus obliquus* CT02, a robust microalgal strain isolated utilizing this strategy, found to exhibit high CO_2 tolerance of up to 20% v/v. In order to expand the suitability towards sustainable cultivation, growth of the isolated strain was subsequently characterized under different media, initial pH, nitrogen sources and phosphate sources. Selection process resulted algae culture broth (ACB) as most favorable growth medium, followed by initial pH as 6, sodium nitrate as nitrogen source and dipotassium phosphate as phosphate source. Under these nutritional conditions, the maximum biomass titer of 0.994 g L^{-1}, productivity of 39.7 mg $L^{-1}day^{-1}$ and CO_2 fixation rate of 66.5 mg $L^{-1}day^{-1}$ was observed. Compositional analysis of biomass grown under suitable nutritional and physicochemical conditions depicted high protein content of 35.96 % w/w and lipid content of 41.21 % w/w, which suggests the viability of CT02 for construction of microalgal biorefinery.

References

1. Arumugam, M., Agarwal, A., Arya, M. C., & Ahmed, Z. (2013). Influence of nitrogen sources on biomass productivity of microalgae *Scenedesmus bijugatus*. Bioresource technology, 131, 246-249.

TH-2951_166106019

2. Benedetti, M., Vecchi, V., Barera, S., & Dall'Osto, L. (2018). Biomass from microalgae: the potential of domestication towards sustainable biofactories. Microbial Cell Factories, 17(1), 1-18.
3. Bhola, V., Swalaha, F., Kumar, R. R., Singh, M., & Bux, F. (2014). Overview of the potential of microalgae for CO_2 sequestration. International Journal of Environmental Science and Technology, 11(7), 2103-2118.
4. Bligh, E. G., & Dyer, W. J. (1959). A rapid method of total lipid extraction and purification. Canadian journal of biochemistry and physiology, 37(8), 911-917.
5. Bradford, M. M. (1976). A rapid and sensitive method for the quantitation of microgram quantities of protein utilizing the principle of protein-dye binding. Analytical biochemistry, 72(1-2), 248-254.
6. Cataldo, D. A., Maroon, M., Schrader, L. E., & Youngs, V. L. (1975). Rapid colorimetric determination of nitrate in plant tissue by nitration of salicylic acid. Communications in soil science and plant analysis, 6(1), 71-80.
7. Chandrashekharaiah, P. S., Paul, V., Kodgire, S., Chawada, H., Thorat, R., Kushwaha, S., & Dasgupta, S. (2021). Photoautotrophic cultivation of *Chlamydomonas reinhardtii* in open ponds of greenhouse. Archives of Microbiology, 203(4), 1439-1450.
8. Difusa, A., Talukdar, J., Kalita, M. C., Mohanty, K., & Goud, V. V. (2015). Effect of light intensity and pH condition on the growth, biomass and lipid content of microalgae *Scenedesmus* species. Biofuels, 6(1-2), 37-44.
9. Dubois, M., Gilles, K. A., Hamilton, J. K., Rebers, P. T., & Smith, F. (1956). Colorimetric method for determination of sugars and related substances. Analytical chemistry, 28(3), 350-356.
10. Goswami, G., Sinha, A., Kumar, R., Dutta, B. C., Singh, H., & Das, D. (2019). Process engineering strategy for cultivation of high density microalgal biomass with improved productivity as a feedstock for production of bio-crude oil via hydrothermal liquefaction. Energy, 189, 116136.

TH-2951_166106019

11. Ho, S. H., Chen, C. Y., Lee, D. J., & Chang, J. S. (2011). Perspectives on microalgal CO_2-emission mitigation systems—a review. Biotechnology advances, 29(2), 189-198.
12. Kang, C. D., An, J. Y., Park, T. H., & Sim, S. J. (2006). Astaxanthin biosynthesis from simultaneous N and P uptake by the green alga *Haematococcus pluvialis* in primary-treated wastewater. Biochemical Engineering Journal, 31(3), 234-238.
13. Mirón, A. S., Garcıa, M. C. C., Camacho, F. G., Grima, E. M., & Chisti, Y. (2002). Growth and biochemical characterization of microalgal biomass produced in bubble column and airlift photobioreactors: studies in fed-batch culture. Enzyme and microbial technology, 31(7), 1015-1023.
14. Muthuraj, M., Kumar, V., Palabhanvi, B., & Das, D. (2014). Evaluation of indigenous microalgal isolate *Chlorella* sp. FC2 IITG as a cell factory for biodiesel production and scale up in outdoor conditions. Journal of Industrial Microbiology and Biotechnology, 41(3), 499-511.
15. Muthuraj, M., Chandra, N., Palabhanvi, B., Kumar, V., & Das, D. (2015). Process engineering for high-cell-density cultivation of lipid rich microalgal biomass of *Chlorella* sp. FC2 IITG. Bioenergy Research, 8(2), 726-739.
16. Palabhanvi, B., Muthuraj, M., Mukherjee, M., Kumar, V., & Das, D. (2016). Process engineering strategy for high cell density-lipid rich cultivation of *Chlorella* sp. FC2 IITG via model guided feeding recipe and substrate driven pH control. Algal Research, 16, 317-329.
17. Parsons, T. R. (2013). A manual of chemical & biological methods for seawater analysis. Elsevier.
18. Pires, J. C. M., & da Cunha Gonçalves, A. L. (Eds.). (2019). Bioenergy with carbon capture and storage: using natural resources for sustainable development. Academic Press.

TH-2951_166106019

19. Pruvost, J., Van Vooren, G., Le Gouic, B., Couzinet-Mossion, A., & Legrand, J. (2011). Systematic investigation of biomass and lipid productivity by microalgae in photobioreactors for biodiesel application. Bioresource technology, 102(1), 150-158.
20. Qiu, R., Gao, S., Lopez, P. A., & Ogden, K. L. (2017). Effects of pH on cell growth, lipid production and CO_2 addition of microalgae *Chlorella sorokiniana*. Algal research, 28, 192-199.
21. Ren, H. Y., Liu, B. F., Ma, C., Zhao, L., & Ren, N. Q. (2013). A new lipid-rich microalga *Scenedesmus* sp. strain R-16 isolated using Nile red staining: effects of carbon and nitrogen sources and initial pH on the biomass and lipid production. Biotechnology for biofuels, 6(1), 1-10.
22. Shen, Y., Yuan, W., Pei, Z., & Mao, E. (2010). Heterotrophic culture of *Chlorella protothecoides* in various nitrogen sources for lipid production. Applied Biochemistry and Biotechnology, 160(6), 1674-1684.
23. Solovchenko, A., & Khozin-Goldberg, I. (2013). High-CO_2 tolerance in microalgae: possible mechanisms and implications for biotechnology and bioremediation. Biotechnology letters, 35(11), 1745-1752.
24. Surkatti, R., & Al-Zuhair, S. (2018). Effect of cresols treatment by microalgae on the cells' composition. Journal of water process engineering, 26, 250-256.
25. U Uggetti, E., Sialve, B., Hamelin, J., Bonnafous, A., & Steyer, J. P. (2018). CO_2 addition to increase biomass production and control microalgae species in high rate algal ponds treating wastewater. Journal of CO_2 Utilization, 28, 292-298.
26. Van Wychen, S., & Laurens, L. (2013). Determination of total carbohydrates in algal biomass. Contract, 303, 275-3000.
27. Wang, H., Nche-Fambo, F. A., Yu, Z., & Chen, F. (2018). Using microalgal communities for high CO_2-tolerant strain selection. Algal research, 35, 253-261.
28. Wang, H., Nche-Fambo, F. A., Yu, Z., & Chen, F. (2018). Using microalgal communities for high CO_2-tolerant strain selection. Algal research, 35, 253-261.

TH-2951_166106019

29. Wu, Y. H., Yu, Y., Hu, H. Y., & Zhuang, L. L. (2016). Effects of cultivation conditions on the production of soluble algal products (SAPs) of Scenedesmus sp. LX1. Algal Research, 16, 376-382.

TH-2951_166106019

Chapter 4

Establishment of biorefinery for bioactive molecules, biofuel, and biofertilizer using Tetradesmus obliquus CT02.

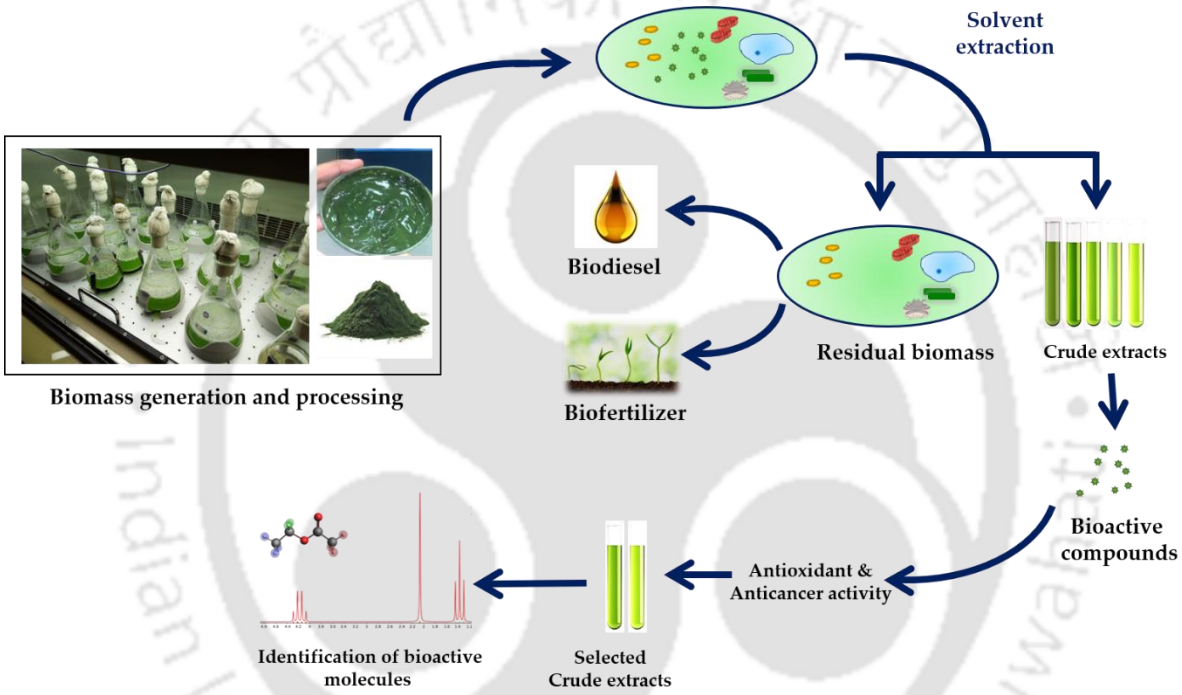

Fig. 4.1 Graphical abstract

4.1. Background and Motivation

Though microalgae have been well documented as feedstock for biofuels, the technology is not completely mature to be realized at the commercial scale owing to low net energy ratio (NER) and sub-optimal economic output [Chisti et. al., 2013]. Microalgal biofuel, one of the most prominent alternatives to the fossil fuel, face major economic challenges in terms of low biomass titer and productivity, biomass harvesting and conversion to biofuel. Many of these steps are high cost and energy intensive, thus hinders the commercialization. To that end,

TH-2951_166106019

biorefineries with sequential multiproduct portfolio are the most promising solutions, implicating efficient utilization of the whole microalgal biomass for co-production of high-value products like biotherapeutics, nutraceuticals, and low value biofuels (biodiesel, bio-crude oil and bioethanol), biofertilizer and bioplastics. With a suitable microalgal strain having diverse pool of macromolecules, the biorefinery strategy can be significantly valorized resulting a positive net energy ratio (NER). For example, *Scenedesmus obliquus* BR003 was sequentially explored for carbohydrate, lipids and pigments as a part of biorefining strategy [Vieira et. al., 2021]. Another study utilized waste water for growth of *Scenedesmus obliquus* and subsequent extraction of high-value products like flavonoids and low-value products like biofuels and biofertilizer [Ferreira et. al., 2019].

In the present study, a biorefinery approach has been established with an indigenous CO_2 tolerant freshwater microalgal isolate *Tetradesmus obliquus* CT02 towards synthesis of bioactive molecules, biofuel, and biofertilizer. The concept of biorefinery with multiple products has been demonstrated in two sequential steps resulting in alternate product cascades: option-1 being bioactive molecules and biodiesel or option-2 being bioactive molecules and biofertilizer. In the first step, solvent-based crude microalgal extracts containing bioactive molecules were screened for their antioxidant and anticancer activities. Crude fractions exhibiting antioxidant and anticancer activities were further characterised through mass spectroscopy to identify the bioactive molecules. The post extracted biomass was subjected to a two-step direct transesterification method for biodiesel production as another product of option-1. In case of option-2, the post extracted biomass obtained from the first step was evaluated for its biofertilizer potential through induced germination of *Solanum lycopersicum* seeds.

TH-2951_166106019

4.2. Materials and Methods

4.2.1. Preparation of microalgal crude extracts

Tetradesmus obliquus CT02 was cultivated under selected nutritional and physicochemical condition (Chapter 3) and the biomass was harvested through centrifugation at 5000 rpm and 4°C. Further, 1 gram finely powered lyophilized biomass was suspended in 50 mL of each of the five solvents *i.e.*, methanol, isopropanol, acetone, ethyl acetate, and hexane. These solvents were chosen based on their difference in polarity (Fig. 4.2). Five different crude extracts were prepared by three rounds of sonication and overnight incubation at 28 °C and 150 rpm, followed by evaporation of the solvent (Fig. 4.2). The crude extracts were stored at 4 °C for subsequent experiments.

4.2.2. Determination of antioxidant activity through DPPH free radical scavenging

The antioxidant activity of the crude extracts was determined in terms of 2,2-diphenyl-1-picrylhydrazyl (DPPH) radical scavenging activity assay [Sen et. al., 2013]. The concentration of each extract required to scavenge 50% of the DPPH (IC_{50}) was calculated based on the correlation (linear regression) between percentage scavenging activity and concentration of the extract. In order to develop the correlation, different concentrations (50 - 1000 µg mL^{-1}) of each crude extract were prepared in methanol. The crude extract in methanol (0.75 mL) was mixed with 0.25 mL of 0.1 mM DPPH, dissolved in methanol, and incubated for 30 min in dark at room temperature. Post incubation, the absorbance of the mixture was recorded at 517 nm. DPPH scavenging activity (%) was calculated as follows:

$$\%\ DPPH\ scavenging\ activity = \frac{A_c - A_t}{A_c} \times 100 \quad (4.1)$$

where A_c is the absorbance of control containing DPPH dissolved in pure methanol and A_t is the absorbance of the test sample together with DPPH.

TH-2951_166106019

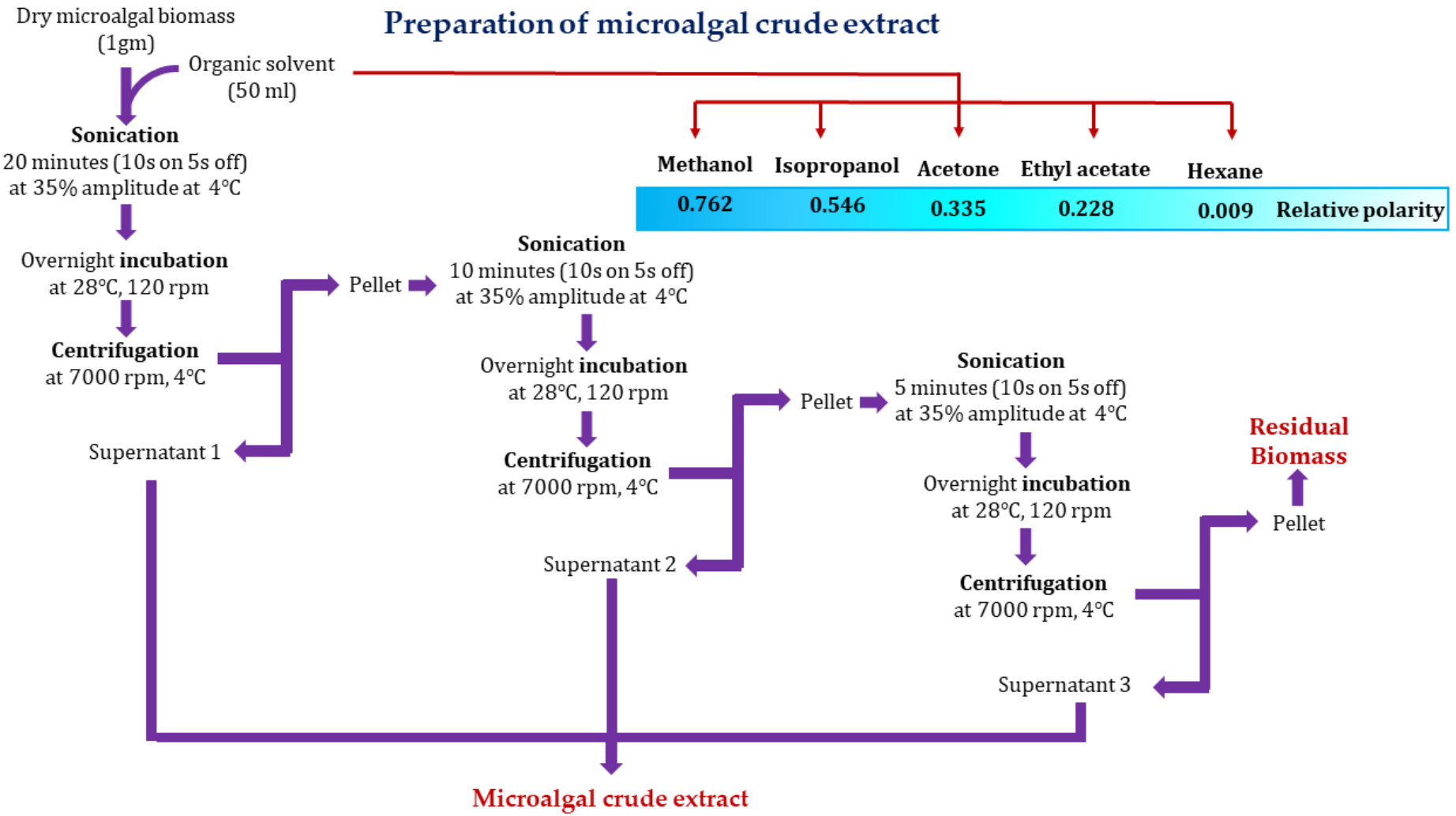

Fig. 4.2. Method for preparation of crude microalgal extracts from *Tetradesmus obliquus* CT02 through solvent extraction

TH-2951_166106019

4.2.3. Screening and estimation of anticancer activity of the crude extracts

The effect of microalgal crude extract on cancer cell growth inhibition was determined *in vitro* through MTT based cell viability assay [Pal et. al., 2020]. In the first step, all five extracts were evaluated for their anticancer activity at a concentration of 100 µg mL^{-1}. Breast cancer cells (MCF7) grown in DMEM high glucose medium, were seeded in 96 well plate (4000 - 5000 cells per well). After 48 h of incubation at 37 °C and 5% v/v CO_2, the monolayer was washed with DPBS. Prior to MTT assay, the cells were treated with the extract or with ethanol (vehicle control) for 72 h. Base line viability was determined by performing the MTT assay for the cells at zero h. Post treatment, monolayer of the cells was washed with DPBS and incubated with 100 µL MTT reagent (0.5 mg mL^{-1}) for 3 h at 37 °C. MTT reagent was then removed, and the formazan crystals were dissolved in DMSO. Absorbance was measured at 570 nm using microplate reader (Infinite Pro M200, Tecan Life Sciences, Switzerland), with 690 nm as the reference. The difference in the absorbance (A_{570} - A_{690}) was considered as the measure for cell viability. Change in viability of ethanol treated cells (control) was assigned as 100%, and those of extract treated cells were expressed as relative to the control. The extract exhibiting highest inhibition to the cell viability was selected for further experiments. The IC_{50} for the selected extract was calculated based on the percentage cell viability observed at different concentrations.

4.2.4. Identification of compounds with antioxidant and anticancer activity using HR-LCMS-QTOF

Phytochemical composition of the selected crude microalgal extracts exhibiting maximum antioxidant and anticancer activities was analysed by high resolution liquid chromatograph mass spectrometer (HR-LCMS,1290 Infinity UHPLC System, Agilent Technologies, USA). The system was aided with Quadrupole Time of Flight Mass Spectrometer (Q-TOF MS). 5 µL sample was injected into the Hypersil Gold C18 column (100 x 2.1 mm – 3 µ particle size). Gradient of water with 0.1% formic acid (solvent A) and acetonitrile with 10% water and 0.1% formic acid (solvent B) was used as mobile phase. With a flow rate of 3 mL min^{-1}, separation was performed

TH-2951_166106019

for 30 min. Compounds were analysed in 6550 iFunnel Q-TOF MS operated in positive ion mode by dual Agilent jet stream electrospray ionization (dual AJS ESI). Mass spectrometric data acquisition was done for the m/z ratio ranging 150 to 1000 with a scanning rate of 1 spectrum per second. Metlin Metabolites AM PCD Library (B.08.00) (Agilent technologies, USA) was used for identification of compounds. The compounds found in abundance were further reviewed for their antioxidant and anticancer activities based on previously reported literatures.

4.2.5. Assessment of post extracted residual microalgal biomass as feedstock for biodiesel production

The FAME content of the post extracted residual microalgal biomass was estimated using sequential two-step direct transesterification method [Muthuraj et. al., 2014]. In the first step, 1 mL alkali catalyst (0.5 N NaOH in methanol) was added to 50 mg of dry biomass followed by incubation at 90 ℃ in a shaker water bath at 150 rpm for 20 min. After cooling down, the second step was performed by adding 1 mL acid catalyst (5% H_2SO_4 in methanol) and incubating at the same conditions. Finally, the FAME fraction was collected by adding equal volume of deionized water and hexane to the transesterified mixture. Hexane layer containing total FAME was washed thrice in order to remove aqueous impurities. The FAME components were analysed using GC-FID (Agilent Technologies, USA). FAME dissolved in hexane was filtered through 0.22 µm nylon filter and injected to GC equipped with HP-5ms Ultra Inert column (30 m × 250 µm × 0.25 µm). Helium was used as carrier gas and the split ratio was set as 10:1. Oven temperature was ramped from 70 ℃ to 180 ℃ at a rate of 15 ℃ min^{-1} and then to 260 ℃ at rate of 2.5 ℃ min^{-1} and the final temperature was held for 5 min. The total runtime for GC-FID analysis was 44.33 min. Supelco 37 component FAME mix (Sigma-Aldrich, USA) was used as the standard for identification and quantification of compounds.

4.2.6. Assessment of post extracted residual microalgal biomass as biofertilizer

TH-2951_166106019

The potential of post extracted residual microalgal biomass as biofertilizer was assessed based on its effect on the germination of *Solanum lycopersicum* (tomato) seeds. In petri plates, 100 gm of air-dried soil (sieved through 2 mm mesh) was mixed with different amounts (11.5 mg, 50 mg, 75 mg, 100 mg, 125 mg, 150 mg, 175 mg, and 200 mg) of residual microalgal biomass or commercial grade NPK (20:20:13) to obtain the different fertilizer doses. Each plate was inoculated with 10 tomato seeds and kept in greenhouse at 25 ℃ temperature and 70% humidity. Fixed amount of tap water was sprinkled on each plate at every 24 h interval. All the plates were monitored for number of seeds germinated every 24 h. At the end of the 10th day, the final germination percentage (FGP) and the germination index (GI) were calculated according to Eq. 4.2 and Eq. 4.3, respectively [Ferreira et. al., 2019].

$$\text{FGP} = \left(\frac{\text{Total no.of seeds germinated at the end of trial}}{\text{number of initial seeds}}\right) \times 100 \qquad (4.2)$$

$$GI = (10 \times \text{N}_1) + (9 \times \text{N}_2) + (8 \times \text{N}_3) + (7 \times \text{N}_4) + (6 \times \text{N}_5) + (5 \times \text{N}_6) + (4 \times \text{N}_7) + (3 \times \text{N}_8) + (2 \times \text{N}_9) + (1 \times \text{N}_{10}) \qquad (4.3)$$

where N_t is the number of seeds germinated on the tth day and value of t varies from 1 to 10. Further to this, NPK content of the residual microalgal biomass was measured to quantitatively establish its biofertilizer capacity. Total nitrogen (N) was determined directly by elemental analyser (EuroEA3000, Italy). Total phosphorus (P) was determined following the procedure described by Feng *et al.,* 2015 and estimated calorimetrically using ascorbic acid method [Parsons et. al., 1984]. For estimation of potassium (K), 10 mL of mixed acid reagent (H_2SO_4:$HCLO_4$::5:1) was added to 0.2 g of biomass and digested at 300 ℃ for 4 h [Jain et. a., 2018]. Quantification of potassium (K) was done using flame photometry.

4.3. Results and Discussion

High protein and lipid content of CT02 under the given nutritional and growth parameters point towards establishing a circular bioeconomy, coupling CO_2 sequestration and multi-product

TH-2951_166106019

portfolio such as high-value bioactive compounds, biofuel, and biofertilizer, in a biorefinery approach. In line with this understanding, the following process sequence was observed.

4.3.1. Evaluation of crude extracts of CT02 for their antioxidant activity

Antioxidants serve as the crucial defence system against free radicals such as reactive oxygen species (ROS) and reactive nitrogen species (RNS) which causes oxidative stress to the cells leading to their death via oxidation of biological macromolecules [Banskota et. al., 2019]. Besides chemically synthesized drugs, several naturally occurring bioactive compounds with antioxidant properties, originating from plants, have been commercially approved [Lourenco et. al., 2019; Sathisha et. al., 2011]. However, increasing market demand owing to population inflammation has motivated the exploration of more cost-effective natural sources like microalgae for these phytochemicals. In the present study, five different solvent based crude extracts of CT02 were evaluated for their antioxidant potential in terms of DPPH free radical scavenging activity (Fig. 4.3). All the five crude extracts exhibited dose-dependent antioxidant activity, with the lowest IC_{50} value of 137 µg mL^{-1} in case of acetone extract. While both isopropanol and ethyl acetate extracts showed antioxidant activity (~ 203 µg mL^{-1}) comparable to that of acetone, hexane extract showed inferior antioxidant activity with an IC_{50} value of 783.2 µg mL^{-1}. Microalgae have been reported to possess a vast range of bioactive compounds which vary in terms of their polarity and thereby solubility in different solvents. This means that the type and concentration of bioactive molecule(s), obtained post solvent extraction, will vary depending on the polarity of the solvent(s) used for the process of extraction. Hence, differential bioactivity may be observed with different solvent extracts. Acetone extract from CT02 recorded superior antioxidant activity in comparison to other microalgae strains such as *Chlorella* sp. with IC_{50} value of 780 - 2590 µg mL^{-1} [Dimova et. al., 2021], *Scenedesmus obliquus* with IC_{50} value of 938 - 2273 µg mL^{-1} [Cengiz et. al., 2019], *Porphyridium sordidum* with IC_{50} value of 286 µg mL^{-1} [Assunção et. al., 2017] and *Haematococcus pluvialis* with IC_{50} value of 528 µg mL^{-1} [Assunção et. al., 2017].

TH-2951_166106019

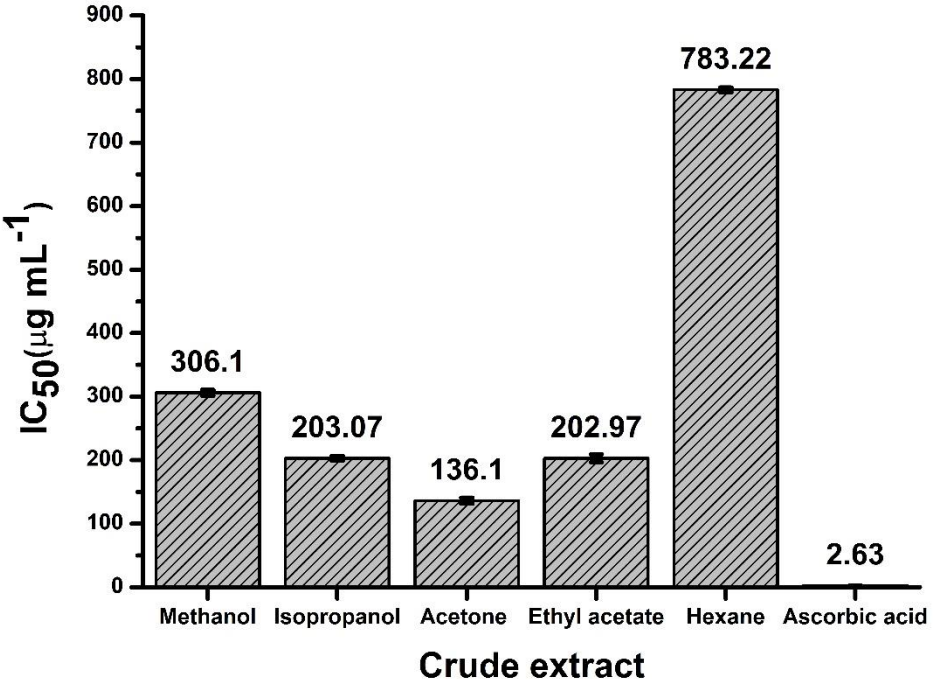

Fig. 4.3. Comparison of antioxidant activity of different crude extracts of *Tetradesmus obliquus* CT02 based on their IC_{50} for DPPH radical scavenging

HR-LCMS-QTOF analysis (Appendix A) of acetone crude extract was carried out to identify the compounds with antioxidant property (Table 4.1). The antioxidant compounds which were found to be present in abundance are fusarochromanone [Ambi et. al., 2021], benzoquinol [Mène et. al., 2010], hexadecanoic acid [Kim et. al., 2020], Nigakihemiacetal A [Jamil et. al., 2020], luciferin [Dubuisson et. al., 2004], convallasaponin A [Salehi et. al., 2020, Puente et. al., 2017], and tridecanol [Dawood et. al., 2020; Shah et. al., 2014]. Further, brassinolide was reported to enhance the activity of antioxidant enzymes in *Chlorella vulgaris* [Bajguz et. al., 2010]. Therefore, the antioxidant activity of acetone extract may be attributed to the coordinated action of these bioactive molecules. The results indicate that acetone extracts of CT02 can be commercially realized as potential sources of antioxidant compounds.

4.3.2. Evaluation of crude extracts of CT02 for their anticancer activity

TH-2951_166106019

In view of the undesired side effects of conventional chemotherapeutic drugs, the pharmaceutical research is now more focused on search for naturally occurring anticancer agents. Crude solvent extracts obtained from CT02 were screened *in vitro* for their anticancer activity.

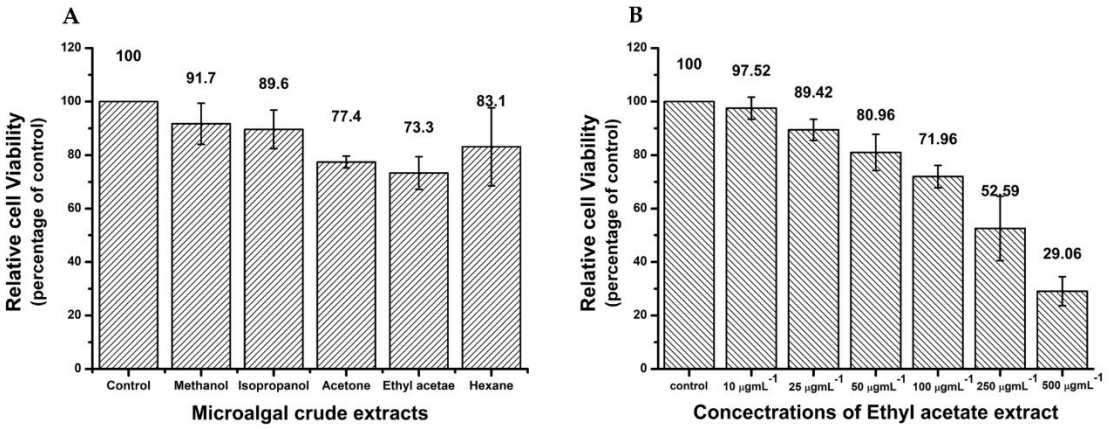

Fig. 4.4 (A) Evaluation of crude extracts of *Tetradesmus obliquus* CT02 for their anticancer activity at a concentration of 100 µgmL-1 and (B) Evaluation of dose dependent anticancer activity of ethyl acetate extract. Experiments were conducted on breast cancer cell line MCF7.

At a concentration of 100 µg mL^{-1}, ethyl acetate extract showed the lowest relative cell viability of 73.3%, followed by acetone (77.4%), hexane (83.1%), isopropanol (89.6%), and methanol (91.7%) (Fig.4.4A). Further, dose-dependent activity of ethyl acetate extract revealed an IC_{50} value of 306.67 µg mL^{-1} (Fig. 4.4B). Similar to the present study, anticancer molecules from

TH-2951_166106019

Table 4.1. List of compounds present in selected crude microalgal extracts for antioxidant and anticancer activity identified via HRLCMS-QTOF

Sl. No.	Name	Formula	Mass	Relative abundance (%) *	References
Antioxidants present in acetone extract					
1	3'-N-Acetyl-4'-O-(14-methylheptadecanoyl) fusarochromanone	$C_{35}H_{56}N_2O_6$	600.41	6.29	Ambi et. al., 2021
2	2-Hexaprenyl-3-methyl-5-hydroxy-6-methoxy-1,4-benzoquinol	$C_{38}H_{58}O_4$	578.43	6.16	Mène et. al., 2010
3	16-Hydroxy hexadecanoic acid	$C_{16}H_{32}O_3$	272.23	5.97	Kim et. al., 2020
4	Nigakihemiacetal A	$C_{22}H_{34}O_7$	410.23	5.71	Jamil et. al., 2020
5	Dinoflagellate luciferin	$C_{33}H_{40}N_4O_6$	588.30	4.86	Dubuisson et. al., 2004
6	Convallasaponin A	$C_{32}H_{52}O_9$	580.37	1.83	Salehi et. al., 2020; Puente et. al., 2017
7	Brassinolide	$C_{28}H_{48}O_6$	480.34	1.74	Bajguz et. al., 2010
8	Tridecan-1-ol	$C_{13}H_{28}O$	200.21	1.36	Dawood et. al., 2020; Shah et. al., 2014
Anticancer agents present in ethyl acetate extract					
1	Dioscin	$C_{45}H_{72}O_{16}$	868.48	20.09	Aumsuwan et. al., 2016
2	(5b,12a), 9-anthracenylmethyl ester, 12-hydroxy- Cholan-24-oic acid	$C_{39}H_{50}O_3$	566.39	18.90	Agarwal et. al., 2016
3	Dinoflagellate luciferin	$C_{33}H_{40}N_4O_6$	588.30	4.97	Kaskova et. al., 2016
4	16-Hydroxy hexadecanoic acid	$C_{16}H_{32}O_3$	272.23	3.73	Kim et. al., 2020
5	Gracillin	$C_{45}H_{72}O_{17}$	883.49	2.58	Min et. al., 2019
6	Phytosphingosine	$C_{18}H_{39}NO_3$	317.29	2.34	Kang et. al., 2017
7	3'-N-Acetyl-4'-O-(14-methylheptadecanoyl) fusarochromanone	$C_{35}H_{56}N_2O_6$	600.41	2.05	Mahdavian et. al., 2014
8	Tridecan-1-ol	$C_{13}H_{28}O$	200.21	1.46	Habila et. al., 2021
9	Decyl butanoate	$C_{14}H_{28}O_2$	228.21	1.45	Han et. al., 2004
10	TG (18:1(11Z)/16:1(9Z)/18:1(11Z)) [iso3]	$C_{55}H_{100}O_6$	856.75	0.31	Aminzadeh et. al., 2017

* Relative abundance (%) $= \frac{abundance\ of\ a\ molecule\ present\ in\ an\ individual\ extract}{\sum abundance\ of\ all\ the\ molecules\ present\ in\ an\ individual\ extract} \times 100$

TH-2951_166106019

various microalgae strains such as *Scenedesmus obliquus, Chlorella sorokiniana, Granulocystopsis* sp., have shown fairly promising clinical significance against cancer cell lines [Marrez et. al. 2019, Martinez et. al., 2018, Tavares et. al., 2020]. HR-LCMS-QTOF analysis (Appendix A) of ethyl acetate crude extract revealed the presence of two most prevalent anticancer compounds dioscin [Aumsuwan et. al., 2016] and cholanoic acid [Agarwal et. al., 2016]. Besides, eight more anticancer molecules were also found to be present in abundance (Table 4.1).

4.3.3. Synthesis of biodiesel from post extracted residual biomass of CT02

Analysis of total lipid content of post extracted residual biomass revealed negligible loss with the total lipid content in case of acetone and ethyl acetate, being 39.1% w/w and 35.7% w/w respectively (Table 4.2). This can be explained by the fact that a major portion of the total microalgal lipid is composed of triacylglycerol, which being non-polar in nature, remains unextracted when polar solvents like acetone and/or ethyl acetate are used. The results suggest that both the residual biomass can be used as suitable feedstock for biodiesel production. A total FAME yield of 36.7% w/w and 33.1% w/w was obtained by direct transesterification of acetone and ethyl extracted biomass respectively (Table 4.2). FAME composition has been reported to influence the fuel properties of biodiesel such as cetane number, viscosity, flow properties, lubricity *etc*. [Cha et. al., 2017]. FAME obtained from both residual biomasses contained palmitic acid (C16:0), stearic acid (C18:0), and elaidic acid (C18:1n9t) as the major constituents (Fig. 4.5), thereby making it suitable for use as biodiesel [Singh et. al., 2020, Kumar et. al., 2014]. The absence of C18:3 or other higher unsaturated fatty acids may be advantageous towards better biodiesel quality as per European standards [Gouveia et. al., 2009]. Further, presence of a high percentage of saturated fatty acids (Table 4.2) may be beneficial in terms of providing higher oxidative stability to biodiesel and improving its performance at low temperature [Aslam et. al., 2018].

TH-2951_166106019

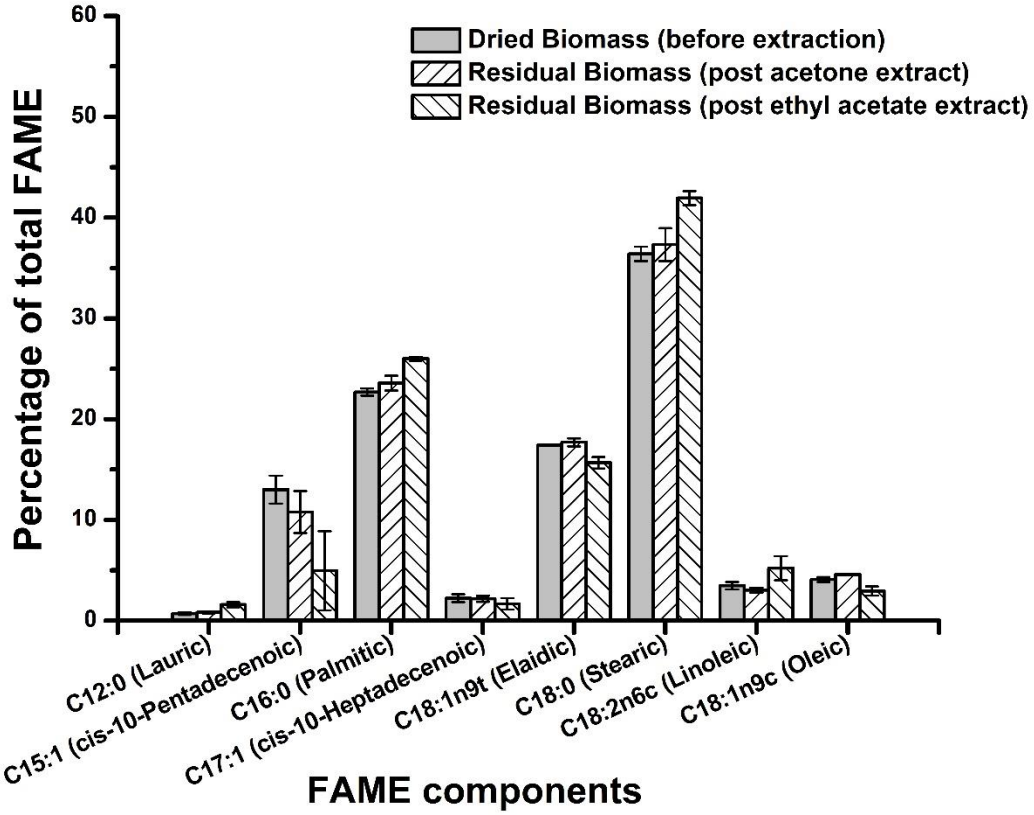

Fig. 4.5 Composition of FAME obtained via direct transesterification of CT02 biomass before and after extraction

Table 4.2 FAME profile obtained via direct transesterification of CT02 biomass, before and after extraction

	Dried biomass (before extraction)	***Residual biomass (post acetone extraction)***	***Residual biomass (post ethyl acetate extraction)***
Total lipid content (Percentage of biomass)	41.2	39.1	35.7
Total FAME content (Percentage of biomass)	38.6 ± 4.2	36.7 ± 2.4	33.1 ± 1.6
Saturated FAME			
(Percentage of total FAME)	59.80 ± 1.19	61.73 ± 2.5	69.54 ± 1.1
(Percentage of biomass)	23.09 ± 1.77	22.65 ± 1.05	23.02 ± 0.79
PUFA			
(Percentage of total FAME)	3.48 ± 0.37	3.03 ± 0.25	5.21 ± 1.2
(Percentage of biomass)	1.34 ± 0.10	1.11 ± .05	1.72 ± 0.06
MUFA			
(Percentage of total FAME)	36.72 ± 2.1	35.24 ± 2.84	25.25 ± 5.5
(Percentage of biomass)	14.17 ± 1.09	12 ± .6	8.36 ± .29

TH-2951_166106019

4.3.4. Application of post extracted residual biomass as biofertilizer

Both the residual biomass, after extraction using acetone and ethyl acetate, has been observed to induce germination of *Solanum lycopersicum* (Tomato) seeds. Compared to control, an increase in final germination percentage (FGP) of 30% and 25% was observed for the residual biomass post acetone and ethyl acetate extraction respectively (Fig. 4.6A). The highest FGP of 80% and 75% was observed for acetone and ethyl extracted biomass at concentrations of 1.25 and 1.5 g per kg soil respectively (Fig. 4.6A). These values were found to be comparable with the FGP value of 85% in case NPK (20:20:13), *albeit* at a lower standard dose of 0.115 g per kg of soil [Mukherjee et., al., 2015]. Based on the daily observation, highest germination index (GI) was recorded to be 118.5 and 117.5 for acetone and ethyl acetate extracted biomass respectively, both at a concentration of 1.25 g per kg of soil (Fig. 4.6A). However, a marginally higher GI value of 150 was calculated for NPK (20:20:13) at a dose of 1g per kg of soil. More than two-fold increase in GI, with respect to control, was observed for both types of residual biomass (Fig. 4.6B). In a similar study, microalgal pellets of *Scenedesmus obliquus* showed approximately 20% increase in FGP and 1.6-fold increase in GI for germination of wheat and barley seeds [Ferrira et. al., 2019]. Elemental composition analysis of both the residual biomass revealed presence of 7 – 8% N, 0.11% P, and 0.5% K (Table 4.3). This N-P-K composition of the post extracted residual biomass of CT02 was found to be similar to that of de-oiled microalgal biomass (DOMBW) of *Scenedesmus* sp. and vermicompost (Table 4.3). While the de-oiled biomass of *Scenedesmus* sp. was demonstrated as a promising biofertilizer for rice production [Nayak et. al., 2019], vermicompost is considered one of the most commercially used biofertilizers [Nayak et. al., 2019]. These results establish the suitability of the post extracted residual biomass of CT02 as biofertilizer.

TH-2951_166106019

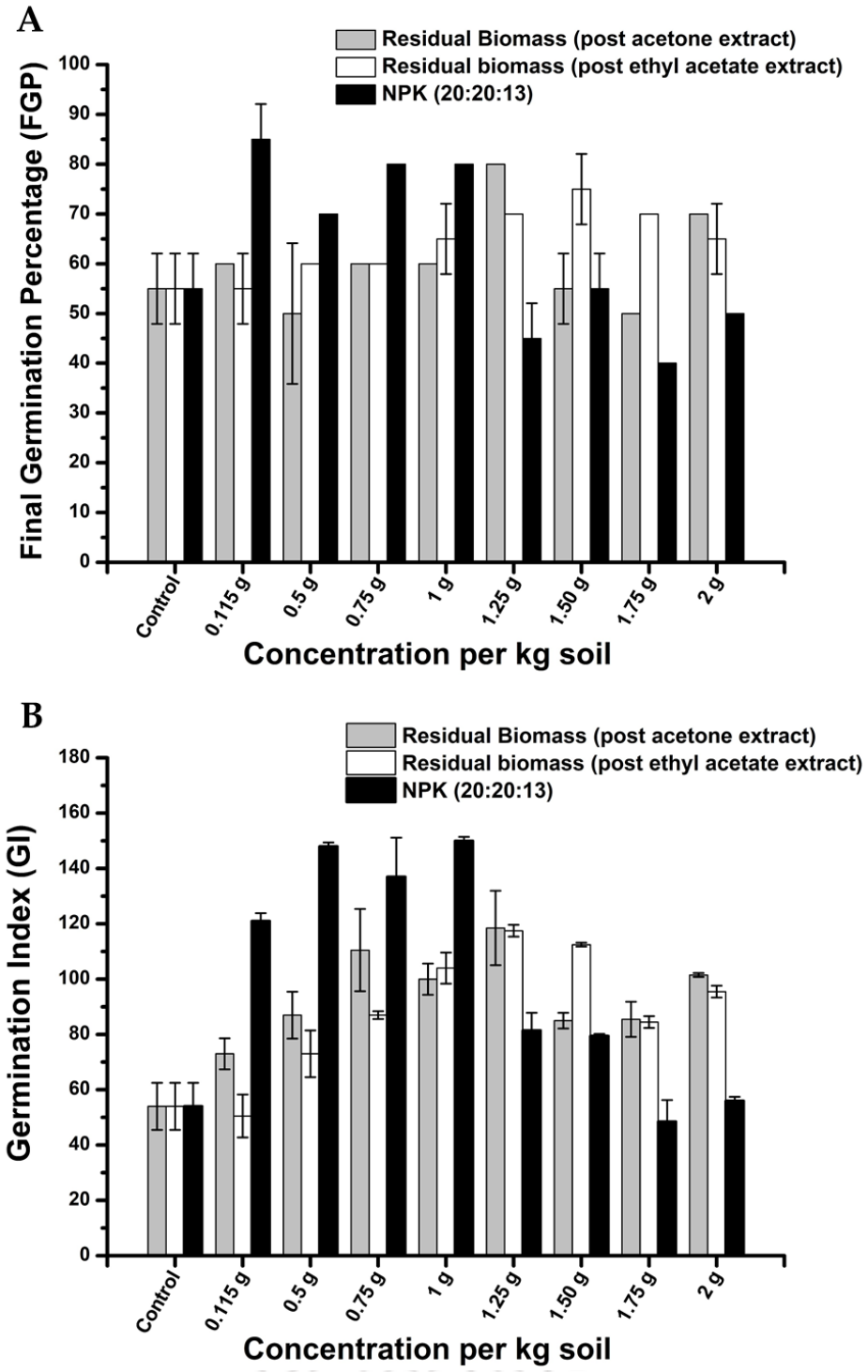

Fig. 4.6 Dose dependent effect of post extracted residual biomass of CT02 and NPK on (A) final germination percentage (FGP) and (B) gemination index (GI) of *Solanum lycopersicum* (tomato) seeds.

TH-2951_166106019

Table 4.3 Elemental composition (N-P-K) of post extracted biomass of CT02, de-oiled microalgal biomass from *Scenedesmus* sp. and vermicompost

Elements (% of biomass)	**Residual biomass post acetone extraction (Current study)**	**Residual biomass post ethyl acetate extraction (Current study)**	**De-oiled microalgal biomass from *Scenedesmus* sp. [**Nayak et. al., 2019**]**	**Vermi compost [**Nayak et. al., 2019**]**
Total N	8.00 ± 0.14	7.30 ± 0.11	7.50 ± 0.08	1.40 ± 0.03
Total P	0.11 ± 0.00	0.12 ± 0.00	1.60 ± 0.03	0.77 ± 0.01
Total K	0.57 ± 0.01	0.50 ± 0.01	0.70 ± 0.02	0.48 ± 0.01

4.4. Conclusions

A microalgal biorefinery approach has been established through bioprospecting of indigenous CO_2 tolerant freshwater isolate *Tetradesmus obliquus* CT02 biomass in two sequential steps, resulting in alternate product cascades of bioactive molecules and biodiesel or biofertilizer. At the onset, different solvent based crude extracts of CT02 biomass resulted in staggeringly high antioxidant activity (IC_{50} value of 137 µg mL^{-1} for acetone extract) and anticancer activity (IC_{50} value of 306.67 µg mL^{-1} for ethyl acetate extract). In the next step, post extracted residual biomass of CT02 yielded high FAME content of 33.1% - 36.7% w/w. Analysis of FAME composition revealed abundance of palmitic acid (C16:0), stearic acid (C18:0), and elaidic acid (C18:1n9t) as the major constituents, proving it suitable for use as biodiesel. When purposed as biofertilizer, the post extracted residual biomass showed significant inductive effect on germination of *Solanum lycopersicum* seeds, comparable to that of commercial grade NPK. In a nutshell, sequential demonstration of CT02 as a cell factory for production of high value bioactive molecules and low

TH-2951_166106019

value biodiesel or biofertilizer designated the strain to be a potential candidate for construction of biorefinery. Furthermore, commercial viability of the process can be enhanced by implantation of process engineering strategies at the cultivation of CT02 aiming high biomass titer and productivity.

References

1. Agarwal, D. S., Anantaraju, H. S., Sriram, D., Yogeeswari, P., Nanjegowda, S. H., Mallu, P., & Sakhuja, R. (2016). Synthesis, characterization and biological evaluation of bile acid-aromatic/heteroaromatic amides linked via amino acids as anti-cancer agents. Steroids, 107, 87-97.
2. Ambi A, Bauchi FP, & Bashir M. (2021) Yellow and Red Varities of *Habiscus sabdariffa* Calyces Contain Novel Antioxidants as Analysed by Liquid Chromatography-Electrospray IonizationTandem Mass Spectrometry (LC-ESI) Acta Scientific NUTRITIONAL HEALTH (ISSN : 2582-1423)
3. Aminzadeh-Gohari, S., Feichtinger, R. G., Vidali, S., Locker, F., Rutherford, T., O'Donnel, M., & Kofler, B. (2017). A ketogenic diet supplemented with medium-chain triglycerides enhances the anti-tumor and anti-angiogenic efficacy of chemotherapy on neuroblastoma xenografts in a CD1-nu mouse model. Oncotarget, 8(39), 64728.
4. Aslam, A., Thomas-Hall, S. R., Manzoor, M., Jabeen, F., Iqbal, M., Uz Zaman, Q., & Tahir, M. A. (2018). Mixed microalgae consortia growth under higher concentration of CO_2 from unfiltered coal fired flue gas: fatty acid profiling and biodiesel production. Journal of Photochemistry and Photobiology B: Biology, 179, 126-133.
5. Assunção, M. F., Amaral, R., Martins, C. B., Ferreira, J. D., Ressurreição, S., Santos, S. D., & Santos, L. M. (2017). Screening microalgae as potential sources of antioxidants. Journal of Applied Phycology, 29(2), 865-877.
6. Aumsuwan, P., Khan, S. I., Khan, I. A., Ali, Z., Avula, B., Walker, L. A., & Dasmahapatra, A. K. (2016). The anticancer potential of steroidal saponin, dioscin, isolated from wild

TH-2951_166106019

yam (*Dioscorea villosa*) root extract in invasive human breast cancer cell line MDA-MB-231 in vitro. Archives of Biochemistry and Biophysics, 591, 98-110.

7. Bajguz, A. (2010). An enhancing effect of exogenous brassinolide on the growth and antioxidant activity in *Chlorella vulgaris* cultures under heavy metals stress. Environmental and Experimental Botany, 68(2), 175-179.
8. Banskota, A. H., Sperker, S., Stefanova, R., McGinn, P. J., & O'Leary, S. J. (2019). Antioxidant properties and lipid composition of selected microalgae. Journal of Applied Phycology, 31(1), 309-318.
9. Chisti, Y. (2013). Constraints to commercialization of algal fuels. Journal of biotechnology, 167(3), 201-214.
10. Dimova, D., Dobreva, D., Panayotova, V., & Makedonski, L. (2021). DPPH antiradical activity and total phenolic content of methanol and ethanol extracts from macroalgae (Ulva rigida) and microalgae (Chlorella). Scripta Scientifica Pharmaceutica, 7(2).
11. Dubuisson, M., Marchand, C., & Rees, J. F. (2004). Firefly luciferin as antioxidant and light emitter: the evolution of insect bioluminescence. Luminescence: the journal of biological and chemical luminescence, 19(6), 339-344.
12. Feng, W., Zhu, Y., Wu, F., Meng, W., Giesy, J. P., He, Z., & Fan, M. (2016). Characterization of phosphorus forms in lake macrophytes and algae by solution 31 P nuclear magnetic resonance spectroscopy. Environmental Science and Pollution Research, 23(8), 7288-7297.
13. Ferreira, A., Ribeiro, B., Ferreira, A. F., Tavares, M. L., Vladic, J., Vidović, S., & Gouveia, L. (2019). *Scenedesmus obliquus* microalga-based biorefinery–from brewery effluent to bioactive compounds, biofuels and biofertilizers–aiming at a circular bioeconomy. Biofuels, Bioproducts and Biorefining, 13(5), 1169-1186.
14. Gouveia, L., & Oliveira, A. C. (2009). Microalgae as a raw material for biofuels production. Journal of industrial microbiology and biotechnology, 36(2), 269-274.

TH-2951_166106019

15. Habila, M. M., Festus, E. A., Morumda, D., Joseph, I., Chinonso, A. D., & Sunday, A. M. FTIR and GC-MS Analysis of the Aqueous and Ethanolic Extracts of Jatropha tanjorensis Leaves.
16. Han, H. S., Kwon, Y. J., Park, S. H., Kim, E. J., Rho, Y. S., Sin, H. S., & Um, S. J. (2004). Potent effect of 5-HPBR, a butanoate derivative of 4-HPR, on cell growth and apoptosis in cancer cells. International journal of cancer, 109(1), 58-64.
17. Jain, M. S., Jambhulkar, R., & Kalamdhad, A. S. (2018). Biochar amendment for batch composting of nitrogen rich organic waste: Effect on degradation kinetics, composting physics and nutritional properties. Bioresource technology, 253, 204-213.
18. Kang, H. M., Son, H. S., Cui, Y. H., Youn, B., Son, B., Kaushik, N. K., & Lee, S. J. (2017). Phytosphingosine exhibits an anti-epithelial–mesenchymal transition function by the inhibition of EGFR signaling in human breast cancer cells. Oncotarget, 8(44), 77794.
19. Kaskova, Z. M., Tsarkova, A. S., & Yampolsky, I. V. (2016). 1001 lights: luciferins, luciferases, their mechanisms of action and applications in chemical analysis, biology and medicine. Chemical Society Reviews, 45(21), 6048-6077.
20. Kim, B. R., Kim, H. M., Jin, C. H., Kang, S. Y., Kim, J. B., Jeon, Y. G., & Han, A. R. (2020). Composition and antioxidant activities of volatile organic compounds in radiation-bred Coreopsis cultivars. Plants, 9(6), 717.
21. Kumar, V., Muthuraj, M., Palabhanvi, B., Ghoshal, A. K., & Das, D. (2014). High cell density lipid rich cultivation of a novel microalgal isolate *Chlorella sorokiniana* FC6 IITG in a single-stage fed-batch mode under mixotrophic condition. Bioresource technology, 170, 115-124.
22. Lourenço, S. C., Moldão-Martins, M., & Alves, V. D. (2019). Antioxidants of natural plant origins: From sources to food industry applications. Molecules, 24(22), 4132.
23. Mahdavian, E., Palyok, P., Adelmund, S., Williams-Hart, T., Furmanski, B. D., Kim, Y. J., & Clifford, J. L. (2014). Biological activities of fusarochromanone: a potent anti-cancer agent. BMC research notes, 7(1), 1-11.

TH-2951_166106019

24. Marrez, D. A., Naguib, M. M., Sultan, Y. Y., & Higazy, A. M. (2019). Antimicrobial and anticancer activities of *Scenedesmus obliquus* metabolites. Heliyon, 5(3), e01404.
25. Mène-Saffrané, L., Jones, A. D., & DellaPenna, D. (2010). Plastochromanol-8 and tocopherols are essential lipid-soluble antioxidants during seed desiccation and quiescence in Arabidopsis. Proceedings of the National Academy of Sciences, 107(41), 17815-17820.
26. Min, H. Y., Jang, H. J., Park, K. H., Hyun, S. Y., Park, S. J., Kim, J. H., & Lee, H. Y. (2019). The natural compound gracillin exerts potent antitumor activity by targeting mitochondrial complex II. Cell death & disease, 10(11), 1-18.
27. Mohd Jamil, M. D. H., Taher, M., Susanti, D., Rahman, M. A., & Zakaria, Z. A. (2020). Phytochemistry, traditional use and pharmacological activity of *Picrasma quassioides*: a critical reviews. Nutrients, 12(9), 2584.
28. Mukherjee, C., Chowdhury, R., & Ray, K. (2015). Phosphorus recycling from an unexplored source by polyphosphate accumulating microalgae and cyanobacteria—a step to phosphorus security in agriculture. Frontiers in microbiology, 6, 1421.
29. Muthuraj, M., Kumar, V., Palabhanvi, B., & Das, D. (2014). Evaluation of indigenous microalgal isolate *Chlorella* sp. FC2 IITG as a cell factory for biodiesel production and scale up in outdoor conditions. Journal of Industrial Microbiology and Biotechnology, 41(3), 499-511.
30. Nayak, M., Swain, D. K., & Sen, R. (2019). Strategic valorization of de-oiled microalgal biomass waste as biofertilizer for sustainable and improved agriculture of rice (Oryza sativa L.) crop. Science of The Total Environment, 682, 475-484.
31. Pal, U., Ghosh, S., & Limaye, A. M. (2020). DNA methylation in the upstream CpG island of the GPER locus and its relationship with GPER expression in colon cancer cell lines. Molecular Biology Reports, 47(10), 7547-7555.
32. Parsons, T. R., Maita, Y., & Lalli, C. M. (1984). Determination of phosphate. A manual of chemical and biological methods for seawater analysis, 22-25.

TH-2951_166106019

33. Puente-Garza, C. A., Meza-Miranda, C., Ochoa-Martínez, D., & García-Lara, S. (2017). Effect of in vitro drought stress on phenolic acids, flavonols, saponins, and antioxidant activity in *Agave salmiana*. Plant physiology and biochemistry, 115, 400-407.
34. Reyna-Martinez, R., Gomez-Flores, R., López-Chuken, U., Quintanilla-Licea, R., Caballero-Hernandez, D., Rodríguez-Padilla, C., & Tamez-Guerra, P. (2018). Antitumor activity of *Chlorella sorokiniana* and *Scenedesmus* sp. microalgae native of Nuevo León State, México. PeerJ, 6, e4358.
35. Sahin, S. C. (2019). *Scenedesmus obliquus*: a potential natural source for cosmetic industry. International Journal of Secondary Metabolite, 6(2), 129-136.
36. Salehi, B., Azzini, E., Zucca, P., Maria Varoni, E., V Anil Kumar, N., Dini, L., & Sharifi-Rad, J. (2020). Plant-derived bioactives and oxidative stress-related disorders: A key trend towards healthy aging and longevity promotion. Applied Sciences, 10(3), 947.
37. San Cha, T., Chen, J. W., Goh, E. G., Aziz, A., & Loh, S. H. (2011). Differential regulation of fatty acid biosynthesis in two *Chlorella* species in response to nitrate treatments and the potential of binary blending microalgae oils for biodiesel application. Bioresource Technology, 102(22), 10633-10640.
38. Sathisha, A. D., Lingaraju, H. B., & Prasad, K. S. (2011). Evaluation of antioxidant activity of medicinal plant extracts produced for commercial purpose. E-Journal of Chemistry, 8(2), 882-886.
39. Sen, S., De, B., Devanna, N., & Chakraborty, R. (2013). Total phenolic, total flavonoid content, and antioxidant capacity of the leaves of Meyna spinosa Roxb., an Indian medicinal plant. Chinese journal of natural medicines, 11(2), 149-157.
40. Shah, M. D., Seelan, J. S. S., & Iqbal, M. (2020). Phytochemical investigation and antioxidant activities of methanol extract, methanol fractions and essential oil of *Dillenia suffruticosa* leaves. Arabian Journal of Chemistry, 13(9), 7170-7182.

TH-2951_166106019

41. Shah, M. D., Yong, Y. S., & Iqbal, M. (2014). Phytochemical investigation and free radical scavenging activities of essential oil, methanol extract and methanol fractions of *Nephrolepis biserrata*. Int. J. Pharm. Pharm. Sci, 6(9), 269-277.
42. Singh, N., Goyal, A., & Moholkar, V. S. (2020). Microalgal bio-refinery approach for utilization of *Tetradesmus obliquus* biomass for biodiesel production. Materials Today: Proceedings, 32, 760-763.
43. Tavares-Carreón, F., De la Torre-Zavala, S., Arocha-Garza, H. F., Souza, V., Galán-Wong, L. J., & Avilés-Arnaut, H. (2020). In vitro anticancer activity of methanolic extract of *Granulocystopsis* sp., a microalgae from an oligotrophic oasis in the Chihuahuan desert. PeerJ, 8, e8686.
44. Vieira, B. B., Soares, J., Amorim, M. L., Bittencourt, P. V. Q., de Cássia Superbi, R., de Oliveira, E. B., & Martins, M. A. (2021). Optimized extraction of neutral carbohydrates, crude lipids and photosynthetic pigments from the wet biomass of the microalga *Scenedesmus obliquus* BR003. Separation and Purification Technology, 269, 118711.

TH-2951_166106019

Chapter 5

Development of process engineering strategy for high cell density cultivation of Tetradesmus obliquus CT02 coupled with CO_2 sequestration.

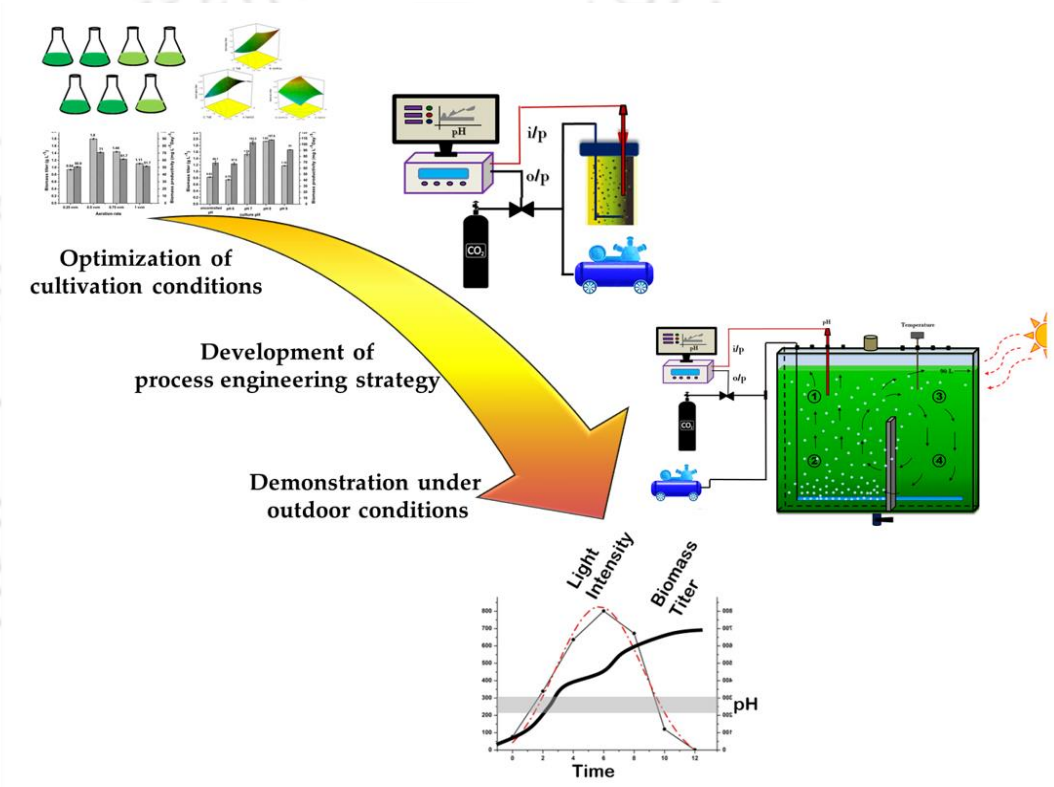

Fig. 5.1 Graphical abstract

5.1 Background and Motivation

The global concern for alarming increase in carbon footprint, especially the atmospheric CO_2 concentration, has mandated the search for feasible carbon capture strategies (CCS). In contrast to the hazardous and energy intensive chemical methods, biological methods using microbial cell factories offer natural and sustainable solution for CO_2 sequestration [Yaashikaa, et. al., 2019, Singh et. al., 2019]. Microalgae, the microorganism capable of simultaneous CO_2 mitigation and

TH-2951_166106019

generation of multiple product array, have gained impetus for building sustainable biorefineries. With the ease of cultivation and multiproduct paradigm, the commercialization potential of microalgae has been immensely encouraged by the scientific community.

In spite of all this advantages, there are handful of commercial scale processes in place for CO_2 sequestration and synthesis of value-added compounds or bulk chemicals using microalgae. The key limitations leading to this status quo are, lack of suitable microalgae strains which can tolerate and grow at higher CO_2 concentration and lower biomass titer and productivity under fluctuating outdoor conditions, which considered to be economical way of biomass generation by harvesting the natural sunlight. To that end, development of optimal process engineering strategies targeting better biomass titer or productivity coupled with improved CO_2 sequestration are vital. Rigorous attempts are being made to upregulate the factors like CO_2 fixation rate [Cabello et. al., 2017], substrate utilization [Goswami et. al., 2019], light availability to cells [Muthuraj et. al., 2015]. and mass transfer of CO_2 [Gonçalves et. al., 2016; Qiu et. al., 2017] towards improved biomass generation. The culture pH, with direct control on solubility of CO_2 and nutrients, stands as one of the most critical factors for the dynamics of microalgal growth [Qiu et. al., 2017]. Several reports also revealed the effect of pH on cell metabolism which has impact on biomass composition i.e., protein and lipid content [Qiu et. al., 2017; Difusa et. al., 2017,8]. Owing to these facts, designing a suitable process engineering strategy for controlling pH in microalgae cultivation is the need of the hour. Further, in order to realize the process engineering strategy at commercial scale, it is important to be validated at large scale and under fluctuating environmental conditions.

5.2. Materials and Methods

5.2.1. Microorganism and inoculum preparation

The indigenous CO_2 tolerant microalga strain *Tetradesmus obliquus* CT02 was subjected to experimentation in search of suitable process engineering strategy for improved biomass titer and productivity. Inoculum for all laboratory scale experiments was prepared by growing the cells in

TH-2951_166106019

algae culture broth (ACB) medium containing (g L^{-1}) $NaNO_3$, 1; K_2HPO_4, 0.25; $MgSO_4$, 0.513; NH_4Cl, 0.050; $CaCl_2$, 0.058; $FeCl_3$, 0.003; in 250 mL Erlenmeyer flasks with working volume of 100 mL, incubated at 28°C temperature and 150 rpm agitation in a shaker incubator (Multitron-Pro, Infors HT, Switzerland). Light intensity was maintained at 50 µE $m^{-2}s^{-1}$ with a light: dark cycle of 16:8 h. For experiments in 100 L airlift photobioreactor, inoculum was prepared using ACB medium in 7.5 L automated photobioreactor (Bioflo115®, Eppendorf, Germany) with 5 L working volume, operated at 200 rpm agitation and 0.5 vvm (volume of air per volume of culture per min) aeration rate. Culture pH was maintained at 8 through automated on-demand supply of CO_2. Light intensity was maintained at 250 µE $m^{-2}s^{-1}$ with a light: dark cycle of 16:8 h. In the present study, inoculum size of 10%, v/v was used for all the experiments.

5.2.2. Media engineering for maximization of biomass titer

With an aim to improve the final biomass titer, response surface methodology (RSM) based 3 factors and 5 levels central composite design (CCD) was employed for optimizing the concentration of key media components such as initial nitrate ($NaNO_3$) concentration, initial phosphate (K_2HPO_4) concentration and initial TME (trace and micro element comprising $MgSO_4$; NH_4Cl; $CaCl_2$ and $FeCl_3$) concentration. 1 unit of TME comprised (g) $MgSO_4$, 0.513; NH_4Cl, 0.050; $CaCl_2$, 0.058; $FeCl_3$, 0.003. Design-Expert® version 7 (Stat-ease Inc., USA) was used for entire design and analysis purpose. Table 5.1 depicts the coded and actual values of the factors where +α, +1 (high); 0 (medium); and–1, −α (Low); correspond to high, medium, and low levels of the variables, respectively. The CCD predicted 19 experimental combinations (Table 5.2) comprising eight factorial points, six axial points and five replicates of centre points. Experiments were performed in shake flask maintained at the same conditions as detailed in section 2.1 and samples were withdrawn at the end of every light cycle to monitor the growth. All subsequent experiments were performed using optimized ACB medium.

TH-2951_166106019

Table 5.1. Different levels (actual and coded experimental values) of each parameter used in response surface design for the maximization of biomass titer.

FACTORS	MEDIA COMPONENTS	UNITS	-ALPHA	-1	0	+1	+ALPHA
A	**Initial Nitrogen ($NaNO_3$) concentration**	**g L^{-1}**	0.5	0.7	1	1.3	1.5
B	**Initial phosphate (KH_2PO_4) concentration**	**g L^{-1}**	0.15	0.19	0.25	0.31	0.35
C	**Initial trace and micro element (TME) concentration**	**Unit L^{-1}**	0.5	0.7	1	1.3	1.5

5.2.3. Growth of CT02 under varied input aeration rate

In order to determine the optimum input aeration rate for growth, CT02 was characterized under four different flow rates of the inlet air stream: 0.25, 0.5, 0.75, and 1 vvm. Experiments were conducted in bubble column photobioreactor (Spectrochem Instruments, India) of 500 mL with working volume of 400 mL. The culture was grown in optimized ACB medium with constant light intensity of 250 µE $m^{-2}s^{-1}$ and light: dark cycle of 16:8 h, maintained with warm white LED. Sample was drawn at the end of every light cycle for analysis of growth. Biomass productivity (P, mg L^{-1} d^{-1}) was calculated using Eq. (1).

$$P = \frac{X_{max} - X_i}{T_{max}} \quad (1)$$

Where, X_{max} and X_i are the maximum and initial biomass concentration (g L^{-1}), respectively. T_{max} is the time required to reach maximum biomass titer (X_{max}).

TH-2951_166106019

Table 5.2. Full factorial, central composite design matrix of three variables along with the response, biomass titer.

Standard Order	*Initial nitrate concentration (g L^{-1})*	*Initial phosphate concentration (g L^{-1})*	*Initial TME concentration (units L^{-1})*	*Biomass titer (gL^{-1})*	
				Observed	**Predicted**
1	0.70	0.19	0.70	1.183	1.180
2	1.30	0.19	0.70	1.130	1.120
3	0.70	0.31	0.70	1.351	1.280
4	1.30	0.31	0.70	1.388	1.360
5	0.70	0.19	1.30	0.907	0.920
6	1.30	0.19	1.30	1.086	1.100
7	0.70	0.31	1.30	1.031	1.030
8	1.30	0.31	1.30	1.377	1.350
9	0.50	0.25	1.00	0.932	0.930
10	1.50	0.25	1.00	1.133	1.140
11	1.00	0.15	1.00	1.079	1.070
12	1.00	0.35	1.00	1.355	1.370
13	1.00	0.25	0.50	1.339	1.360
14	1.00	0.25	1.50	1.144	1.130
15	1.00	0.25	1.00	1.210	1.190
16	1.00	0.25	1.00	1.193	1.190
17	1.00	0.25	1.00	1.191	1.190
18	1.00	0.25	1.00	1.195	1.190
19	1.00	0.25	1.00	1.189	1.190

5.2.4. Growth of CT02 under different pH of the culture

To evaluate the effect of culture pH on the growth performance of CT02, batch cultivation was conducted at five different static pH i.e. 6,7,8,9 and10. Experiments were performed in 7.5 L automated bioreactor (Bioflo115®, eppendorf, Germany) with working volume of 3 L and light intensity was maintained at 250 µE $m^{-2}s^{-1}$ with a light: dark cycle of 16:8 h. Input aeration was maintained at optimal value obtained from the previous experiments and fixed agitation of 200 rpm was introduced for better mixing. For precise maintenance of culture pH throughout entire period of cultivation, 0.5 Molar HCL and 0.5 Molar NaOH solution was fed to the reactor through feedback loop with pH sensor. Sample was taken at the end of each light phase and analysed for determination of biomass titer and productivity.

TH-2951_166106019

5.2.5. Effect of simulated diurnal variation of light intensity on growth and culture pH of CT02

With the aim of large-scale cultivation of the strain under outdoor condition, experiments were designed to analyse the influence of diurnal variation in incident light intensity on the interconnected dynamics of light intensity, growth and culture pH. In order to mimic the diurnal light pattern of outdoor condition, real time sunlight intensity data was recorded at an interval of 2 hr for the daytime at different days for two different seasons i.e., summer (April to August) and winter (November to February). Average of the dynamic light intensity profile for different days were then fitted using Gauss amp distribution function and simulated profiles for variation in light intensity at different time points of a day in summer and winter were obtained via regression analysis (Fig. 5.2). Two parallel batch experiments were set up to obtain dynamics of growth and variation of culture pH under the simulated diurnal variation of light intensity in two different seasons. The organism was cultivated in bubble column photobioreactor as described in section 5.2.3 and aeration rate at its optimal value was maintained throughout the batch. The light: dark cycle of 12:12 h was implemented and the incident light intensity was changed at every 2 hr during 12 hr of light phase, according to the simulated sunlight profiles of different seasons. Segments of exponential growth phase were closely monitored for change in biomass concentration and culture pH.

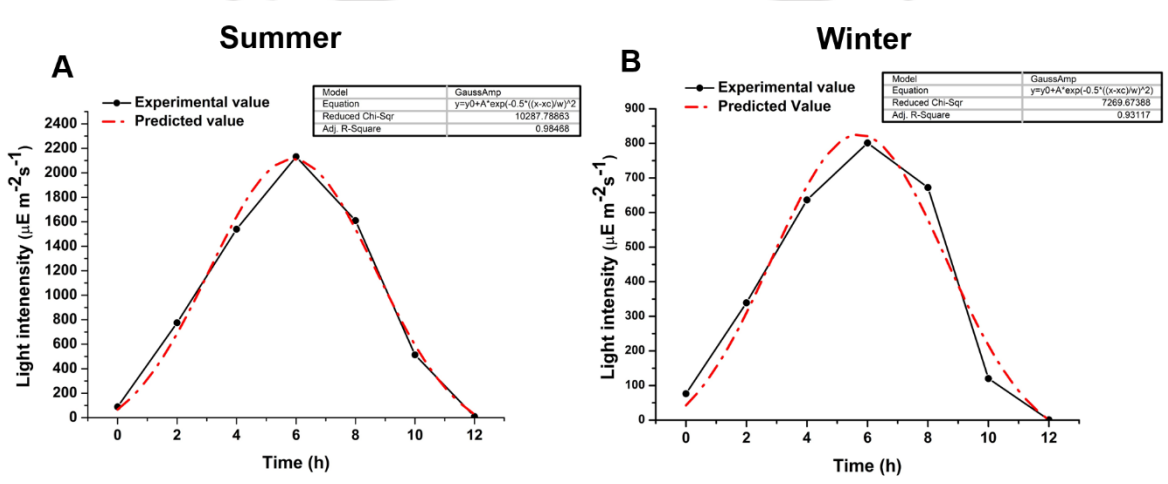

Fig. 5.2 Simulated profile of diurnal variation in sunlight intensity for (A) summer and (B) winter season.

TH-2951_166106019

Specific growth rate (μ, h^{-1}) of the organism was calculated based on biomass titer using Eq. (2).

$$\mu = \frac{\ln\left(\frac{X_2}{X_1}\right)}{T_2 - T_1} \quad (2)$$

Where, X_1 and X_2 are the biomass concentration (g L^{-1}) at time (h) T_1 and T_2, respectively.

5.2.6. Cultivation of CT02 under diurnal variation of light intensity coupled with pH based CO_2 feeding

Based on the understanding (as obtained from the previous experiments in the section 5.2.5) of interdependent dynamics of light intensity, growth and culture pH, cultivation of the strain with improved biomass titer and productivity was targeted by employing a process engineering strategy, based on on-demand supply of CO_2 for maintaining optimal culture pH and under diurnal variation of light intensity. The strain was grown under batch mode in bubble column photobioreactor with working volume of 400 mL, maintaining the optimal aeration rate of 0.5 vvm and with the variation of incident light intensity as per the simulated profile for the winter season (light: dark cycle of 12:12 h). The pH of the culture was maintained at its optimal value of 8, via cascade control with CO_2 feeding using solenoid valve which was guided by the pH sensor. The growth performance of the strain under the application of process engineering strategy was compared with the batch with uncontrolled pH and without feeding of pure CO_2 at any point of time. Both the batches were monitored for their growth at the beginning of every light cycle and the culture pH was recorded online at every 10 min interval for the whole cultivation period. CO_2 fixation rate (R_{CO_2}, mg L^{-1} day^{-1}) was calculated using Eq. (3)

$$R_{CO_2} = C_C P \frac{M_{CO_2}}{M_C} \quad (3)$$

where, C_C is elemental carbon content of biomass. M_{CO_2} and M_C are the molar mass of CO_2 and C (g mol^{-1}), respectively.

TH-2951_166106019

5.2.7. Cultivation of CT02 in 100 L airlift bioreactor under outdoor fluctuating environmental condition

Growth performance evaluation of the strain under outdoor condition was carried out in 100 L flat plate airlift bioreactor (FP-ABR) with working volume of 90 L (Fig. 5.3). The FP-ABR was built using 8 mm thick transparent acrylic panels with dimensions of 75 (H)× 90 (L)× 15 cm (W) and equipped with the automated CO_2 based pH control and pH data logging facility. The batch with optimal static pH was fed with pure CO_2 as per the feedback control with pH sensor, while the batch with uncontrolled pH had no input CO_2 except its normal presence in air.

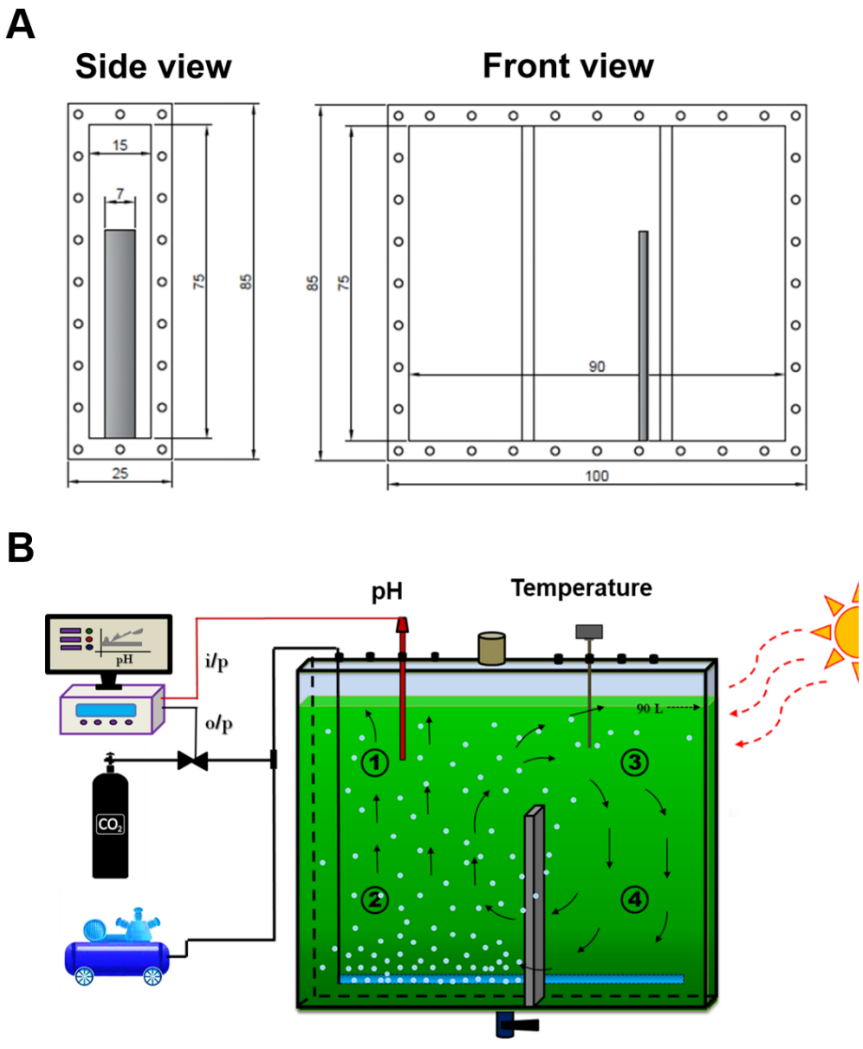

Fig. 5.3. Schematic diagram of 100 L FP-ABR showing (A) dimensions (in cm) used for construction of the bioreactor; (B) working principle of the bioreactor including pH based CO_2 feeding system and mixing pattern.

TH-2951_166106019

Aeration rate required for the scaled-up condition was calculated based on the criteria of equal volumetric power consumption rate ($\frac{P_G}{V_L}$) for both laboratory scale bubble column reactor and large-scale FP-ABR [Guler et. al., 2019].

The volumetric power consumption rate was calculated using Eq. (4)

$$\frac{P_G}{V_L} = \rho_L \times g \times U_G \quad (4)$$

where P_G is the power supply by aeration (J s^{-1}), V_L is the volume of culture medium (L), ρ_L is the density of the liquid (kg m^{-3}), g is the gravitational acceleration (m s^{-2}), and U_G is the superficial gas velocity in the aerated zone (m s^{-1}). The volumetric aeration rate was calculated from its corelation with superficial gas velocity (U_G) according to Eq. (5).

$$U_G = \frac{Q}{A_C} \quad (5)$$

Where Q is the volumetric gas flow rate (m^3) and A_C is the cross-sectional area (m^2).

As the volumetric power requirement ($\frac{P_G}{V_L}$) is constant for both the bubble column photobioreactor and FP-ABR.

So, $\rho_{L_1} \times g \times U_{G_1} = \rho_{L_2} \times g \times U_{G_2}$

Where ρ_{L_1} = density of the liquid in bubble column photobioreactor

U_{G_1} = superficial gas velocity in bubble column photobioreactor

ρ_{L_2} = density of the liquid in FP-ABR

U_{G_2} = superficial gas velocity in FP-ABR

g =gravitational acceleration (m s^{-2})

For bubble column photobioreactor,

Radius (r) = 0.036 m

$A_{C_1} = (\pi \times 0.036^2)\ m^2$

$= 0.0041\ m^2$

TH-2951_166106019

$Q_1 = 0.2\ L\ min^{-1}$ (0.5 vvm for 0.4 L culture volume)

$= 0.000003\ m^3\ s^{-1}$

$$U_{G_1} = \frac{Q_1}{A_{C_1}}$$

$= 0.00074\ m\ s^{-1}$

Assuming negligible change in culture density compared to density of water for both the cultivation system,

$U_{G_1} = U_{G_2}$

For flat plate airlift bioreactor (FP-ABR),

Length (L) = 0.9 m

Width (W) = 0.15 m

$A_{C_2} = 0.9 \times 0.15\ m^2$

$= 0.135\ m^2$

So, $Q_2 = \frac{U_{G_2}}{A_{C_2}}$

$= 5.994\ Lmin^{-1}$

$\approx 6\ Lmin^{-1}$

The experiments were carried out from 06th July 2021 to 19th August 2021. The growth of the culture was measured at every 4 h interval for the 12 h of daytime starting from 4:30 AM (Approximate time of sunrise). The incident sunlight intensity (Average of intensity at 4 equidistant points for each side of the reactor surface, Fig. 5.3B) and culture temperature was recorded at every 2 h for the daytime from 4:30 AM to 6:30 PM. Utilization of nitrate and phosphate was monitored every day by analysing the culture sample collected at sunrise.

5.2.8. Analysis of growth and substrate utilization

The growth of the organism was determined by measuring the optical density at 690 nm (OD_{690}) using UV-Vis spectrophotometer (Cary 100, Agilent Technologies, USA). Biomass concentration was calculated using the experimentally established linear correlation, 1 OD_{690} = 0.1853 g dry cells L^{-1} (R^2 = 0.99). For analysis of substrate utilization, known volume of sample was

TH-2951_166106019

centrifuged at 10000 rpm for 10 minutes and the cell supernatant was collected and subjected to chemical assays.

5.2.8.1. Analysis of phosphate utilization

Phosphate estimation was carried out using ascorbic acid method with potassium hydrogen phosphate (dibasic) as standard [Persons et. al., 1984]. Combined reagent (0.16 mL) comprising (5 N) sulfuric acid, (0.018 M) antimony potassium tartrate, (0.102 M) ammonium molybdate and (0.1 M) ascorbic acid was used for estimating the phosphate content in the supernatant of 1mL. The absorbance was read at 880 nm after incubation for 10 minutes at room temperature.

5.2.8.2. Analysis of nitrate utilization

Estimation of nitrate present in the supernatant was done using salicylic acid method and keeping sodium nitrate as the standard [Cataldo et. al., 1975]. In this method, 0.1 mL of the supernatant was mixed with 0.4 mL of 5 % (w/v) salicylic acid in sulfuric acid followed by incubation for 20 minutes at room temperature which yields a yellow-coloured solution after neutralization with 9.5 mL of 2N NaOH. The absorbance was observed at 410 nm after cooling the tubes to room temperature.

5.3. Results and Discussion

5.3.1. Optimization of cultivation conditions for growth of CT02

5.3.1.1. Media engineering for maximization of biomass

Statistical model-based optimization method is preferred over conventional one as it considers the interaction between input parameters and also rationally search their optimal value throughout the input range. To that end, the media components for growth of CT02 were optimized using response surface methodology (RSM) based central composite design (CCD) where a total of 19 experiments were performed. The biomass titres obtained from these experiments were used as response towards development of quadratic model. The estimated regression coefficients and their significance (p-value) as obtained from Analysis of Variance (ANOVA) is shown in Table 5.3. All linear, square and interaction terms of the model were found to be significant except the

TH-2951_166106019

interaction between initial concentration of phosphate and TME. The significance of the model was depicted by high regression coefficient (R^2 of 0.99). The model was rationally expressed as second order polynomial equation (Eq.6) which depicted the relationship between biomass titer and media components. Interactive effect of the media components on the biomass titer is shown as 3D surface plot (Fig. 5.4).

$$\text{Biomass Titer} = 1.19 + 0.064 \times A + 0.089 \times B - 0.069 \times C + 0.035 \times AB + 0.060\ AC + 0.003 \times BC - 0.054 \times A^2 + 0.012 \times B^2 + 0.02 \times C^2 \quad (6)$$

Further, validation of the model was confirmed by comparing the predicted biomass titer (1.38 g L^{-1}) with the experimental value (1.35 g L^{-1}) at optimized concentration of nitrate (1.11 g L^{-1}), phosphate (0.31 g L^{-1}) and TME (0.71unit L^{-1}). CCD-RSM based optimization of the process variables resulted in 36.8% increase in biomass titer while compared to un-optimized condition. Similar to the present study, various studies have shown CCD-RSM based media optimization as an effective strategy towards improvement in biomass titer [Makut et. al., 2019; Verma et. al., 2020; Fawzy et. al., 2017].

Table 5.3. Analysis of variance (ANOVA) for the selected quadratic model of biomass titer.

Source	Sum of Squares	Degree of freedom (d_f)	Mean Square	F value	p-value Prob > F
Model	0.3214	9	0.03571	140.456	< 0.0001
A-nitrate	0.0559	1	0.05585	219.670	< 0.0001
B-phosphate	0.1074	1	0.10740	422.409	< 0.0001
C-TME	0.0646	1	0.06461	254.125	< 0.0001
AB	0.0100	1	0.01001	39.375	0.0001
AC	0.0292	1	0.02916	114.694	< 0.0001
BC	0.0001	1	0.00007	0.260	0.6223
A^2	0.0395	1	0.03953	155.466	< 0.0001
B^2	0.0018	1	0.00184	7.218	0.0249
C^2	0.0057	1	0.00570	22.417	0.0011
Residual	0.0023	9	0.00025		
Lack of Fit	0.0023	5	0.00046	914.508	< 0.0001
Pure Error	0.0000	4	0.00000		
Cor Total	0.3237	18			
R^2	0.9929	Adjusted R^2	0.9859	Predicted R^2	0.9463

TH-2951_166106019

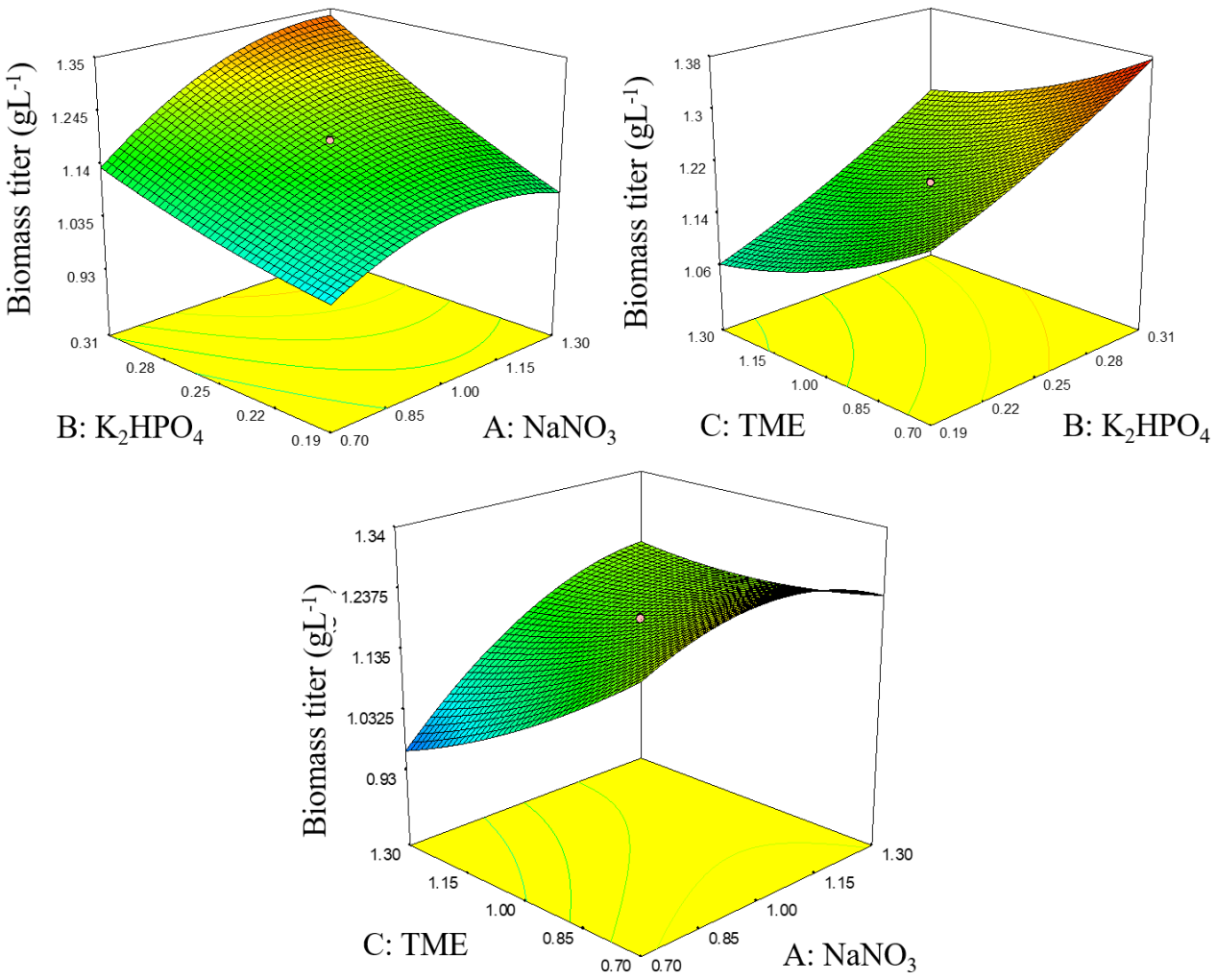

Fig. 5.4. 3D response surface plot showing the interactive effect of the media components on the biomass titer of CT02.

TH-2951_166106019

5.3.1.2. Growth of CT02 under the variation of input aeration rate

In any microbial cultivation system, in particular air lift or bubble column, aeration plays critical role on gas liquid mass transfer [Zhang et. al., 2002], mixing [Yaqoubnejad et. al., 2021] and substrate utilization efficiency [Tang et. al., 2015] and in turn, on growth performance of the organism. Further, finding the optimal level of aeration is also important for avoiding any possible shear stress to the microbial cells [Zhao et. al., 2015]. Therefore, the effect of input aeration rate on growth of CT02 was evaluated at four different aeration rates ranging from 0.25 vvm to 1 vvm (Fig 5.5). The highest biomass titer and productivity of 1.8 g L^{-1} and 71 mg L^{-1} day^{-1} was recorded for the aeration rate of 0.5 vvm (Fig. 5.5B). However, growth performance of the organism was linearly compromised with increase in flow rate beyond 0.5 vvm (Fig. 5.5A and 5.5B).

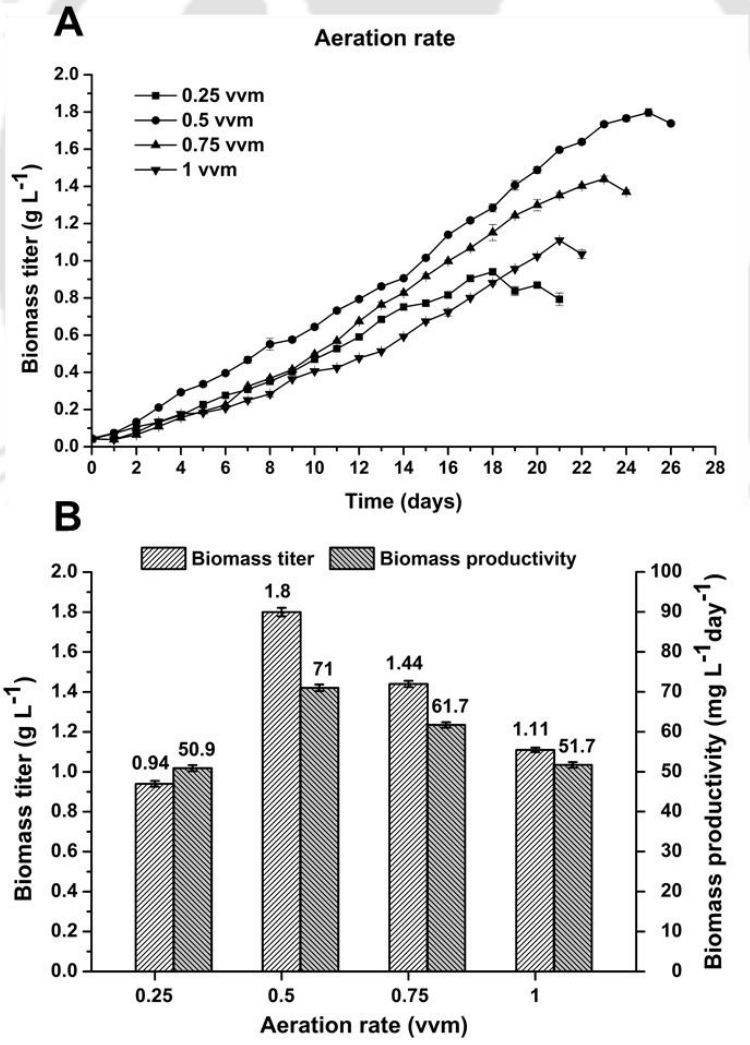

TH-2951_166106019

Fig. 5.5. Effect of varied aeration rate on the growth performance of CT02 cultivated under photoautotrophic condition: (A) Dynamic profile of growth, (B) Biomass titer and productivity.

The inferior growth performance of the organism at relatively higher aeration rate may be attributed to the enhanced dissolved oxygen (DO) content, which might have caused inhibition in photosynthetic pathways [Tang et. al., 2015]. A significantly reduced biomass titer of 0.94 g L^{-1} and productivity of 50.9 mg L^{-1} day^{-1} was observed at lower air flow rate of 0.25 vvm (Fig. 5.5B). This strongly resembled with the fact that lower aeration rate can cause reduced gas liquid mass transfer coefficient for CO_2 and inefficient mixing [Goswami et. al., 2019; Zhao et. al., 2015]. Therefore, an aeration rate of 0.5 vvm was used in all subsequent experiments.

5.3.1.3. Growth of CT02 under different culture pH

Culture pH has been shown to exert significant impact on metabolic activity of the cells [Chen et. al., 1994; Qiu et. al., 2017], solubility of nutrients and availability of carbonaceous compounds [Qiu et. al., 2017; Difusa et. al., 2015]. In particular, for photosynthetic organism like microalgae, the speciation of dissolved inorganic carbon is tightly regulated by culture pH, leading to the formation of bicarbonate (HCO_3^-) pool, which, further ensures sufficient supply of CO_2 for the activity of RuBisCo during photosynthesis and reduces counterproductive oxygenase activity [Umetani, et. al., 2021]. Therefore, finding optimal value of culture pH and its maintenance throughout the cultivation period become imperative for developing a microalgae cultivation process. In the present, CT02 was characterized under four different culture pH ranging from 6 to 9 (Fig. 5.6A). Amongst all, the culture with pH 8 showed highest biomass titer and productivity of 1.93 g L^{-1} and 107.6 mg L^{-1} day^{-1}, respectively, followed by pH 7 (1.53 g L^{-1} and 103.2 mg L^{-1} day^{-1}) and pH 9 (1.18 g L^{-1} and 91 mg L^{-1} day^{-1}) (Fig. 5.6B). The biomass titer achieved at culture pH 8 increased by 132.5 % while compared to the batch with uncontrolled pH. However, cultivation at pH 6 resulted in reduce biomass titer and productivity as compared to uncontrolled pH. The result of the current study was found to be in line with the study on *Scenedesmus* sp. where decline in biomass productivity was prominent high acidic (pH 5 to 6) and

TH-2951_166106019

alkaline (pH 9) condition of the culture [Difusa et. al., 2015]. Therefore, culture pH of 8 was found to be optimum for CT02 and was considered for designing the process engineering strategy.

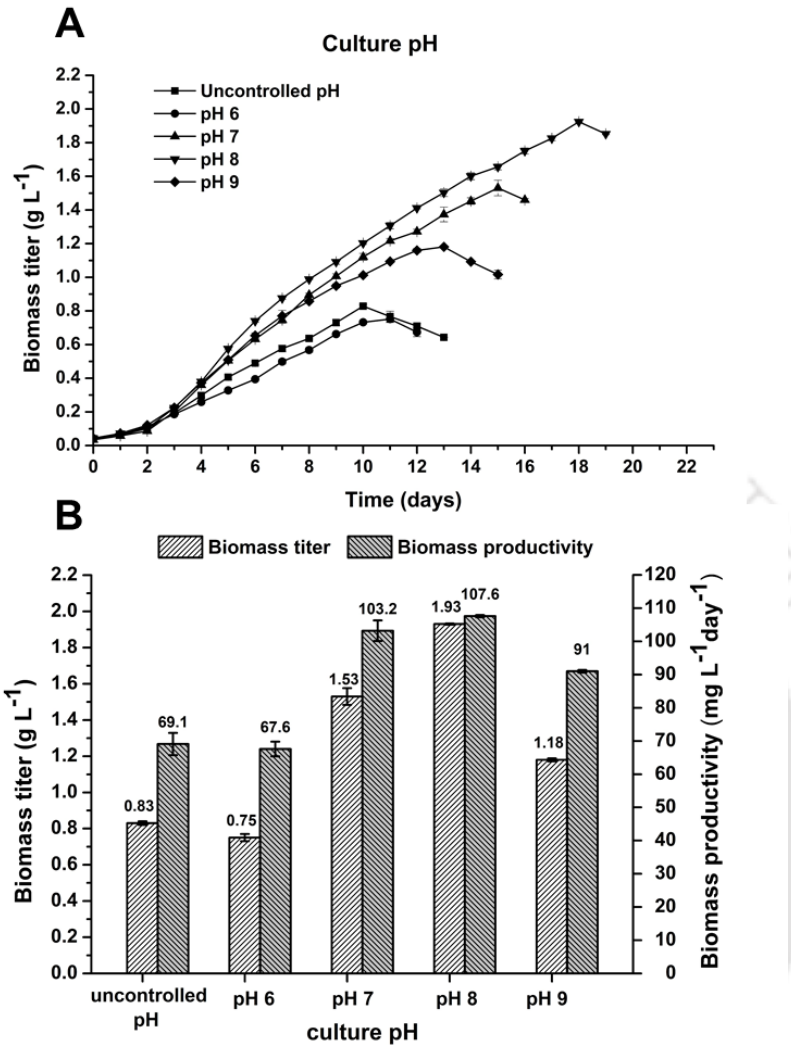

Fig. 5.6. Effect of different culture pH on the growth performance of CT02 cultivated under photoautotrophic condition: (A) Dynamic profile of growth, (B) Biomass titer and productivity.

5.3.2. Characterization of growth and culture pH under simulated diurnal variation of light intensity

Photoautotrophic growth of microalgae critically depends on optimal availability of light as source of energy and CO_2 as source of carbon (and in turn culture pH). In view of the economic feasibility and positive net energy ratio (NER), commercial scale cultivation of microalgae is recommended to be carried out under outdoor condition, harvesting natural sunlight [Koley et. al., 2019, El Shenawy et.

TH-2951_166106019

al., 2020]. However, under outdoor condition the organism is subjected to both diurnal and seasonal variation in incident light intensity and temperature. Therefore, in order to design an effective process engineering strategy, one would require to understand the complex interplay between diurnal and seasonal change in light intensity, growth of the organism and change in culture pH. Variation in growth and associated change in culture pH was evaluated under diurnal variation of simulated light intensity in two different seasons summer and winter (Fig. 5.7). In the summer, the incident light intensity was varied from 88 to 2132 µE $m^{-2}s^{-1}$ and for winter the same was varied from 76 to 801 µE $m^{-2}s^{-1}$. In order to capture micro level change in growth and pH profile during light cycle of three different growth phases vis-à-vis early log (96- 156 h), mid log (240- 300 h) and late log (384- 444 h), sampling was performed at an interval of 4 h for growth and 2 h for culture pH. In both the seasons, during initial half of the light cycle (4-8 h), concomitant increase in specific growth rate was observed with the increase in light intensity, followed by a decline in specific growth rate as the light intensity went down in the later phase of the light cycle. Further, sharp increase in pH of the fermentation broth from ~ 7.5 to ~10 was observed during increment in specific growth rate, which was linked to the elevated utilization of CO_2 as carbon source. It is important to note that the after attaining its peak, pH of the broth remained at its maximum till the end of the light phase. The results indicate that, during majority of the light cycle, the organism was exposed to a pH significantly higher than its optimal value (pH 8), causing suboptimal growth. The increase in broth pH was evidently higher with progression of the culture age, as observed from the pH profile in mid log phase and late log phase of the growth. Based on this result it can be concluded that the growth of the organism was negatively regulated from dual action of higher culture pH and limitation of carbon source. This implies the need of developing a process engineering strategy enabling the growth of the microalgae at optimal pH and without experiencing any possible CO_2 limitation.

TH-2951_166106019

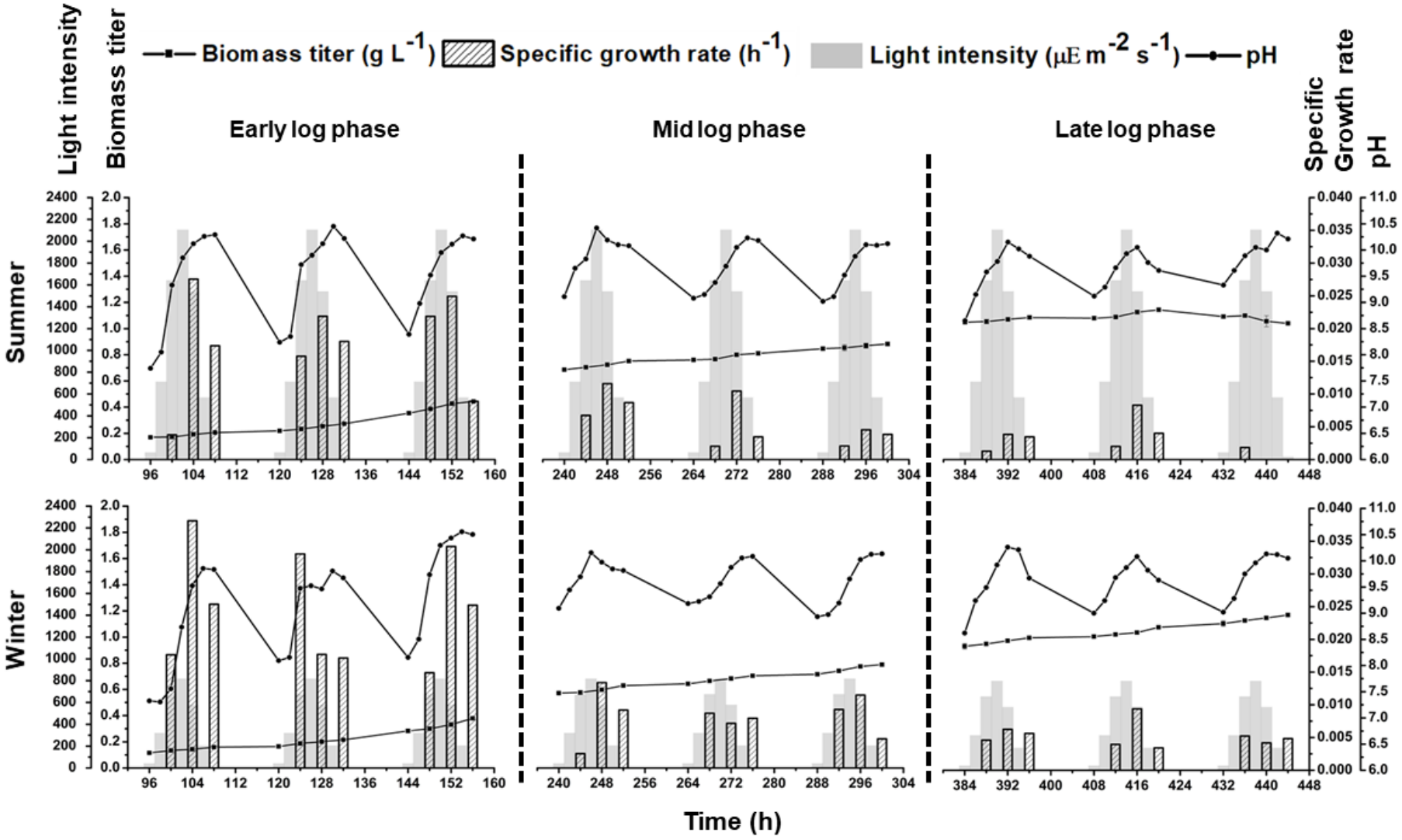

Fig. 5.7. Dynamic profile of biomass titer, specific growth rate and culture pH at different phases of logarithmic growth of CT02 under simulated diurnal sunlight intensity with seasonal variations.

TH-2951_166106019

5.3.3 Cultivation of CT02 coupled with pH guided CO_2 feeding under simulated sunlight

In case of phototrophic growth of microalgae, pH of the broth provides indirect measurement of CO_2 availability to the organism. This offers scope to design a process engineering strategy where pH of the culture can be maintained at its optimal value via cascade control with CO_2 feeding. Interdependent dynamics of light intensity, growth and culture pH (as obtained from the section 5.3.2), indicate that such process engineering strategy, based on on-demand supply of CO_2 under varied light intensity, may results in improved biomass titer and productivity by maintaining optimal culture pH and eliminating CO_2 limitation. Two parallel batches of CT02 were performed where all the growth parameters were kept identical except in one batch, the pH of the culture was maintained at optimal value of 8 through cascade driven intermittent purging of CO_2 and in another batch, culture pH remained uncontrolled (Fig. 5.8B). The batch with controlled pH resulted in maximum biomass titer of 1.87 g L^{-1} (Fig. 5.8A), an improvement by 53.3% when compared with the batch with uncontrolled pH (1.22 g L^{-1}). The improvement in the growth performance of the organism was also marked in terms of higher biomass productivity 114.8 g L^{-1} day^{-1} and average specific growth 0.25 day^{-1}, when culture pH was maintained at its optimal value (Fig. 5.8A) via pH based CO_2 feeding strategy. The inferior growth performance of the pH uncontrolled batch attributed to the gradual increase in culture pH from 8 at the beginning of the batch to 10.7 at the end of the batch (Fig. 5.8B). Further, this increase in culture pH depicts CO_2 limitation to the organism. The process engineering strategy involving pH based CO_2 feeding was able to eliminate both, pH stress to the organism and limitation of the carbon source and thereby, resulted in improved growth performance even under fluctuating light condition (Fig. 5.8C). The CO_2 fixation rate of the pH controlled batch was calculated to be 200 mg L^{-1} day^{-1} which was 92.7 % increase compared to the batch with uncontrolled pH (103.8 mg L^{-1} day^{-1}) (Fig. 5.9). Many studies on microalgal cultivation technology reported to observe similar improvement in growth using CO_2 feeding

TH-2951_166106019

strategies [Mohsenpour et. al., 2016; Lakshmikandan et. al., 2020; Zhao et. al., 2015; Patil et. al., 2019]. However, in majority of the cases, CO_2 supply remained non-systematic and or did not focus on optimal utilization of the input gas. To that end, the on-demand CO_2 injection based on culture pH offer optimal balance between growth and bio sequestration of CO_2 ensuring maximum utilization of input gas abating re-emission of CO_2 back to the environment.

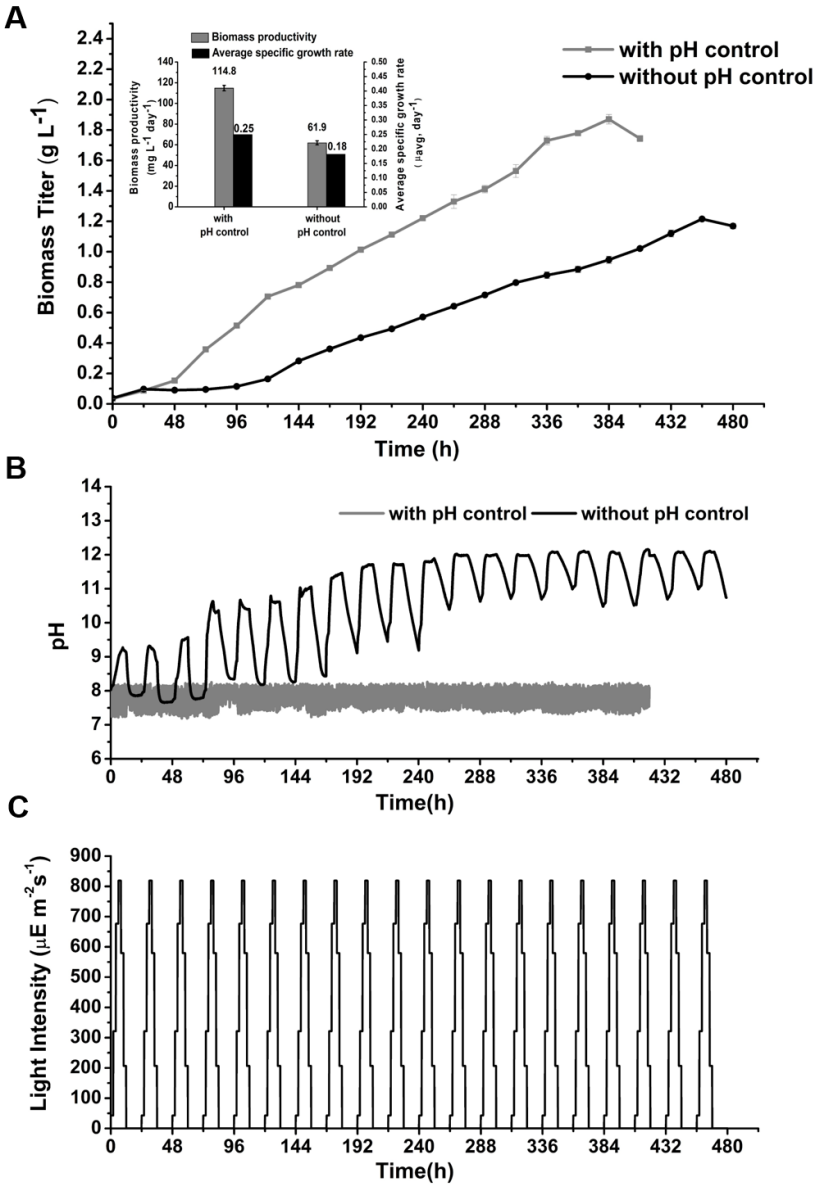

Fig. 5.8. Batch cultivation of CT02 under simulated diurnal sunlight intensity implementing process engineering strategy with pH based CO_2 feeding. Dynamic profiles of (A) biomass titer

TH-2951_166106019

(with comparative data for biomass productivity and average specific growth rate); (B) culture pH and (C) light intensity.

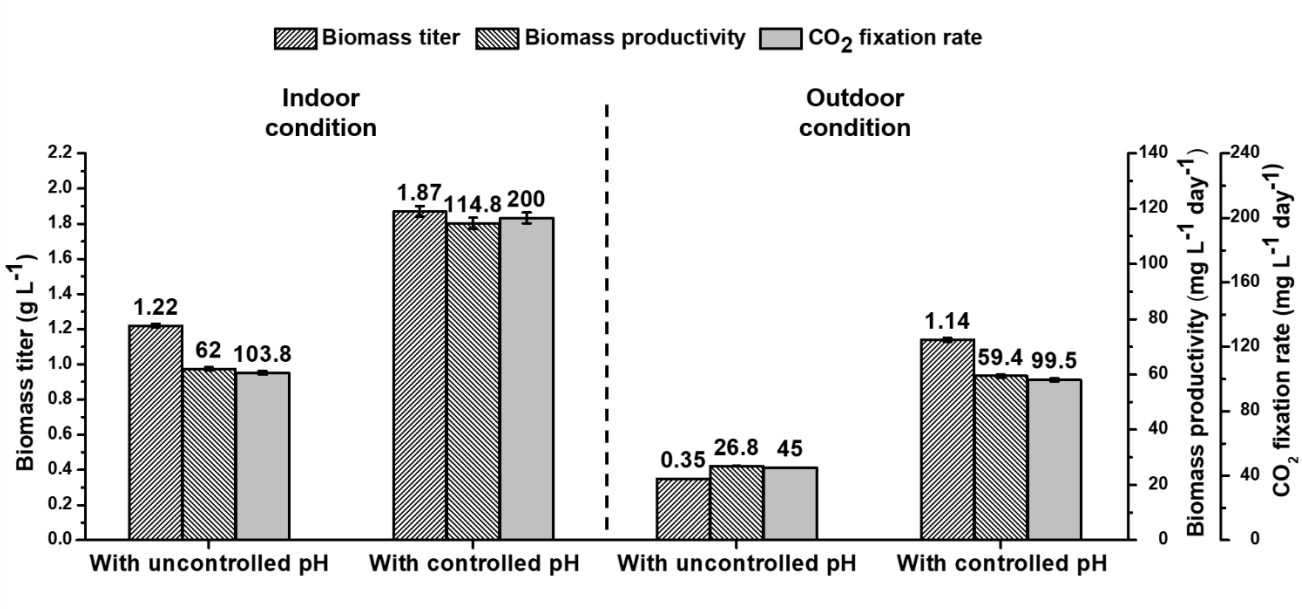

Fig. 5.9. Comparison of different growth kinetic parameters for batch cultivation of CT02 with or without pH guided CO_2 feeding.

5.3.4 Large scale cultivation of CT02 using process engineering strategy under fluctuating outdoor condition

The appropriation of the process engineering strategy developed lies in its scalability and effectiveness under fluctuating outdoor conditions. To that end, the organism CT02 was cultivated in 100 L FP-ABR under the outdoor fluctuating environmental condition, both under controlled and uncontrolled culture pH. The batch with optimal culture pH of 8, resulted in biomass titer of 1.14 g L^{-1} with productivity of 59.4 mgL^{-1} day^{-1} (Fig. 5.10A). This biomass titer and productivity was significantly higher than the pH uncontrolled batch, the corresponding value for the same was recorded as 0.35 g L^{-1} and 26.8 mg L^{-1} day^{-1}(Fig. 5.10A). However, the biomass titer and productivity achieved in pH controlled batch under outdoor scale-up condition was found to be lower than that obtained for indoor condition. This was

TH-2951_166106019

attributed to the fluctuating temperature range of 26 ℃ to 40℃ (Fig. 5.10B) and variation in the range of diurnal sunlight intensity (Fig. 5.10D).

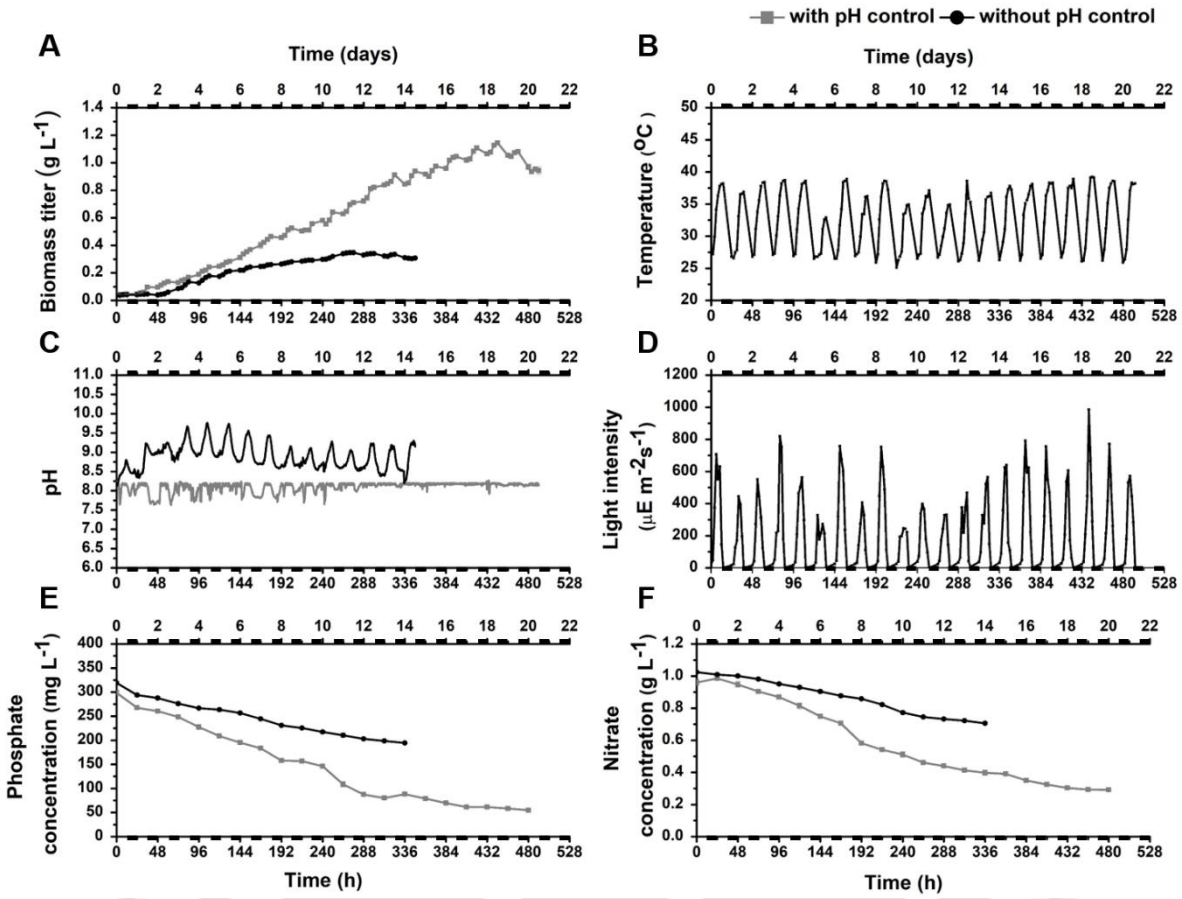

Fig. 5.10. Batch cultivation of CT02 in 100L FP-ABR using the process engineering strategy under fluctuating outdoor environmental condition. Dynamic profiles of (A) biomass titer; (B) temperature (C) culture pH; (D) light intensity; (E) phosphate utilization and (F) nitrate utilization.

As oppose to indoor condition, the pH of the culture in uncontrolled batch under outdoor condition was found to increase from 8 to 9.7 in the initial phase of the fermentation, followed by gradual decrease, which was attributed to the decrease in growth and in turn in CO_2 utilization (Fig. 5.10C). In context of CO_2 fixation rate, 121 % improvement was observed for batch with the process engineering strategy (99.5 mg L^{-1} day^{-1}) compared to batch with

TH-2951_166106019

uncontrolled pH (Fig. 5.9). The improved growth performance of the organism in pH controlled batch also corroborated well with the utilization pattern of nitrate and phosphate (Fig. 5.10E and 5.10F). Most of the reports on outdoor cultivation of microalgae have not adopted proper CO_2 feeding strategy or did not follow the cardinal rule of scale up [Qiu, et. al., 2017, Gupta et. al., 2019]. In contrast to that. the present study made significant progress in microalgal biomass generation by pH guided CO_2 sequestration strategy, efficient utilization of available natural light source and maintaining optimal aeration rate thus minimal operational expenses.

5.4. Conclusion

Tetradesmus obliquus CT02, an indigenous microalgal strain was subjected to the stepwise optimization of cultivation conditions followed by development of process engineering strategy involving pH based CO_2 feeding which resulted in significant improvement in both biomass titer and productivity. Characterization of CT02 under simulated diurnal variation of sunlight revealed that there was an interdependency between growth, culture pH and light intensity, leading to the establishment of culture pH was as guiding parameter for CO_2 feeding. The strategy, not only offers systematic guidance to CO_2 feeding, but also enables to maintain the desired pH of the culture throughout entire phase of cultivation and in turn, cells maintain their biological machinery at their optimal metabolic state. The key feature of the strategy remains its ability to offer improved growth performance of the organism, even under fluctuating outdoor environmental conditions. Extent of CO_2 sequestration, being linked to the growth, was also co-elevated with the improvement in biomass titer and productivity.

References

1. Cabello, J., Morales, M., & Revah, S. (2017). Carbon dioxide consumption of the microalga *Scenedesmus obtusiusculus* under transient inlet CO_2 concentration variations. Science of the Total Environment, 584, 1310-1316.
2. Cataldo, D. A., Maroon, M., Schrader, L. E., & Youngs, V. L. (1975). Rapid

TH-2951_166106019

colorimetric determination of nitrate in plant tissue by nitration of salicylic acid. Communications in soil science and plant analysis, 6(1), 71-80.

3. Chen, C. Y., & Durbin, E. G. (1994). Effects of pH on the growth and carbon uptake of marine phytoplankton. Marine Ecology-Progress Series, 109, 83-83.
4. Difusa, A., Talukdar, J., Kalita, M. C., Mohanty, K., & Goud, V. V. (2015). Effect of light intensity and pH condition on the growth, biomass and lipid content of microalgae *Scenedesmus* species. Biofuels, 6(1-2), 37-44.
5. El Shenawy, E. A., Elkelawy, M., Bastawissi, H. A. E., Taha, M., Panchal, H., kumar Sadasivuni, K., & Thakar, N. (2020). Effect of cultivation parameters and heat management on the algae species growth conditions and biomass production in a continuous feedstock photobioreactor. Renewable Energy, 148, 807-815.
6. Fawzy, M. A. (2017). Fatty acid characterization and biodiesel production by the marine microalga Asteromonas gracilis: statistical optimization of medium for biomass and lipid enhancement. Marine Biotechnology, 19(3), 219-231.
7. Gonçalves, A. L., Rodrigues, C. M., Pires, J. C., & Simões, M. (2016). The effect of increasing CO_2 concentrations on its capture, biomass production and wastewater bioremediation by microalgae and cyanobacteria. Algal research, 14, 127-136.
8. Goswami, G., Sinha, A., Kumar, R., Dutta, B. C., Singh, H., & Das, D. (2019). Process engineering strategy for cultivation of high density microalgal biomass with improved productivity as a feedstock for production of bio-crude oil via hydrothermal liquefaction. Energy, 189, 116136.
9. Guler, B. A., Deniz, I., Demirel, Z., Oncel, S. S., & Imamoglu, E. (2019). Transition from start-up to scale-up for fucoxanthin production in flat plate photobioreactor. Journal of Applied Phycology, 31(3), 1525-1533.
10. Gupta, S., Pawar, S. B., Pandey, R. A., Kanade, G. S., & Lokhande, S. K. (2019).

TH-2951_166106019

Outdoor microalgae cultivation in airlift photobioreactor at high irradiance and temperature conditions: effect of batch and fed-batch strategies, photoinhibition, and temperature stress. Bioprocess and biosystems engineering, 42(2), 331-344.

11. Koley, S., Mathimani, T., Bagchi, S. K., Sonkar, S., & Mallick, N. (2019). Microalgal biodiesel production at outdoor open and polyhouse raceway pond cultivations: a case study with *Scenedesmus accuminatus* using low-cost farm fertilizer medium. Biomass and Bioenergy, 120, 156-165.
12. Lakshmikandan, M., Murugesan, A. G., Wang, S., Abomohra, A. E. F., Jovita, P. A., & Kiruthiga, S. (2020). Sustainable biomass production under CO_2 conditions and effective wet microalgae lipid extraction for biodiesel production. Journal of Cleaner Production, 247, 119398.
13. Makut, B. B., Das, D., & Goswami, G. (2019). Production of microbial biomass feedstock via co-cultivation of microalgae-bacteria consortium coupled with effective wastewater treatment: A sustainable approach. Algal Research, 37, 228-239.
14. Mohsenpour, S. F., & Willoughby, N. (2016). Effect of CO_2 aeration on cultivation of microalgae in luminescent photobioreactors. Biomass and Bioenergy, 85, 168-177.
15. Muthuraj, M., Chandra, N., Palabhanvi, B., Kumar, V., & Das, D. (2015). Process engineering for high-cell-density cultivation of lipid rich microalgal biomass of *Chlorella* sp. FC2 IITG. Bioenergy Research, 8(2), 726-739.
16. Parsons, T. R., Maita, Y., & Lalli, C. M. (1984). Determination of phosphate. A manual of chemical and biological methods for seawater analysis, 22-25.
17. Patil, L., & Kaliwal, B. (2017). Effect of CO_2 concentration on growth and biochemical composition of newly isolated indigenous microalga *Scenedesmus bajacalifornicus* BBKLP-07. Applied biochemistry and biotechnology, 182(1), 335-348.
18. Qiu, R., Gao, S., Lopez, P. A., & Ogden, K. L. (2017). Effects of pH on cell growth,

TH-2951_166106019

lipid production and CO_2 addition of microalgae *Chlorella sorokiniana*. Algal research, 28, 192-199.

19. Singh, J., & Dhar, D. W. (2019). Overview of carbon capture technology: microalgal biorefinery concept and state-of-the-art. Frontiers in Marine Science, 6, 29.
20. Tang, C. C., Zuo, W., Tian, Y., Sun, N., Wang, Z. W., & Zhang, J. (2016). Effect of aeration rate on performance and stability of algal-bacterial symbiosis system to treat domestic wastewater in sequencing batch reactors. Bioresource Technology, 222, 156-164.
21. Umetani, I., Janka, E., Sposób, M., Hulatt, C. J., Kleiven, S., & Bakke, R. (2021). Bicarbonate for microalgae cultivation: a case study in a chlorophyte, *Tetradesmus wisconsinensis* isolated from a Norwegian lake. Journal of Applied Phycology, 33(3), 1341-1352.
22. Verma, R., Kumari, K. K., Srivastava, A., & Kumar, A. (2020). Photoautotrophic, mixotrophic, and heterotrophic culture media optimization for enhanced microalgae production. Journal of Environmental Chemical Engineering, 8(5), 104149.
23. Yaashikaa, P. R., Kumar, P. S., Varjani, S. J., & Saravanan, A. (2019). A review on photochemical, biochemical and electrochemical transformation of CO_2 into value-added products. Journal of CO_2 Utilization, 33, 131-147.
24. Yaqoubnejad, P., Rad, H. A., & Taghavijeloudar, M. (2021). Development a novel hexagonal airlift flat plate photobioreactor for the improvement of microalgae growth that simultaneously enhance CO_2 bio-fixation and wastewater treatment. Journal of Environmental Management, 298, 113482.
25. Zhang, K., Kurano, N., & Miyachi, S. (2002). Optimized aeration by carbon dioxide gas for microalgal production and mass transfer characterization in a vertical flat-plate photobioreactor. Bioprocess and biosystems engineering, 25(2), 97-101.

TH-2951_166106019

26. Zhao, B., Su, Y., Zhang, Y., & Cui, G. (2015). Carbon dioxide fixation and biomass production from combustion flue gas using energy microalgae. Energy, 89, 347-357.

भारतीय प्रौद्योगिकी संस्थान गुवाहाटी • Indian Institute of Technology Guwahati •

TH-2951_166106019

Chapter 6

Conclusions

The present study deals with the development of microalgae based sustainable commercial technology and cumulatively addresses the major bottlenecks of like suitability of microalgal strain for CO_2 sequestration, low biomass titer and productivity. At the onset of the study, *Tetradesmus obliquus* CT02, a potential CO_2 tolerant indigenous microalgal strain, was isolated through a novel CO_2 selection pressure-based screening strategy. The strain exhibited a high CO_2 tolerance of 20% v/v, supporting its suitability towards biological CCS. Broad characterization of the isolated microalgal strain was performed stepwise, in order to select the suitable culture medium, initial pH, limiting nutrient sources (nitrogen and phosphate). Under selected nutritional and physicochemical conditions, CT02 was found to hold high protein and lipid content of 35.96% w/w and 41.21% w/w respectively which divulged the multiproduct potential of the strain. With the aim of developing economically viable process, a biorefinery approach was adopted for CT02 biomass in two sequential steps, resulting in alternate product cascades of bioactive molecules and biodiesel or biofertilizer. As the first step, bioprospecting of CT02 was performed for five different solvent based crude extracts. Amongst the five crude extracts screened for their antioxidant and anticancer activities, acetone extract showed highest antioxidant activity with IC_{50} value of 137 µg mL^{-1} and ethyl acetate extract exhibited maximum anticancer activity with IC_{50} value of 306.67 µg mL^{-1}. HR-LCMS analysis of the selected extracts depicted the presence of an array of bioactive molecules which may be contributing to their antioxidant and anticancer activities. Further, the residual biomass of CT02 post solvent extraction was evaluated for its potential towards biodiesel production.

TH-2951_166106019

High FAME yield of 33.1% - 36.7% w/w was obtained from both acetone and ethyl acetate extracted biomass. Analysis of FAME composition revealed abundance of palmitic acid (C16:0), stearic acid (C18:0), and elaidic acid (C18:1n9t) as the major constituents, proving it suitable for use as biodiesel. While evaluated for biofertilizer potential, the post extracted residual biomass showed significant inductive effect on germination of *Solanum lycopersicum* seeds. The highest final germination percentage and germination index was estimated to be in the range of 75% - 80% and 117.5 - 118.5, respectively which were comparable to that of commercial grade NPK.

In order to improve the achieve improved biomass titer and productivity for large scale outdoor cultivation of CT02, a process engineering strategy was developed stepwise. Media engineering via RSM-CCD based optimization resulted in 36.8 % and 26.5% improvement in biomass titer and productivity respectively. Following the optimization of batch cultivation parameters like input aeration rate and culture pH, the strain was characterised for its growth performance under diurnal variation of simulated sunlight intensity. The close corelation between growth, culture pH and incident light intensity observed in this case. The observation led to the development of pH-guided CO_2 feeding strategy which eliminated the negative action of higher culture pH and limitation of carbon source on microalgal growth. Implementation of the strategy in laboratory scale under simulated sunlight have significantly increased the growth rate of the organism resulting in maximum biomass titer of 1.87 g L^{-1} and biomass productivity of 114.8 g L^{-1} day^{-1}. Moreover, the CO_2 fixation rate of pH-controlled batch was calculated to be 200 mg L^{-1} day^{-1} which was 92.7 % increase compared to the batch with uncontrolled pH (103.8 mg L^{-1} day^{-1}). When cultivated at large scale in 100L FP-ABR under outdoor fluctuating environmental condition, the developed strategy recorded 226% and 122% improved biomass titer and productivity compared to the batch with uncontrolled pH.

TH-2951_166106019

Future Prospects

- ✓ Commercial scale evaluation of the strain's potential towards multiproduct biorefinery.
- ✓ Development of energy efficient technology for harvesting of CT02 biomass and subsequent downstream processing for extraction of value-added compounds.
- ✓ Understanding the biosynthesis pathways and appropriate metabolic engineering for improved product yield.
- ✓ Technoeconomic feasibility analysis of the end-to-end technology for microalgal biorefinery coupled with CO_2 sequestration using *Tetradesmus obliquus* CT02.

TH-2951_166106019

Appendix A

Identification of compounds with antioxidant and anticancer activity using HR-LCMS-QTOF

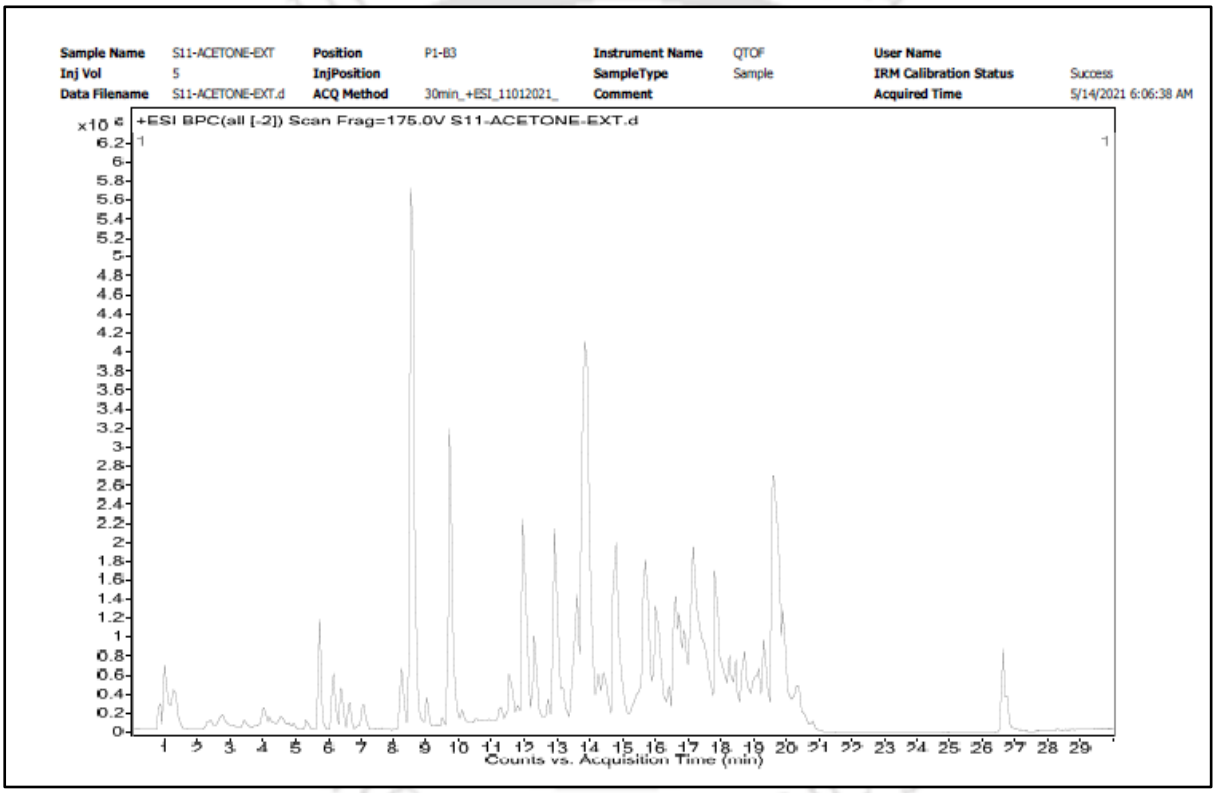

Fig. A1. HR-LCMS-QTOF chromatogram of acetone extract of CT02

Compounds with antioxidant activity present in acetone extract

1. 3'-N-Acetyl-4'-O-(14-methylheptadecanoyl) fusarochromanone
   Molecular formula: $C_{35}H_{56}N_2O_6$ **M/Z ratio:** 601.4218 **Molecular mass:** 600.42

TH-2951_166106019

Compound structure

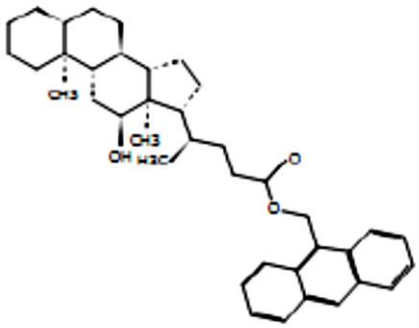

MS spectrum

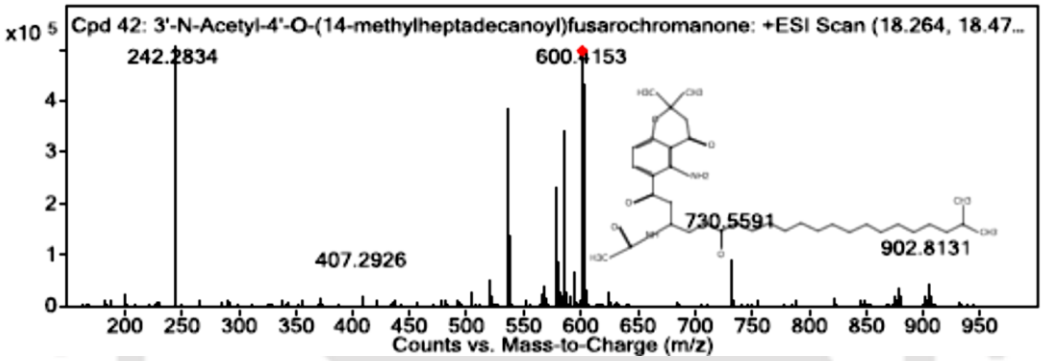

2. 2-Hexaprenyl-3-methyl-5-hydroxy-6-methoxy-1,4-benzoquinol
Molecular formula: $C_{38}H_{58}O_4$ **M/Z ratio:**583.41 **Molecular mass:** 578.43

Compound structure

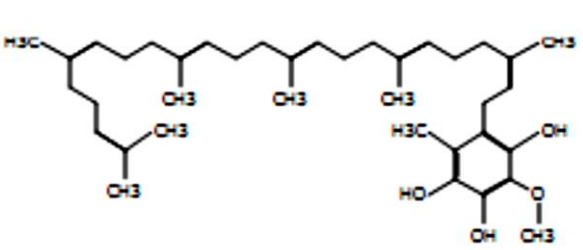

MS spectrum

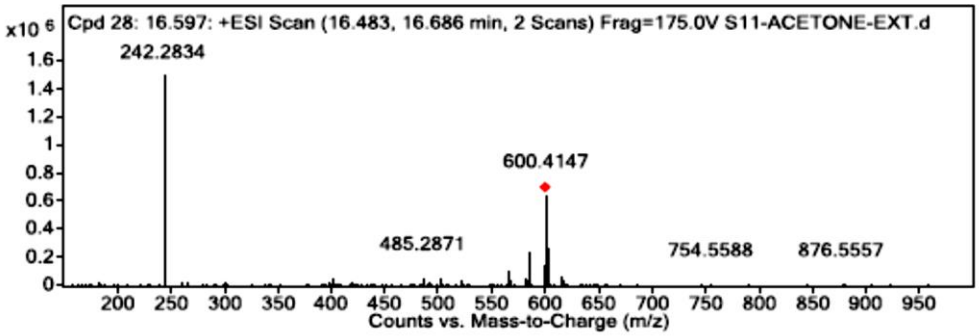

3. 16-Hydroxy hexadecanoic acid

TH-2951_166106019

Molecular formula: $C_{16}H_{32}O_3$ **M/Z ratio:** 290.27 **Molecular mass:** 272.23

Compound structure

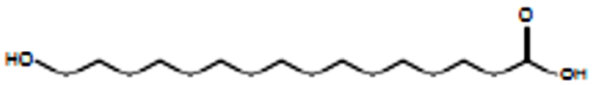

MS spectrum

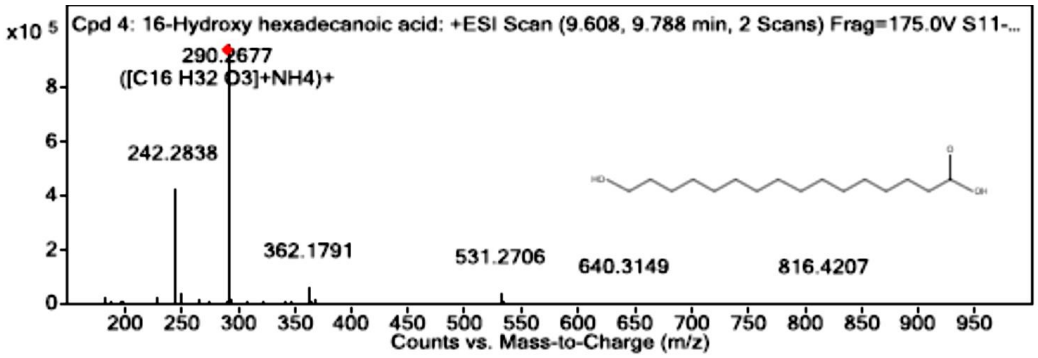

4. Nigakihemiacetal A

Molecular formula: $C_{22}H_{34}O_7$ **M/Z ratio:** 415.21 **Molecular mass:** 410.23

Compound structure

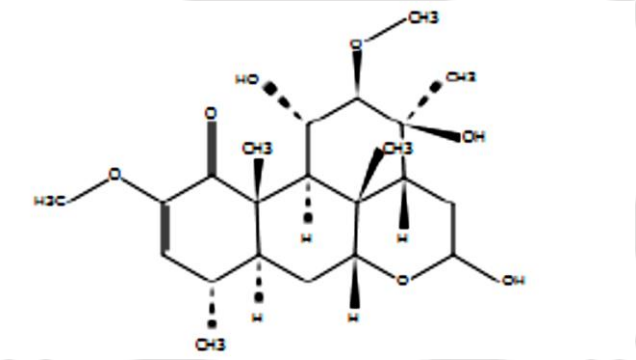

MS spectrum

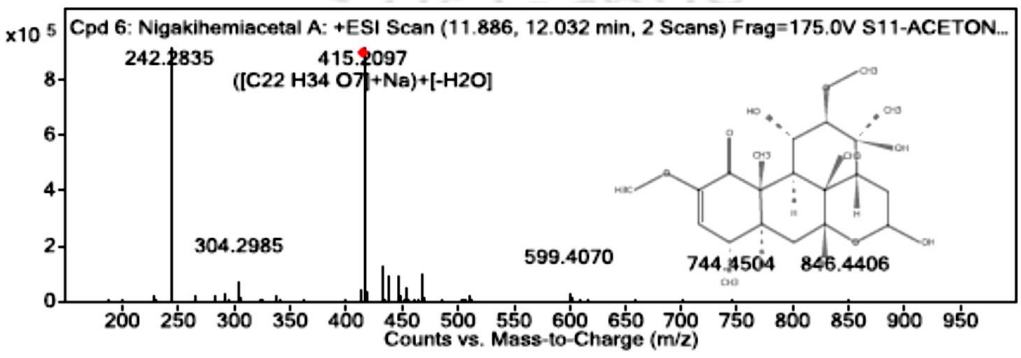

5. Dinoflagellate luciferin

Molecular formula: $C_{33}H_{40}N_4O_6$ **M/Z ratio:** 593.27 **Molecular mass:** 588.29

TH-2951_166106019

Compound structure

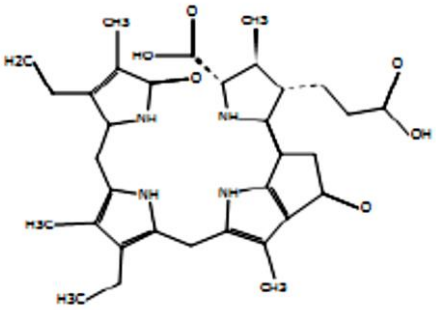

MS spectrum

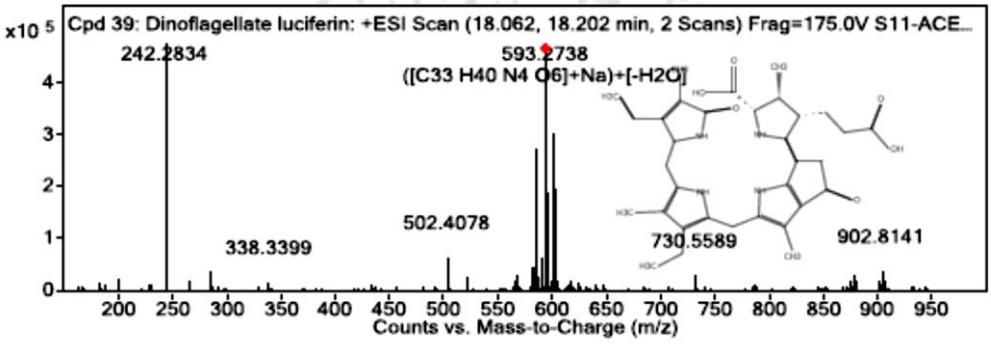

6. Convallasaponin A

Molecular formula: C_{32} H_{52} O_9 **M/Z ratio:** 598.40 **Molecular mass:** 580.37

Compound structure

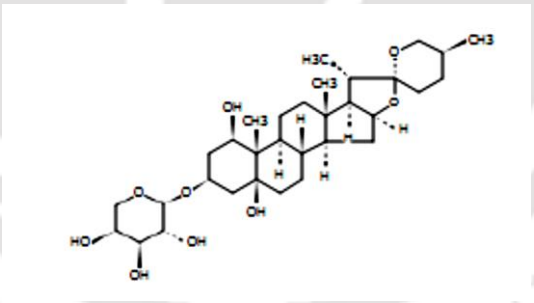

MS spectrum

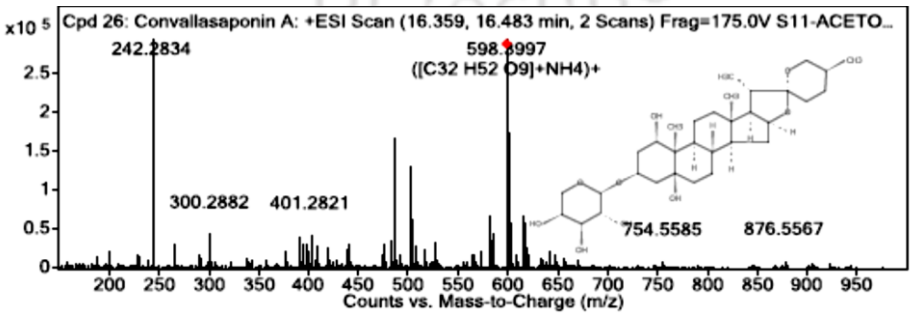

TH-2951_166106019

7. Brassinolide

Molecular formula: $C_{28}H_{48}O_6$ **M/Z ratio:** 498.38 **Molecular mass:** 480.34

Compound structure

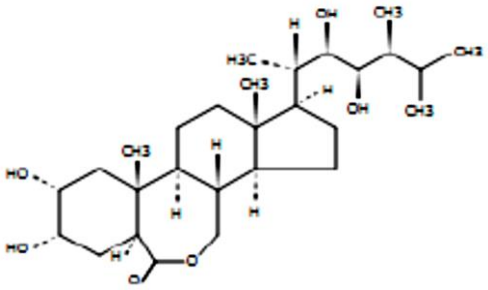

MS spectrum

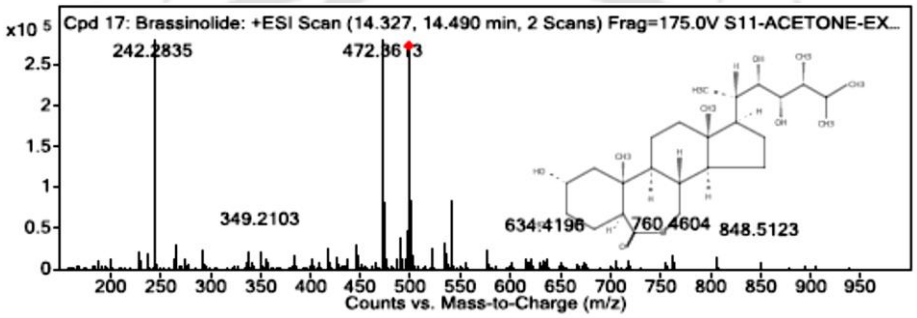

8. Tridecan-1-ol

Molecular formula: $C_{13}H_{28}O$ **M/Z ratio:** 200.24 **Molecular mass:** 200.21

Compound structure

MS spectrum

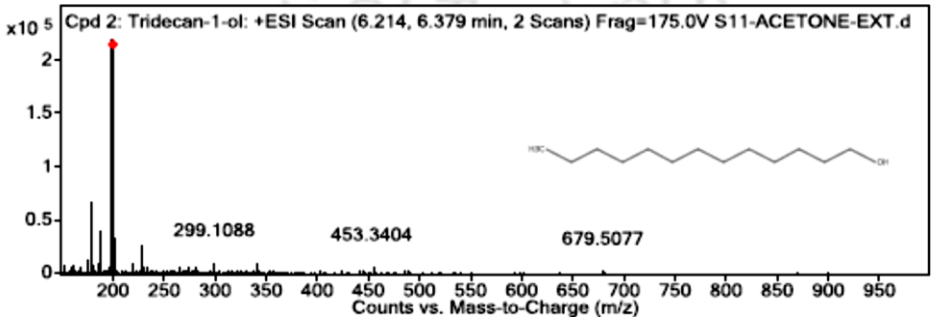

TH-2951_166106019

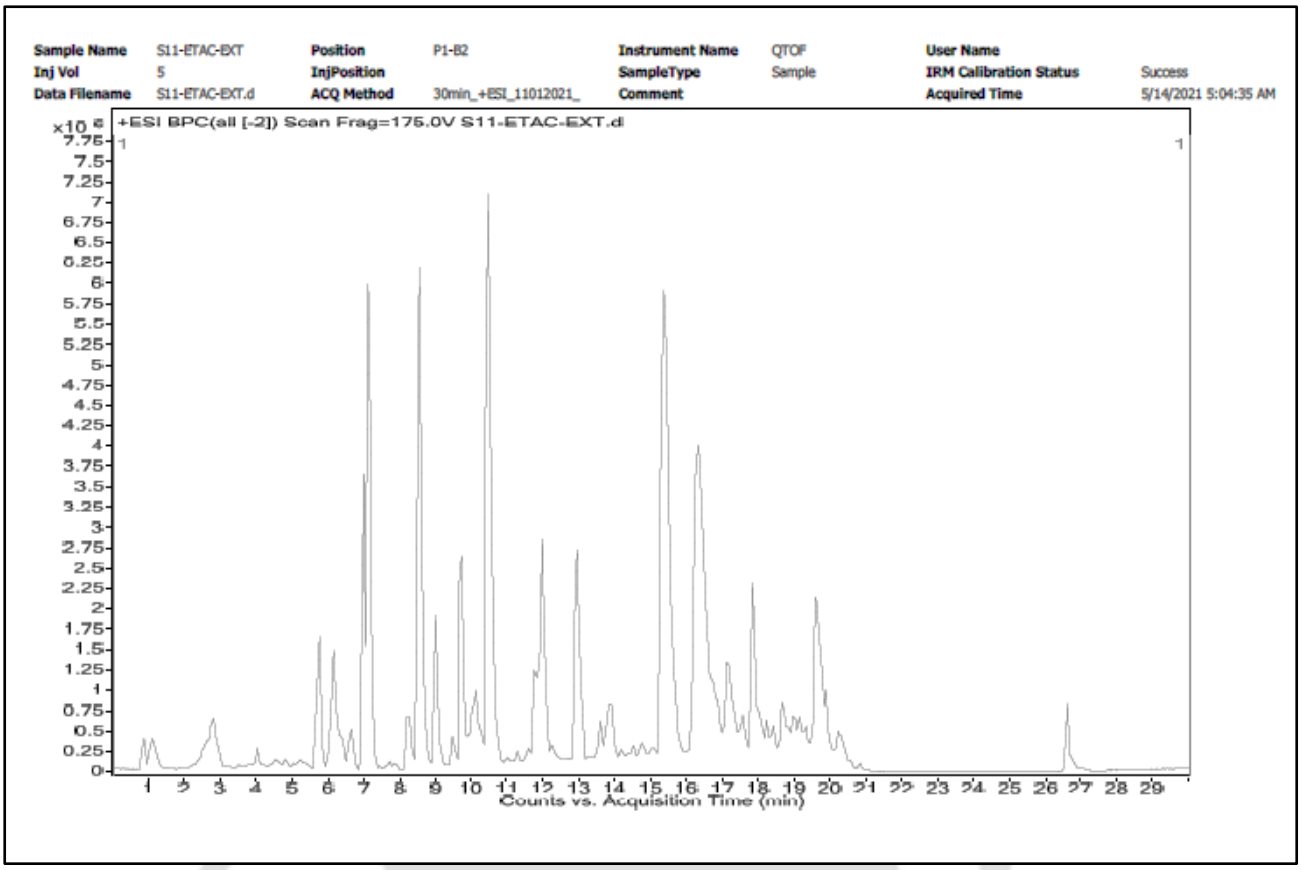

Fig. A2. HR-LCMS-QTOF chromatogram of ethyl acetate extract of CT02

Compounds with anticancer activity present in ethyl acetate extract

1. Dioscin

Molecular formula: $C_{45}H_{72}O_{16}$ **M/Z ratio:** 868.5 **Molecular mass:** 868.48

Compound structure

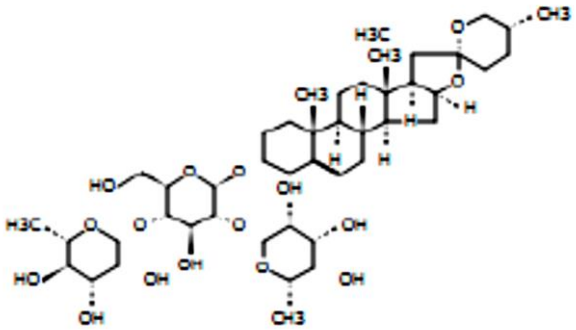

TH-2951_166106019

MS spectrum

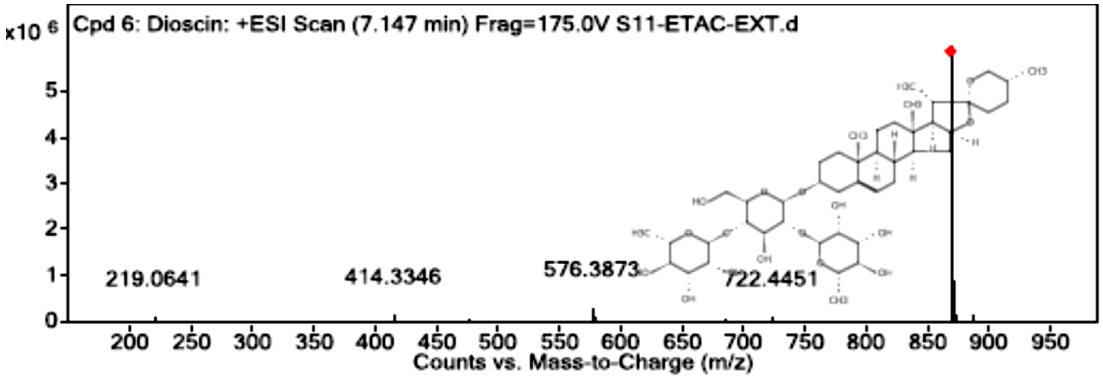

2. (5b,12a), 9-anthracenylmethyl ester, 12-hydroxy- Cholan-24-oic acid
Molecular formula: $C_{39}H_{50}O_3$ **M/Z ratio:** 584.42 **Molecular mass:** 566.39

Compound structure

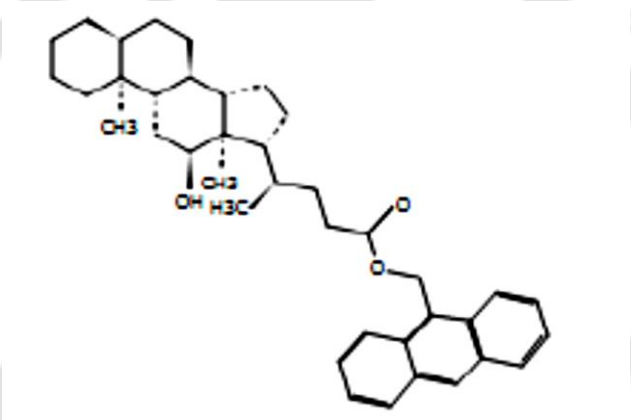

MS spectrum

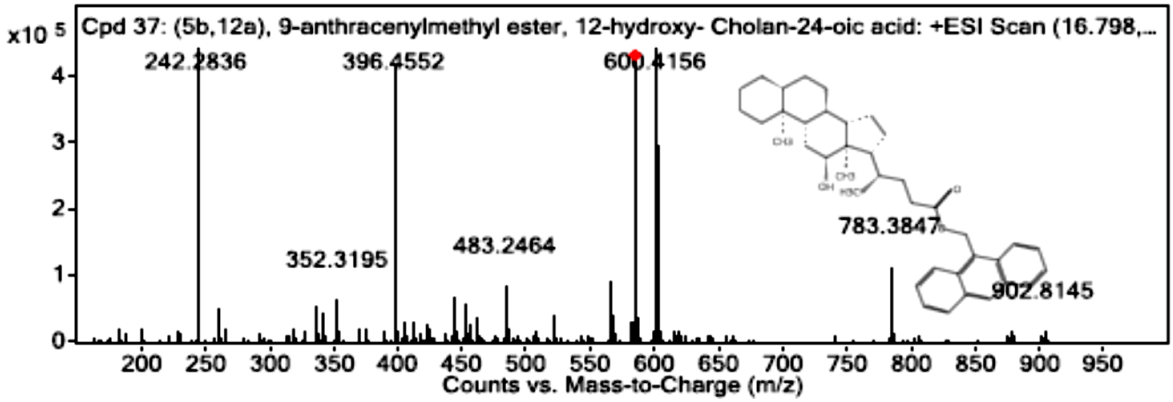

3. Dinoflagellate luciferin

TH-2951_166106019

Molecular formula: $C_{33}H_{40}N_4O_6$ **M/Z ratio:** 593.27 **Molecular mass:** 588.3

Compound structure

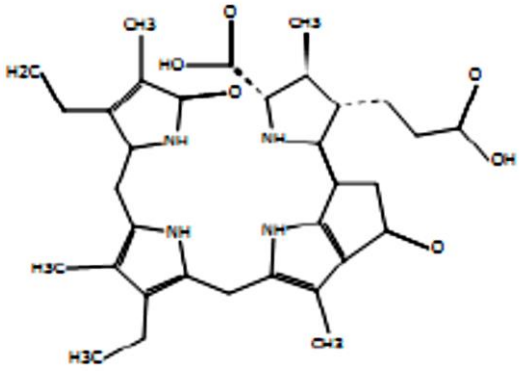

MS spectrum

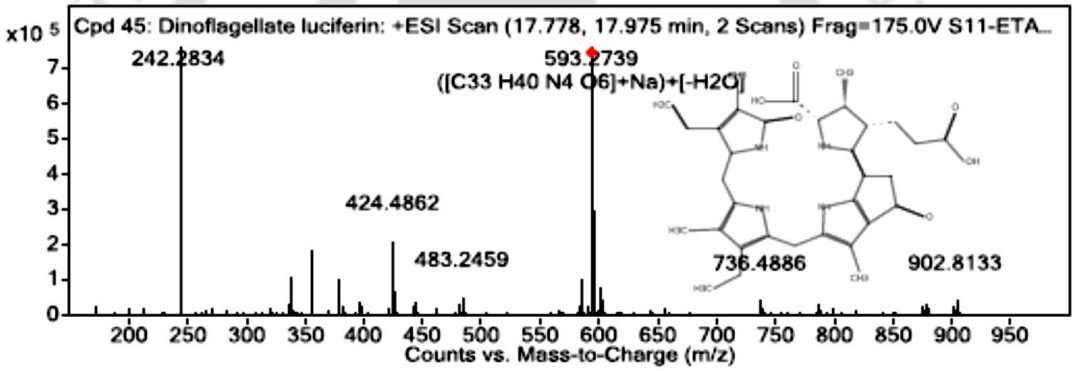

4. 16-Hydroxy hexadecanoic acid

Molecular formula: $C_{16}H_{32}O_3$ **M/Z ratio:** 290.27 **Molecular mass:** 272.23

Compound structure

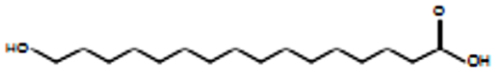

MS spectrum

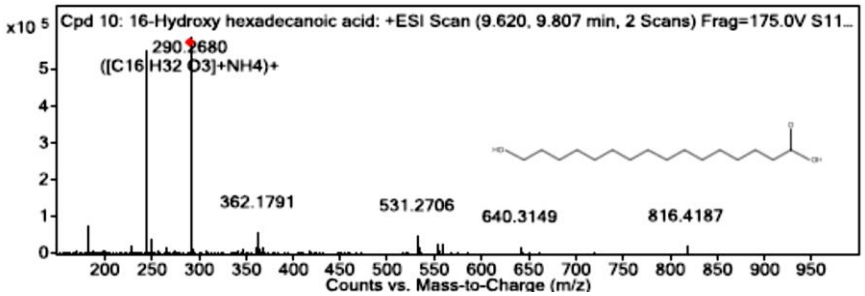

5. Gracillin

TH-2951_166106019

Molecular formula: $C_{45}H_{72}O_{17}$ **M/Z ratio:** 884.5 **Molecular mass:** 883.5

Compound structure

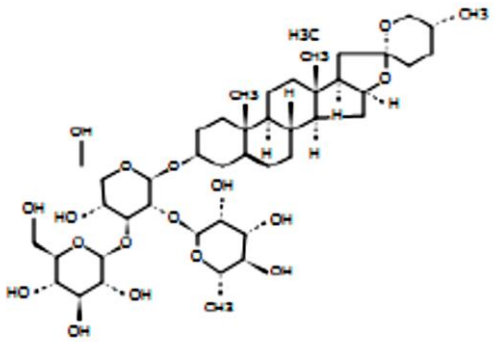

MS spectrum

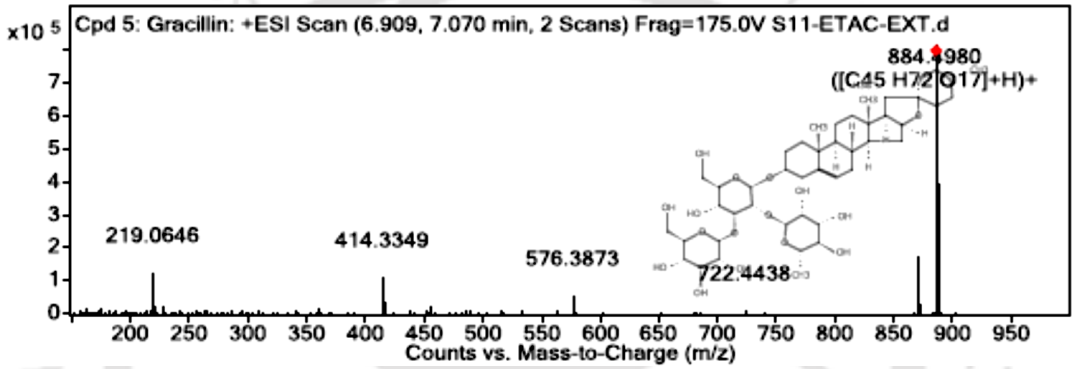

6. Phytosphingosine

Molecular formula: $C_{18}H_{39}NO_3$ **M/Z ratio: 300.29 Molecular mass: 317.29**

Compound structure

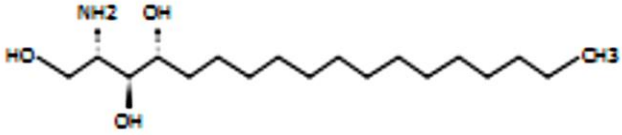

MS spectrum

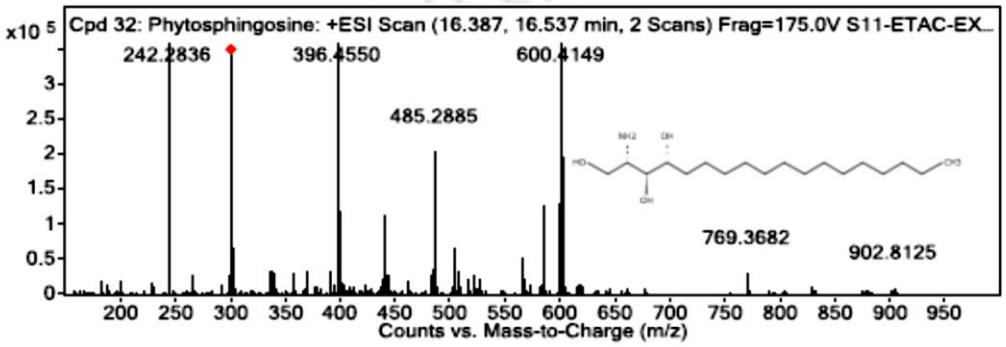

7. 3'-N-Acetyl-4'-O-(14-methylheptadecanoyl) fusarochromanone

TH-2951_166106019

Molecular formula: $C_{35}H_{56}N_2O_6$ **M/Z ratio:** 601.42 **Molecular mass:** 600.41

Compound structure

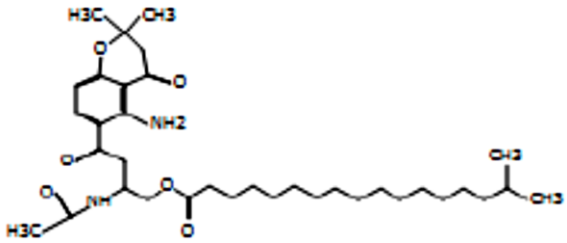

MS spectrum

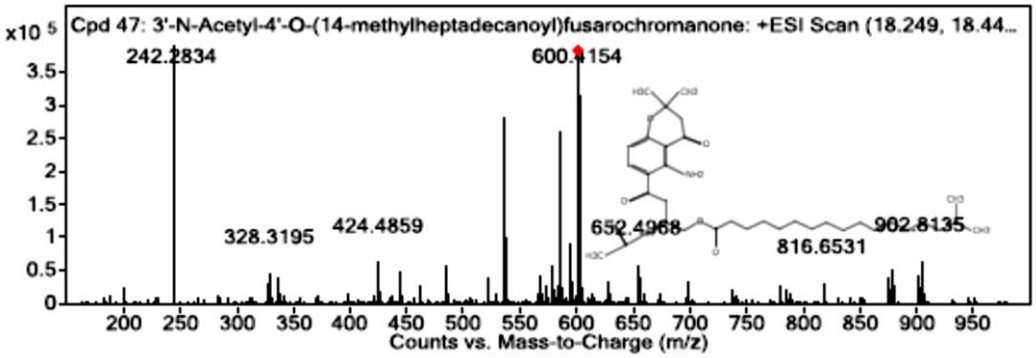

8. Tridecan-1-ol

Molecular formula: $C_{13}H_{28}O$ **M/Z ratio:** 200.24 **Molecular mass:** 200.21

Compound structure

MS spectrum

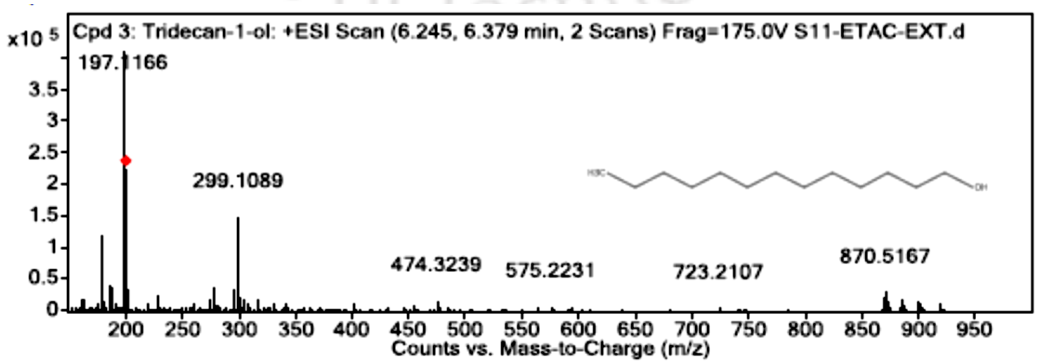

9. Decyl butanoate

TH-2951_166106019

Molecular formula: $C_{14}H_{28}O_2$ **M/Z ratio:** 228.23 **Molecular mass:** 228.21

Compound structure

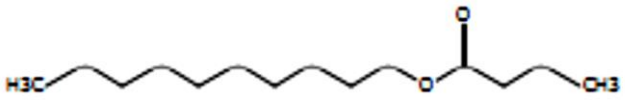

MS spectrum

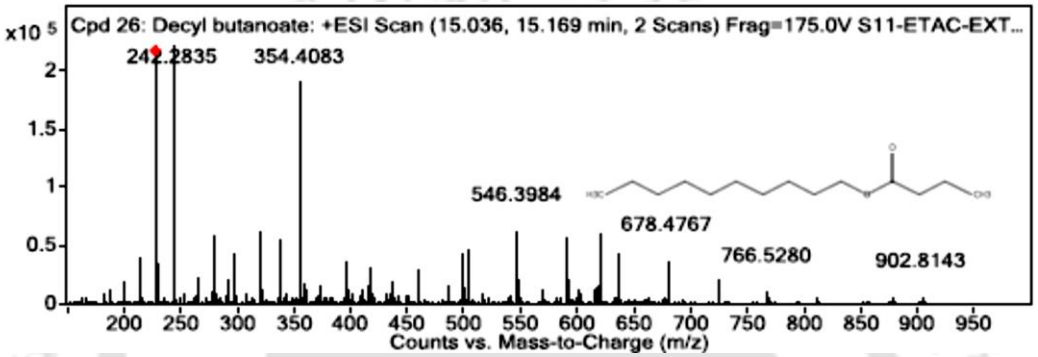

10. TG (18:1(11Z)/16:1(9Z)/18:1(11Z)) [iso3]
Molecular formula: $C_{55}H_{100}O_6$ **M/Z ratio:** 874.78 **Molecular mass:** 856.75

Compound structure

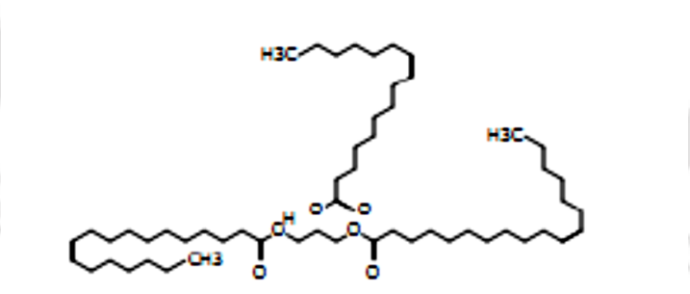

MS spectrum

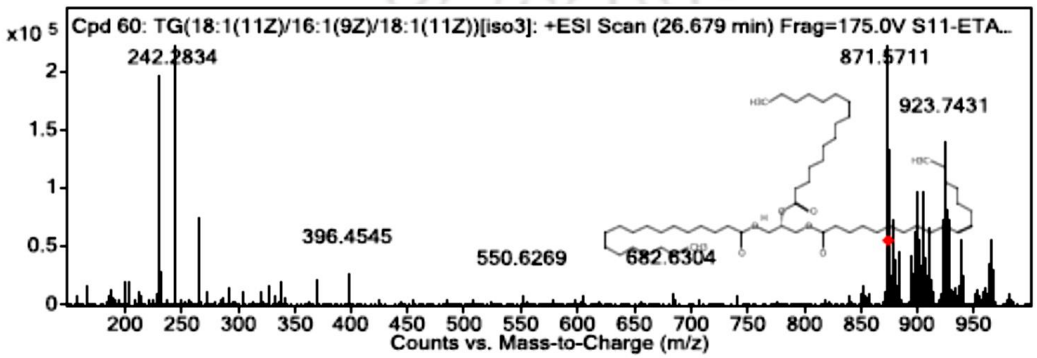

TH-2951_166106019

List of Publications

Articles from thesis work

- **Sinha, A**., Kumar, R., Goswami, G., & Das, D. (2022). Process Engineering Strategy for Large Scale Outdoor Cultivation of *Tetradesmus Obliquus* CT02 Coupled with pH Guided CO_2 Feeding. *Journal of environmental management*, 318,115539.
- Sinha, A., Goswami, G., Kumar, R., & Das, D. (2021). A microalgal biorefinery approach for bioactive molecules, biofuel, and biofertilizer using a novel carbon dioxide-tolerant strain Tetradesmus obliquus CT02. *Biomass Conversion and Biorefinery*, 1-14.

Articles from collaborative work.

- Kumar, R., Goswami, G., Debnath, D., **Sinha, A**., & Das, D. (2022). Screening and evaluation of novel microalga *Desmodesmus pannonicus* CT01 for CO_2 sequestration potential and aqua feed application. *Biomass Conversion and Biorefinery*, 1-12.
- Goswami, G., Kumar, R., **Sinha, A.,** Birazee, B., Dutta, B. C., Bhutani, S., & Das, D. (2022). ALGLIQOL: A two stage integrated process towards synthesis of renewable transportation fuel via catalytic hydrothermal liquefaction of lipid enriched microalgae biomass and distillation. *Energy Conversion and Management*, 263, 115696.
- Goswami, G., Kumar, R., Sinha, A., Maiti, S. K., Dutta, B. C., Singh, H., & Das, D. (2019). A low-cost and scalable process for harvesting microalgae using commercial-grade flocculant. RSC Advances, 9(67), 39011-39024.
- Goswami, G., Sinha, A., Kumar, R., Dutta, B. C., Singh, H., & Das, D. (2019). Process engineering strategy for cultivation of high density microalgal biomass with improved productivity as a feedstock for production of bio-crude oil via hydrothermal

TH-2951_166106019

liquefaction. Energy, 116-136

- Dineshbabu, G., Goswami, G., Kumar, R., Sinha, A., & Das, D. (2019). Microalgae–nutritious, sustainable aqua-and animal feed source. Journal of Functional Foods, 62, 103-545.

Patent applications from collaborative work

- Goswami G, Kumar R, Sinha A, Dutta B C, Singh H, Das D, "Process for production of liquid transportation fuel via catalytic hydrothermal liquefaction of microalgae biomass". Indian Patent Application No. 202111055352, filed on November 30, 2021
- Goswami G, Kumar R, Sinha A, Dutta B C, Singh H, Das D, "Scalable harvesting method for production of microalgal Biomass feedstock". Indian Patent Application No. 201911018574, filed on May 09, 2019.
- Goswami G, Sinha A, Kumar R, Dutta B C, Singh H, Das D, "Process for enhancing biomass productivity by high density cultivation of microalgae", Indian Patent Application No. 201811041629, filed on November 02, 2018.

TH-2951_166106019

List of Conferences/Workshops

- Sinha A, Kumar R, Goswami G, Das D, "A novel method for screening and isolation of potential CO_2 tolerant microalgae", BESCON 2019, IIT Madras.
- Sinha A, Kumar R, Goswami G, Dutta B C, Das D, "Screening and isolation of potential CO_2 tolerant microalgae form industrial waste water via CO_2 selection pressure:", Bioprocessing India 2017, IIT Guwahati.
- GIAN course on "Biofuel Cell Technology: Fundamentals and Applications"; April 23-27,2018; IIT Guwahati
- 20^{th} Indo-US Flow Cytometry Symposium cum Workshop on "Applications of Flow Cytometry in Biotechnology"; March 13-16,2019; IIT Guwahati.

TH-2951_166106019

Vitae

The author was born on July 21st 1991 in Asansol, West Bengal. He passed his higher secondary examination with first class from Birbhum Rastriya Vidyalaya, Suri, Birbhum, West Bengal in 2009. He completed his Bachelor of Technology in Biotechnology from Haldia Institute of Technology under West Bengal University of Technology, in 2014. He did his Master of Technology in Biotechnology from National Institute of Technology Durgapur, in 2016.

Ankan Sinha joined the Ph.D. programme in July 2016 at Department of Biosciences and Bioengineering, Indian Institute of Technology Guwahati, Assam, India. He received the junior and senior research fellowships from ONGC PanIIT Centre for Bioenergy. He presented his Ph.D. synopsis on 7th October 2021 in an open seminar and recommended for thesis submission. He presented his final viva-voce seminar on 21st July 2022.

TH-2951_166106019